PAPER BASED CELL CULTURE: ELECTROSPIN-COATED PAPER AS NATURAL EXTRACELLULAR MATRIX INSPIRED BIOPOLYMER SCAFFOLD

NG KELVIN

FACULTY OF ENGINEERING
UNIVERSITY OF MALAYA
KUALA LUMPUR

2021

PAPER BASED CELL CULTURE: ELECTROSPIN-COATED PAPER AS NATURAL EXTRACELLULAR MATRIX INSPIRED BIOPOLYMER SCAFFOLD

NG KELVIN

THESIS SUBMITTED IN FULFILMENT OF THE REQUIREMENTS FOR THE DEGREE OF DOCTOR OF PHILOSOPHY

FACULTY OF ENGINEERING
UNIVERSITY OF MALAYA
KUALA LUMPUR

2021

UNIVERSITY OF MALAYA

ORIGINAL LITERARY WORK DECLARATION

Name of Candidate: Ng Kelvin

Matric No: KHA150073/17035737/1

Name of Degree: Doctor of Philosophy

Title of Project Paper/Research Report/Dissertation/Thesis ("this Work"):

Paper based cell culture: electrospin-coated paper as natural extracellular matrix inspired biopolymer scaffold

Field of Study: Biomedical Engineering

I do solemnly and sincerely declare that:

(1) I am the sole author/writer of this Work;
(2) This Work is original;
(3) Any use of any work in which copyright exists was done by way of fair dealing and for permitted purposes and any excerpt or extract from, or reference to or reproduction of any copyright work has been disclosed expressly and sufficiently and the title of the Work and its authorship have been acknowledged in this Work;
(4) I do not have any actual knowledge nor do I ought reasonably to know that the making of this work constitutes an infringement of any copyright work;
(5) I hereby assign all and every rights in the copyright to this Work to the University of Malaya ("UM"), who henceforth shall be owner of the copyright in this Work and that any reproduction or use in any form or by any means whatsoever is prohibited without the written consent of UM having been first had and obtained;
(6) I am fully aware that if in the course of making this Work I have infringed any copyright whether intentionally or otherwise, I may be subject to legal action or any other action as may be determined by UM.

Candidate's Signature Date:

Subscribed and solemnly declared before,

Witness's Signature Date:

Name:

Designation:

PAPER BASED CELL CULTURE: ELECTROSPIN-COATED PAPER AS NATURAL EXTRACELLULAR MATRIX INSPIRED BIOPOLYMER SCAFFOLD

ABSTRACT

Paper has recently found widespread applications in biomedical fields, especially as an alternative scaffolding material for cell culture, owing to its properties such as fibrous nature, porosity, and flexibility. However, paper on its own is not an optimal material for cell culture and modification is necessary for its scaffold application. The present study focuses on modification of filter paper through electrospin-coating and dip-coating with polycaprolactone (PCL), a promising biomaterial in tissue engineering. Morphological analysis, physical properties analysis, evaluation of cell viability, alkaline phosphatase (ALP) activity and live/dead assays were conducted to study the potential of the modified paper-based scaffold. The results were compared to filter paper (FP) and electrospun PCL (ES-PCL) as reference samples. The results indicate that electrospin-coating is a simple and efficient way of modifying FP. It not only improves the morphology of the deposited electrospun layer through reduction of fiber diameter by nearly 75%, but also greatly reduces the scaffold fabrication time compared to ES-PCL. The tensile properties of electrospin-coated filter paper (ES-PCL/FP) are significantly higher than other scaffolds, which indicates the synergistic effect of modifying FP with electrospin-coating method. Furthermore, the electrospin-coating of PCL on FP creates a bimodal scaffold that resembles the hierarchical structure of ECM, which could be beneficial toward improving biocompatibility. In vitro studies were conducted on these scaffolds, by using human fetal osteoblast (hFOB) and human adipose derived stem cells (ADMSC), to study the cellular interaction with these scaffolds in the aspect of proliferation, adhesion, and differentiation. The biochemical assays (Resazurin assay) conducted on hFOB and

ADMSC show an up-regulated proliferation rate over the time points, ES-PCL/FP provides significantly higher readings compared to all other groups. The immunofluorescent stain results also show improved cell-distribution and cell-scaffold attachment all over the ES-PCL/FP. Medium sorption and retention capability of the scaffolds, and the effect towards cell proliferation, have also been highlighted in this study.

Keyword: Electrospinning, Tissue engineering, Paper-based Scaffolds, Cell Proliferation, Polycaprolactone

PENGKULTURAN SEL BERASASKAN KERTAS: KERTAS SALUTAN ELEKTRONSPIN SEBAGAI BAHAN PERANCAH POLIMER INSPIRASI DARIPADA MATRIK EXTRASELULAR SEMULA JADI.

ABSTRAK

Pada masa ini, kertas digunakan secara meluas dalam bidang bioperubatan, terutama sebagai bahan perancah alternatif untuk pengkulturan sel disebabkan oleh sifatnya yang berserabut, berliang dan mudah lentur. Namun begitu, penggunaan kertas sahaja bukanlah satu bahan yang optimum untuk pengkulturan sel dan ia memerlukan pengubahsuaian dalam aplikasinya untuk digunakan sebagai perancah biobahan. Kajian ini tertumpu pada pengubahsuaian kertas penapis, melalui kaedah salutan elektrospin dan salutan-celupan dengan menggunakan polycaprolactone (PCL), satu biobahan yang berguna dalam bidang kejuruteraan tisu. Ujian seperti Analisis morfologi, penilaian keupayaan sel, aktiviti alkali fosfatase (ALP) dan esei hidup/mati dijalankan bagi mengkaji potensi perancah berasaskan kertas yang diubah suai. Perbandingan dibuat antara keputusan yang diperoleh dari eksperimen dengan kertas penapis dan PCL(ES-PCL) yang telah dielektrospin. PCL (ES-PCL) berfungsi sebagai sampel rujukan dalam perbandingan ini. Keputusan menunjukkan kertas salutan elektrospin adalah cara yang paling mudah dan berkesan dalam modifikasi FP. Ia dapat menambahbaik bentuk lapisan mendapan elektrospin dengan pengurangan diameter serat sebanyak 75% dan juga mengurangkan masa fabrikasi jika dibandingkan dengan ES-PCL. Kekuatan sifat ketegangan kertas turas salutan elektrospin adalah jauh lebih tinggi berbanding perancah yang lain, di mana ia menunjukkan kesan sinergistik hasil daripada pengubahsuaian kertas turas salutan elektrospin. Tambahan pula, salutan elektrospin kertas turas menggunakan PCL membentuk perancah bimodal yang menyerupai struktur hierarki ECM, di mana ia boleh memberi faedah ke arah meningkatkan keserasian biologi. Kajian in vitro telah dilakukan pada perancah, dengan menggunakan osteoblast (hFOB) dan sel induk adipos manusia

(ADMSC), untuk mengkaji interaksi antara sel dan perancah dari aspek percambahan, lekatan dan pembezaan. Ujian biokimia (Resazurin assay) dilakukan ke atas hFOB dan ADMSC menunjukkan kadar percambahan terkawal berdasarkan titik masa, membuktikan yang ES-PCL/Fp memberikan bacaan yang tinggi berbanding kumpulan yang lain. Keupayaan perancah untuk menyerap dan mengekalkan media, dan kesannya kepada percambahan sel turut ditekankan dalam kajian ini.

Kata kunci: Salutan elektrospin, Kujuruteraan tisu, Bahan perancah kertas, Penyebaran sel osteoblast, Polycaprolactone.

ACKNOWLEDGEMENTS

I want to thank my supervisors, Assoc. Prof. Ir. Dr Belinda Pingguan-Murphy and Prof. Dr Xu Feng for their guidance throughout my studies. Their valuable time and advice have helped me through up and downs in my research. I felt grateful that I was given the opportunity to work under them, as their invaluable teaching and guidance have made me a better researcher. I deeply value their effort in helping me to prepare my manuscript. Despite their tight schedule, they are willing to spare their precious time to revise my manuscript and thesis.

I want to thank my brothers and sisters in Tissue engineering lab for their guidance and supports. The lab technologist, Miss Liyana, is always there to help in lab-related issue and experimental preparation work. Poon Chi Tat, Dr Salfarina and Izzah are the lovely people that always provide me advice and technical support in experiment related matter. Special thanks to Prof. Dr Xu Feng and for welcoming me to his great research group, Bioinspired Engineering and Biomechanics Centre (BEBC), and provided me with the wonderful opportunity to grow as a researcher. Brother and sisters in BEBC such as Dr Ze Dong, Dr Hao Liu, Dr Meng Wang, Dr Yan Gong, and Mo Xiao Lee have never ceased to provide me support and encouragement when needed. The life-changing experience in BEBC have opened my eye, it gives me a glimpse to the world of high impact research.

Above all else, I would express my deepest gratitude to my family for supporting me throughout my research. I am always in debt to my parent, Ng Yuen Kit and Tan Mei Ngor for their selfless love, unconditioned support, and care throughout my entire life. I felt grateful to have great siblings, Ng Ferrine and Mok Wai Loon, who are always be there to support me. It is a blessing to have aunties and relatives that never stop showering me with encouragement and bits of advice.

TABLE OF CONTENTS

LIST OF FIGURES

LIST OF TABLES

LIST OF SYMBOLS AND ABBREVIATIONS

Adipose-Derived Stem Cells	ADSCs
Alkaline Phosphatase	ALP
Bone Marrow-Derived Mesenchymal Stem Cells	BMMSCs
Cell-In-Gel-In-Paper	CiGiP
Degree Celcius	^{o}C
Dip-Coating Of Filter Paper	DFP
Electrospin-Coated Filter Paper	ES-PCL/FP
Electrospun Polycaprolactone	ES PCL
Embryonic Stem Cells	ESCs
Field Emission Scanning Electron Microscopy	FESEM
Filter Paper	FP
Glycidyl Methacrylate Polymer	pGMA
Human Adipose Derived Stem Cells	ADMSC
Human Fetal Osteoblast	hFOB
Human Induced Pluripotent Stem Cells	hiPSCs
Hydroxylpropyl Cellulose	HPC
Infrapatellar Fat Pad	IFP
Initiator Chemical Vapor Deposition	iCVD
International Society For Cellular Therapy	ISCT
Mesenchymal Stem Cells	MSCs
Micron	µ
Nano	n
Natural Extracellular Matrices	ECM
Perfluorodecyl Acrylate Polymer	pFDA
Phosphate Buffer Saline	PBS
Polycaprolactone	PCL
Stem Cells	SSCs
Stromal Vascular Fraction	SVF
The International Federation For Adipose Therapeutics And Science	IFATS
Thermally Induced Phase Separation	TIPS
Three-Dimensional	3D
Two Dimensional	2D

LIST OF APPENDICES

CHAPTER 1: INTRODUCTION

1.1 Research Background

Paper, with history dating back thousands of years，is an essential human invention, that was proved to be revolutionary for humanity**.** It was initially invented as a tool to record and preserve information has recently found widespread application in biomedical fields, such as paper-based electronics (H. Liu et al., 2017), low-cost and disposable analytical platforms (M. L. Cheng et al., 2008; J. Hu et al., 2014; A. W. Martinez et al., 2007), microfluidic devices for drug screening (Hong et al., 2016), and disease modeling (R. Derda et al., 2009; R. Derda et al., 2011; B. Mosadegh et al., 2014; H. J. Park et al., 2014). As a biomaterial, paper offers several advantages such as low cost of production, biocompatibility, ease of chemical alteration, and physical modifiability (Jie Hu et al., 2014). For example, paper has shown great potential as an alternative scaffolding material for cell culture owing to its properties such as fibrous nature, porosity, and flexibility. Its porous structure produces a wicking capability which allows the flow of medium across the paper, thus facilitating the transportation of nutrients and exchange of waste products (Cai et al., 2014). The cellulose fibers in the paper provide a platform for physical and biological support of the cultured cells, enabling them to grow into functioning tissue in an *in vitro* environment (Diban & Stamatialis, 2011; K. Ng et al., 2017; O'Brien, 2011; Suwantong, 2016). These advantages exhibited by versatile paper materials have enticed researchers into further exploring the potential of paper as a cell culture scaffold.

Although paper has several favorable properties for biomedical applications, on its own, it is not an optimal material for cell culture. Some properties, such as lack of cell adhesion moiety (A. Qi et al., 2014) and relatively large pore size, have been found to create difficulty for cell migration along the paper scaffold, in which the cell will need to take a longer path in the situation where the void gap is too wide for the filopodia to bridge (Lowery et al., 2010). Several studies have shown that modification of paper is

necessary to manipulate its chemical and physical properties to create a more feasible environment for cell proliferation, migration, and differentiation (Levy et al., 2002; Oliveira et al., 2015). Various modification methods for paper have been reported, including binding of ceramics to the paper surface with latex binder to modify the topography (H. Juvonen et al., 2013), chemical vapor deposition of polymers onto paper to increase the cell adhesion moiety for better cell growth (H.-J. Park et al., 2014), wax printing on paper to manipulate the proliferation direction of cells, mineralization of paper scaffold prior to cell seeding to dictate stem differentiation (Camci-Unal et al., 2016), and the addition of hydrogels to permit better cell migration within a stacked-up paper scaffold (R. Derda et al., 2011; B. Mosadegh et al., 2014). Most of these modification methods used polymers to modify the properties of paper scaffolds to be more biochemically favorable for cell culture. For scaffolding applications, it is critically important to maintain the porous structure of paper upon the addition of polymer (Agrawal & Ray, 2001). Some of the modification methods mentioned previously used heat or chemicals that might damage paper's natural fibrous microstructure. Natural extracellular matrices (ECM), which is an interwoven random fibrous hierarchical structure primarily made of proteins (mainly collagen and elastin), proteoglycans, and glycosaminoglycans (Azari et al., 2018; Ong & Guda, 2017), plays a crucial role in providing support for cell attachment and growth as well as serving as a reservoir of water, nutrients, cytokines, and growth factors for maintenance of tissue homeostasis (Ong & Guda, 2017). An ideal scaffold must mimic the structure and geometry of ECM to significantly enhance tissue formation (O'Brien, 2011) and provide explicit biophysical and biochemical cues to distinctly modulate cellular response for promoting tissue restoration.

The electrospinning technique has gained popularity in recent years as a feasible method to fabricate biomimetic polymeric scaffolds that resemble native ECM (Aghdam

et al., 2014; Christopherson et al., 2009; Dettin et al., 2015; Nune et al., 2013). Among a wide range of polymers that have been electrospun , there has been a gradual increase of polycaprolactone (PCL) for biomaterial and tissue engineering. PCL has found extensive application in bone tissue engineering, both micro and nano-seized PCL fibers have shown good cell compatibility and promote osteogenic differentiation of stem cells. PCL is soluble in organic solvents, such as chloroform, and toluene at room temperature with low cost of synthesis (E. Malikmammadov et al., 2018). When PCL is electrospun, apart from its favorable intrinsic properties, it also gains advantages such as high surface-area-to-volume ratio, high porosity and an interconnected porous network, all of which are crucial in a biomimetic material (C. T. Yew et al., 2018). Unfortunately, the hydrophobic nature of PCL is not favorable for cell adhesion as it prevents cells from proliferating into the pores of the scaffold, leading to low cell affinity and uncontrolled biological interactions with the scaffold (A Cipitria et al., 2011; E. Malikmammadov et al., 2018). Hence, additional treatment is often required to alter the surface hydrophobicity for the improvement of cell affinity (Amini et al., 2012; Webb et al., 1995). Blending or using PCL in combination with other hydrophilic biopolymers has been a very popular strategy to address some of the shortcomings of PCL (A Cipitria et al., 2011). A recent study has reported the modification of nitrocellulose membranes with electrospun PCL, where electrospun PCL was able to alter the wicking properties of the membrane and enhanced the protein binding as well as improving detection sensitivity of nucleic acid-based lateral flow assays (C. T. Yew et al., 2018). Protein binding is an important aspect of scaffolds for cell anchoring, and a combination of paper and PCL has the potential to produce a scaffold with a controllable degree of hydrophilicity and wicking properties. Further, electrospinning PCL on paper could resolve the morphological issue of paper for cell work and produce an ECM like scaffold, with paper performing as a reservoir basement

layer to enhance the nutrient delivery. The potential of modification of paper-based scaffolds with electrospun PCL has not yet been explored.

The demand for improved scaffolding materials to function as an artificial ECM to facilitate tissue regeneration in the desired anatomical sites of the body is never ending (Iqbal et al., 2019). Tissue engineering inspired therapies are the subject of studies *in vivo* and *in vitro* due to their significant role in the acceleration of bone tissue regeneration. Paper-based platforms have shown great potential in osteogenic differentiation of stem cells (J. Li et al., 2019; H. J. Park et al., 2014). Previously, both osteoblast and stem cells have shown to be very sensitive to the surface topologies where they were seeded (J. R. Venugopal et al., 2008). It will be very interesting to elucidate what paper scaffolds can do to differentiated cell (osteoblast cells) and undifferentiated cell (stem cells) in term of cell behaviour. The promising results obtained in previous studies motivated us to use osteoblast cell and stem cell to evaluate the *in vitro* performance of our scaffold designs. Researcher has reported that paper scaffold are capable as guiding-template that could induce osteoblast mineralization and accelerate bone growth (Camci-Unal et al., 2016). Another study also reported on paper's great potential as a bioactive, functional, and cost-effective scaffold platform for stem cell-mediated bone tissue engineering (H.-J. Park et al., 2014). Although the translation of *in vivo* results into practice is more straightforward, *in vitro* studies provide a more cost-effective initial insight in terms of cell viability and scaffolds capability in maintaining phenotype and functionality (Groeber et al., 2011). Besides, progress in understanding the causes of *in vivo* transplantation failure has led to improvements in design of scaffolding materials to provide more accurate results in relevance to future transplantation trials (Groeber et al., 2011; Polak, 2013).

This study focuses on the modification of paper with PCL, with scaffold properties such as physical and morphological assessed. Cell-material interactions were assessed as well. Two types of cells were used for this study namely, adipose derived stem cells and

human fetal osteoblasts cells. To evaluate the effect of a combination of the filter paper (FP) and PCL, two groups of samples were prepared through electrospin-coating and dip-coating. FP and electrospun PCL (ES-PCL) were used as reference samples.

1.2 Research Question

i. Does modification of paper with PCL have any effect on the paper in terms of physical properties such as mechanical strength, porosity, pore size and fiber diameter?

ii. Does modification of paper with PCL have any effect on the interaction of paper with cells in terms of cell viability, proliferation, and differentiation?

1.3 Research Objectives

This study focuses on the fabrication and characterization of paper-based scaffold with PCL, followed by *in* vitro studies to evaluate cell-material interactions. The objectives of this study are as follows:

i. To study the effect of different modification methods on composite materials (paper with PCL) on physical properties such as mechanical strength, porosity, pore size and fiber diameter.

ii. To evaluate osteoblast and adipose derived stem cell bioactivity responses, such cell proliferation, viability and osteogenic potential of the PCL-modified paper scaffold.

iii. To investigate the ability of scaffold in sustaining cell growth under medium deprivation conditions.

1.4 Research Framework

Including the current introductory chapter, this thesis comprises 5 chapters, its contents are briefly as follows:

Chapter 1 provides a brief overview of the research background, research question, research objectives, and the content of each chapter.

Chapter 2 provides a brief review of the research background, which includes the role of scaffold materials in tissue engineering applications. The clinical applications of paper as a diagnostic tool, a sensor, and a disease model are discussed. An intensive review of various surface modification techniques that have been conducted on paper for *in vitro* and *in vivo* studies is included. This chapter also contains selected figures and table reprinted in part from my review articles as follows:

-Ng, K., Gao, B., Yong, K. W., Li, Y., Shi, M., Zhao, X., Li Z.d., Zhang X.H., Murphy B.P., Xu H.Y., Xu F. (2017). Paper-based cell culture platform and its emerging biomedical applications. Materials Today, 20(1), 32-44.

Chapter 3 contains all the related fabrication and characterization methods used in this study, which includes the fabrication procedure of paper-based scaffold and characterization of the scaffold. The cell culture related techniques for both cell lines and stem cells are explained in detail. Stem cell isolation and cell characterization protocols are also included.

Chapter 4 contains results and discussion. An in-depth discussion about the changes in properties and cellular behavior in response to the modifications is presented. This

chapter contains selected figures and table reprinted in part from my research articles as follows:

-Ng, K., Azari, P., Nam, H. Y., Xu, F., & Pingguan-Murphy, B. (2019). Electrospin-Coating of Paper: A Natural Extracellular Matrix Inspired Design of Scaffold. Polymers, 11(4), 650.

Chapter 5 contains thesis contributions, findings of the study, and future work.

CHAPTER 2: LITERATURE REVIEW

2.1 Introduction

Injuries and lesion, brought by disease or trauma, has caused high mortality among patients, the limited regeneration capability of organ and tissue is to blame. Although tissue transplantation treatment, autograft and allograft, is the preferable option in clinical application, however, organ from the donor is a scarce medical resource which most patients do not have the privilege to access (Jin et al., 2018). The tissue-engineered scaffold has stepped in and emerged as a promising solution for this problem. Scaffold material is capable of a temporary structural template to fill in tissue lesions, and it took the role of matrices for cellular ingrowth and new tissue formation (Smith & Ma, 2004).

The search for biological restoration materials has been an endless quest in tissue engineering. For years, scientists have been searching for biological substitutes that could repair and restore damaged tissue or organ functionality. Various materials were developed to meet the goal of clinically useful materials for tissue replacement. However, this goal is far from being realized due to the ever-increasing demand for a new and better material. The requirement for a biological substitute has been changing throughout the years, in the early year, inert materials are favorable, but as time progresses the requirement has changed. The requirement for an ideal biological substitute has become more stringent by today's standard, being inert alone is no longer suffice, the biological substitute has to be biomimicking structurally and mechanically, at the same time need to biocompatible and biodegradable (O'Brien, 2011).

Conventionally, there are three types of materials used in tissue engineering to fabricate scaffold, namely metals (Alvarez & Nakajima, 2009; Peuster et al., 2001; Yusop et al., 2012), ceramics(Amin & Ewais, 2017; Ravaglioli et al., 2008), and polymer (Xiaohua Liu & Ma, 2004; Smith & Ma, 2004). Metals and ceramic are frequently used as implanting materials in hard tissue engineering (e.g., dental, and orthopedic surgery) to facilitate the repair of tissues damaged beyond the natural healing capacity of the bone.

Metals and ceramic have shown advantages such as mechanical stability, adequate mechanical strength, resistance to corrosion/degradation, and wear resistance. The limitation of metals and ceramic are the non-degradable nature, difficult in processing, metal ion induced allergy and stress shielding caused by stiffness mismatch (Alvarez & Nakajima, 2009). Polymers have become a popular scaffold material in recent years, mainly due to its great tailorability, and degradability. Polymers can be fabricated into two-dimensional (2D) and three-dimensional (3D) materials by using techniques such as molding and electrospinning (Karageorgiou & Kaplan, 2005; Sobral et al., 2011). Most of the polymers are inherently hydrophobic (Elbay Malikmammadov et al., 2018), and this is not favorable for biomedical applications such as lateral flow assays(C.-H. T. Yew et al., 2018),and cell culture platforms (Shalumon et al., 2013). Modifications are required to improve the hydrophilicity for better performance (A. Cipitria et al., 2011).

Paper has recently attracted increasing attention as a substrate for various biomedical applications, as a result of the significant advances in biotechnology. Papers are extensively used in a variety of biomedical applications, such as the production of low-cost and disposable analytical test papers in healthcare applications (Y.-H. Chen et al.; Andres W Martinez et al., 2007; Pollock et al., 2012), flexible electronics (Russo et al., 2011; Tobjörk & Österbacka, 2011), paper-based biosensors (Ge et al., 2012; Lewis et al., 2012; Parolo & Merkoçi, 2013). Paper, given its fibrous, porous and flexible properties (Figure 2. 1 a), has shown great potential as an alternative platform for cell culture (Figure 2. 1c). The unique features of paper-based system in supporting 3D cell culture enables it to be utilized for a range of studies, such as the development of normal or disease models *in vitro* by manipulating the physical or chemical properties of the paper to control nutrient and oxygen diffusion (Figure 2. 1 b & d)) (Ratmir Derda et al., 2009; Ratmir Derda et al., 2011), and study cell-drug interactions in a high-throughput manner (Figure 2. 1e) (R Derda et al., 2009; Bobak Mosadegh, Borna E. Dabiri, et al., 2014b). The wicking and absorbing ability of paper also render it a good carrier in cell

cryopreservation application (Figure 2. 1 f)(Y. Kim et al., 2012; X. Zhang et al., 2011). The reason why paper is gaining its popularity in Tissue Engineering applications is mostly attributed to its attractive intrinsic properties These properties will be further explained in detail in upcoming sections.

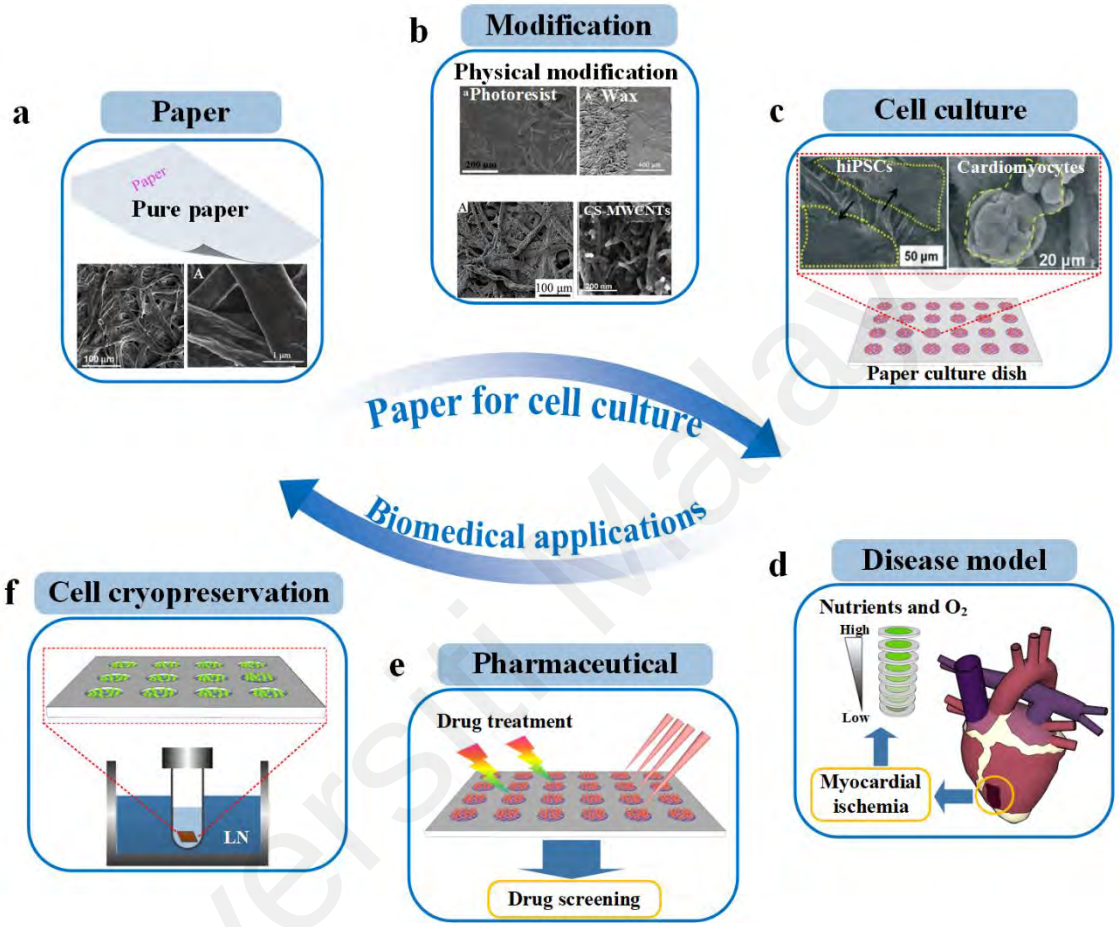

Figure 2. 1: Schematic of outline for paper-based cell culture and its emerging biomedical applications**.** a) Paper fibrous scaffold b) Modification of physical and chemical properties of paper c) Paper for cell culture, c) Disease model that capable of controlling nutrient and oxygen diffusion mimicking the healthy and diseased environment in vivo. e) The cell culture models can also be used to study the cell-drug interactions in a high-throughput manner for drug screening. f) The absorbing ability of paper renders it able to become a holder that reduces the vitrification solution around cells and can be for cell cryopreservation. Images reproduced from (Ratmir Derda et al., 2009; Y. Kim et al., 2003; Lee et al., 2013; Bobak Mosadegh, Borna E Dabiri, et al., 2014; Mosadegh et al., 2015). Adapted from K. Ng et al. (2017).

2.2 Extracellular matrix mimics

In human body, a mixture of cellular and non-cellular component exists in the extracellular interstitial compartment, which organized into a heterogeneous complex called Extracellular Matrix (ECM). ECM play an essential role in determining the cellular behaviour and cell function development (G. Huang et al., 2017). ECM served as a physical foundation for cellular constituent, which at the same time, provide biochemical and biomechanical cues that regulate cell behaviours such as cell proliferation, cell migration, tissue morphogenesis, differentiation and homeostasis (Theocharis et al., 2016). ECM are fundamentally composed of polysaccharides, water and protein, however, the composition and structural properties of ECM varies in different tissue, each tissue develop a distinct characteristic through its dynamic reciprocal interaction with microenvironment in vicinity (Goody & Henry, 2010). The ECM consists of various macromolecules that varies in size, composition, and structure among different anatomical location. For examples, the cornea and cartilage comprise of ECM that are similar but not identical, cartilage play mechanical roles in providing structural and mechanical integrity, while cornea play an important role in visual system with its unique optical properties (Malandrino et al., 2018). The two main classes of macromolecules in ECM are fibrous protein and proteoglycans. The major constituent of fibrous ECM proteins are collagens (Kadler et al., 2007). Collagens are the most abundant fibrous protein in ECM. Collagen is the main structural element in ECM that provide mechanical support, regulate cell adhesion, provide frame for cell migration and chemotaxis. Proteoglycans exist in the form of hydrated gel and were found mostly in extracellular interstitial space within tissue. Proteoglycans have a wide variety of functions that reflect their unique buffering, hydration, binding and force-resistance properties (Frantz et al., 2010). These fibrous macromolecules form a hierarchical structure with porosity and fiber size that range from macro to nano scale. This structure is important in providing

biochemical and biophysical cues that regulate cell behaviours such as cell spreading, motility, self-renewal and differentiation (G. Huang et al., 2017)

Recently, the concept of "ECM mimicking" was integrated into the design and fabrication of tissue engineering scaffold. The influence of ECM's physical and biochemical properties on fundamental cellular processes has enticed researchers' interest in the development of synthetic ECM scaffold for the tissue-culture model. Scaffolding biomaterials that resemble natural ECM have shown promising results in the constructive remodeling of tissues in human clinical applications and animal studies (Badylak et al., 2009). The synthetic strategy used in fabricating ECM mimicking scaffolds focuses on recapitulating the composition, stiffness, and topological structure of the ECM macromolecular organization, such as collagen, glycoprotein, and glycosaminoglycan. The structural features and physical stimuli of the ECM mimicking scaffolds have marked effects upon the host response and the remodeling events that determine the eventual clinical outcome. For instance, cellulose and polymer based fibrous scaffolds were engineered to mimic the structure of fibrillar collagen in ECM, in particular, the highly porous architecture with high specific surface and interconnected pores (H. Li et al., 2020). A few recent studies have demonstrated that native nanocellulose fibers (*e.g.,* bacterial nanocellulose & nanofibrillar cellulose) show good biocompatibility to human cells in 3D cell culture due to their native ECM-mimicking structure and dimension (Bäckdahl et al., 2008; Bhattacharya et al., 2012; Klemm et al., 2011).

2.3 Paper scaffold and its biomedical applications

Paper is an interesting alternative substrate/scaffold to the conventional cell culture materials (*e.g.,* ceramic, glass and polymer) due to its dimensional versatility and tailorable porosity (Choi et al., 2015; Jie Hu et al., 2014; Helka Juvonen et al., 2013). Paper is essentially a fibrous composite in which rigid cellulose microfibrils are embedded in a soft matrix mainly composed of lignin and hemicelluloses. Paper comes

in the form of continuous woven sheet that possesses adequate mechanical strength and porous structure (Figure 2. 1 a). The strong cellulose fibers in paper provide sufficient mechanical properties to reshape and to stack into the structure that favors cell growth, with no detrimental effect on the bulk properties of paper (Ratmir Derda et al., 2011; Bobak Mosadegh, Borna E Dabiri, et al., 2014; Sapp et al., 2015). As mentioned previously, paper with sufficient mechanical properties can also be stacked up layer-by-layer to create 3D scaffolds, which recapitulate the native cell microenvironment where cells reside in a 3D ECM (Figure 2. 1 c) (Abbott, 2003; Cukierman et al., 2001; Frey et al., 2014; Rismani Yazdi et al., 2015; Sapp et al., 2015; F. Wang et al., 1998; Wolf et al., 2003). Such 3D cell culture can generate a precise physiological gradient of oxygen and nutrient, and also provides a physiologically relevant fluid flow, which can better reflect the native situation compared to the conventional *in vitro* 2D model (Bissell, 2003; Ratmir Derda et al., 2011; Frey et al., 2014; G. Huang, Wang, et al., 2012; Bobak Mosadegh, Borna E Dabiri, et al., 2014; Rismani Yazdi et al., 2015; Sapp et al., 2015; Yan et al., 2013). The native 3D cell microenvironment consists of a complex cell-cell, cell-ECM interactions and mass transfer barriers (Abbott, 2003). Compared to a 2D platform, 3D cell culture platform can better mimic the *in vivo* microenvironment with microscale tissue geometry, ECM-like stiffness, and complex organization of ECM.

The highly porous structure of the paper, that closely mimic the structure of fibrillar collagen in ECM, facilitates diffusion of oxygen and nutrients as well as the removal of waste products. By altering the porosity of paper, the amount of nutrient and oxygen reaching the targeted tissue can be precisely controlled that helps in creating an accurate normal or diseased tissue model (Figure 2. 1 d) (Deiss et al., 2013; Ratmir Derda et al., 2009; Bobak Mosadegh, Borna E Dabiri, et al., 2014; Aisha Qi et al., 2014; Sapp et al., 2015; Yan et al., 2013). Paper as a 3D cell culture platform has a great diversity on its surface topography and internal porous microstructure, which enables it to manipulate cell behavior (Ratmir Derda et al., 2011; Bobak Mosadegh, Borna E Dabiri, et al., 2014;

H.-J. Park et al., 2014; Aisha Qi et al., 2014). Furthermore, paper has an inherent ability to wick fluids by capillary action due to its porous structure and large void volume (Y.-H. Chen et al.; Z. Liu et al., 2015), making cell migration inside the paper based scaffolds possible (Ratmir Derda et al., 2009; Ratmir Derda et al., 2011). This water absorbing ability of paper has found its use in cryopreservation technology (AbdelHafez et al., 2010; Chong et al., 2009; Magalhães et al., 2012; Magalhaes et al., 2008; X. Zhang et al., 2011). Cryopreservation has been widely used for long-term storage of biospecimens, such as cells, cell aggregates and tissues. Among various cryopreservation methods, vitrification holds the advantages of maintaining viability, genetic profiles, and cytoskeletal structure of cells (AbdelHafez et al., 2010; Chong et al., 2009; Magalhães et al., 2012; Magalhaes et al., 2008; X. Zhang et al., 2011). Vitrification methods include open pulled straw (Vajta et al., 1998), quartz microcapillary (He et al., 2008), cryotop (Kuwayama, 2007), cryoloop (Lane et al., 1999) and electron microscope grid methods (Martino et al., 1996) have been adopted to vitrify mammalian embryos and successfully maintained the functional properties of post-thawing embryos. However, these methods require special devices to acquire a small volume to achieve high cooling rate for vitrification, which may be expensive and not be suitable for large-scale cryopreservation of embryos (Matsunari et al., 2012). Paper-based cell culture platform can serve as a more convenient and inexpensive platform to achieve minimized vitrification droplet and efficient embryo vitrification through its favorable absorbing property (Figure 2. 2) (Y. Kim et al., 2012; Lee et al., 2013).

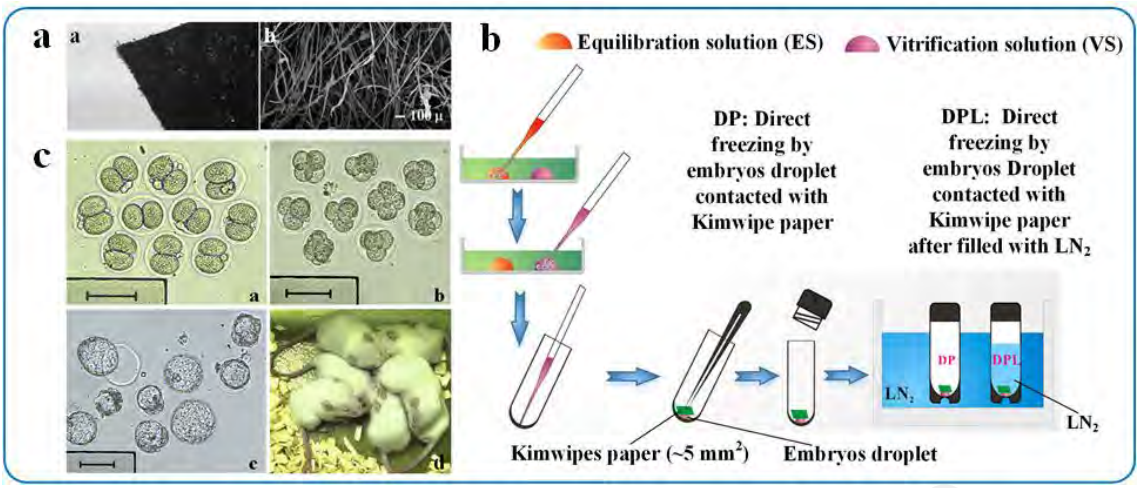

Figure 2. 2: Paper-based cryopersearvation. **a)** Microscope observation of the paper used for bovine blastocysts vitrification: (a) inverted microscope, (b) scanning electron microscope (Y. Kim et al., 2012); **b)** Vitrification of mouse embryo in cryotube using Kimwipes paper (KP) as cell holder; **c)** Representative embryos and living pups born from mouse embryos vitrified in paper-based cryotubes. (a) Two-celled embryos before vitrification, (b) four celled embryos after warming and culturing, (c) blastocysts after warming and culturing, (d) Living pups were born from vitrified embryos (Lee et al., 2013). Adapted from K. Ng et al. (2017).

A hydrogel-based scaffold is a platform that was popular in tissue engineering studies because of its many merits, such as ECM mimicking, minimal immune response, biodegradable and abundant at a low price. However, engineering hydrogel into a functioning structure remains challenging. The relatively weak physical properties and dimensional stability hinder it being used in the load-bearing site. Handling and transfer of such fragile scaffold is also a present problem, as the dimension of the scaffold would easily compromise due to weak mechanical strength. In order to overcome the limitation presented by hydrogel, papers which are made of fibers (provide strong mechanical support) has been used as a frame to support and maintain the thin dimension and mechanically fragile hydrogel, and this application can be seen in so-called cell-in-gel-in-paper (CiGiP) platform (Figure 2. 3 a) (G. Huang, Zhang, et al., 2012), and this system allows repeat handling of the cell-laden paper without significant disruption of cell behavior (Ratmir Derda et al., 2011; Bobak Mosadegh, Borna E Dabiri, et al., 2014; Aisha

Qi et al., 2014). Another advantage of paper is its thickness can be tailored to 200 μm or less to ensure sufficient delivery of oxygen to all cells. Furthermore, a multiple paper unit containing different cell types can also be created by stacking up multiple cell laden papers with a defined spatial distribution to recapitulate native 3D architecture *in vivo* (Figure 2. 3 b-c) (Ratmir Derda et al., 2011; Bobak Mosadegh, Borna E Dabiri, et al., 2014; Xu et al., 2011). Paper can withstand various chemical, thermal and UV sterilization processes without suffering drastic changes in its properties and this property is very useful for cell culture.

In vitro 3D cellular models that mimic a normal or diseased tissue structure *in vivo* are of great importance for an understanding of the cellular physiological or pathological behavior (Abbott, 2003; Bobak Mosadegh, Borna E Dabiri, et al., 2014; Sapp et al., 2015; Lin Wang et al., 2014). Many studies have proved that a paper-based cell culture platform can be used to mimic various native pathophysiological microenvironments (Figure 2. 3b) (Bobak Mosadegh, Borna E Dabiri, et al., 2014; Sapp et al., 2015; Li Wang et al., 2015; Yan et al., 2013). Functional changes in the microenvironment, such as inadequate oxygen supply, adaptive changes in metabolism and changes in the pH in the microenvironment, can be achieved with a paper-based culture platform.

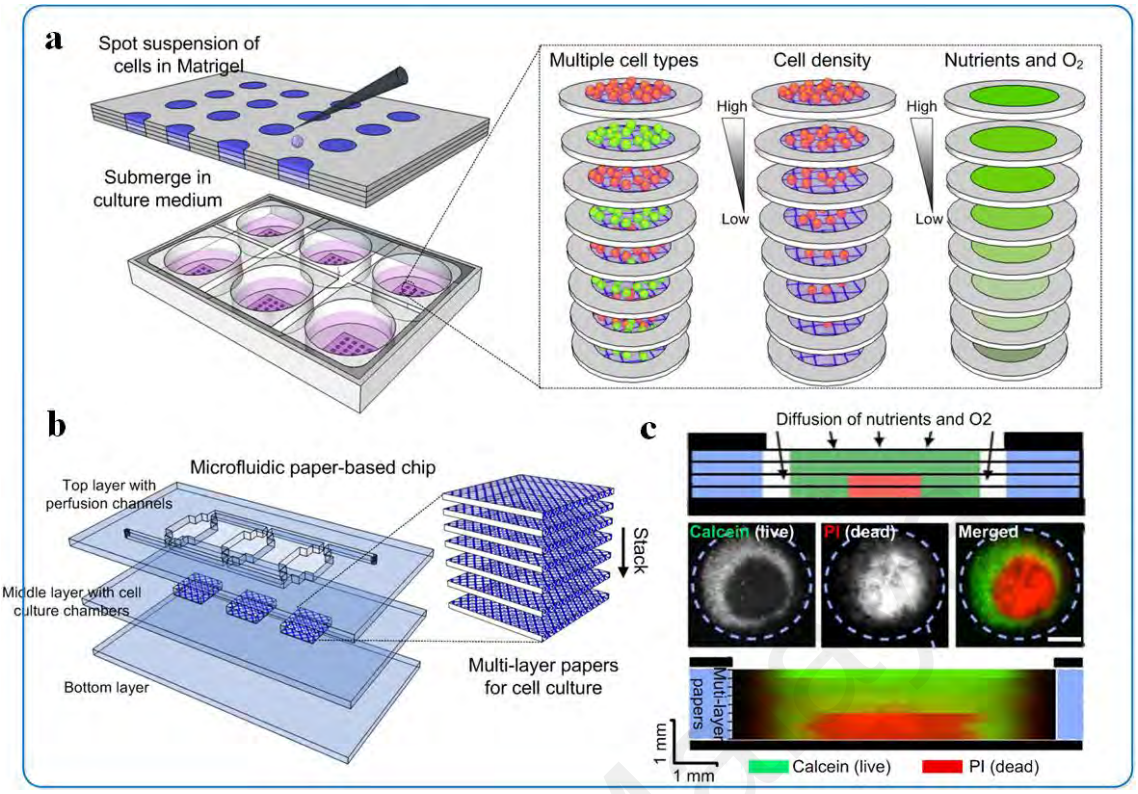

Figure 2. 3: Disease model using paper-based cell culture platform. a) Construction of Cell in Gel in Paper (CiGiP) model (Bobak Mosadegh, Borna E Dabiri, et al., 2014); b) 3D breast cancer model (Yan et al., 2013); c) Fluorescent images depicting the distributions of living (green) and dead (red) cells in a multilayered paper-based cell culture model (Ratmir Derda et al., 2011). Adapted from K. Ng et al. (2017)

Cell-based drug screening through monitoring of cell responses (*e.g.,* cell apoptosis and cell metabolic products) to the drug treatment is of great importance for new drug development (Johnstone, 2002; Pérez-Tomás, 2006). Therefore, significant efforts have been made on the development of various methods for sensitive and specific detection of drug stimulated cell responses. Compared to conventional plastic based platforms, paper provides distinct advantages including low cost, eco-friendliness, short time of testing, and small reagent volume consumed (Y. H. Chen et al., 2015). Particularly, paper can provide a 3D microstructure for *in vitro* cell culture mimicking native 3D microenvironment (R Derda et al., 2009; Bobak Mosadegh, Borna E. Dabiri, et al., 2014a), thus holding great promise for drug screening.

Monitoring cell responses to drug treatment has been developed recently for drug screening. The monitoring of cell response to drug treatment is an effective way for drug screening. Paper-based platforms are capable for high-throughput cell culture by physical modification (*e.g.,* wax printing) forming multiple cell zones defined by barriers in paper (Figure 2. 4). The paper-based platform has demonstrated promising ability for multiple detection of cell responses to various drugs. Furthermore, a common laboratory filter paper modified with plasmonic gold nanorods can act as a highly sensitive 3D platform for cancer biomarker detection due to its excellent flexibility, good wicking properties and high specific surface area, which provides potential for cancer cell responses monitoring (Tian et al., 2012). Considering that the cell responses are normally at an extremely low level, the paper-based electrochemical detection methods are widely used for detection of cell responses due to their highly sensitive, selective and quantitative nature (Zedong Li et al., 2015). In addition, high-throughput electrochemical detection of cell responses can be achieved by using the separated electrodes on paper cell zone to achieve high throughput drug screening applications.

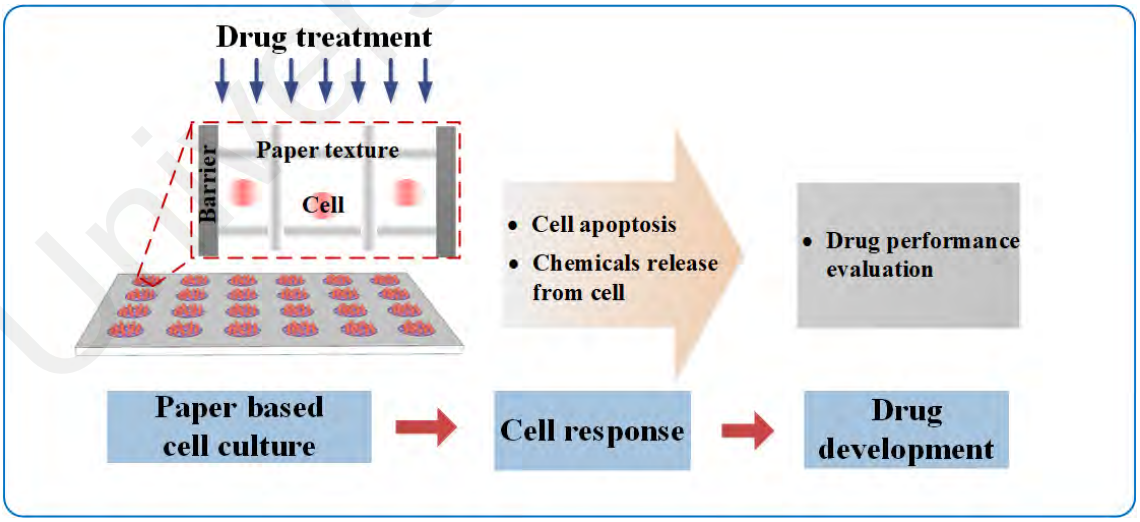

Figure 2. 4: Schematic diagram on the working principle of paper-based cell culture platform for cell-based drug screening.

Although there are many advantages to use paper as a cell culture platform, before that, some of its limitations must be addressed. Paper by itself is not a suitable material

for cell culture, this is due to the absence of cell adhesion moieties (Aisha Qi et al., 2014). The main factor that affects cell adhesion and proliferation on a cell culture platform is the presence of cell adhesion moieties. Unfortunately, paper does not have these natural biological ligands attached to it. It is essential to attach these cell adhesion moieties biomolecules (*e.g.,* peptides or nucleotides) onto paper prior to cell culture. Another limitation of the paper is, it is very rigid hence difficult to stretch hence making the evaluation of mechanically induced cell response difficult and the mechanical property of paper decline overtime as a cell culture platform in long-term immersion of cellulose pulp (composition of paper) in the culture medium which might destroy the bonding between the cellulose pulps and cause cells to lose their anchoring sites, thus disrupting cell-matrix adhesion. This cellulose pulp is bound together through mechanical interlocking and intermolecular hydrogen bonds which provide paper with sufficient mechanical strength (Holik, 2013; Aisha Qi et al., 2014). Therefore, the modification of paper's chemical and physical properties has become an inevitable and essential part of paper-based cell culture to create a more feasible environment for cell growth. To date, various modification methods have been developed to manipulate the chemical and physical properties of paper to fit different cell culture applications. A variety of commercially available papers are currently used in cell culture and biomedical applications. The detailed comparison between the papers is listed in Table 2. 1.

Table 2. 1: Paper types and their characteristics in biomedical applications.

Paper types	**Pore size**	**Roughness**	**Thickness**	**Cell types**	**Applications**
Whatman filter paper #114	25 µm	Rough	190 µm	Cardiomyocyte/ Aortic valvular interstitial cell/Human acute promyelocytic leukemia cell	Cell culture/Disease model/ Drug screening
Whatman® Protran® nitrocellulose membrane	1.0 µm	Smooth	130 µm ~160 µm	Human breast cancer cell	Cell culture/ Disease model
Janus paper	/	Smooth	/	Human lung fibroblast	Disease model
Kimwipe Kimberly Clark 34155	/	Smooth	100 µm ~160 µm	Mouse embryonic fibroblast	Cell cryopreservation
Weighing paper	/	Smooth	100 µm ~200 µm	Bovine blastocyst Human adipose-derived stem cell	Cell culture/Disease model

2.3.1 Modification of paper's chemical properties for cell culture

The surface chemistry of paper is an important factor for cell attachment and proliferation (Feinberg et al., 2008; Helka Juvonen et al., 2013). Paper can be easily modified chemically by conjugating with many biomolecules (*e.g.,* peptides or nucleotides) (Y.-H. Chen et al.). The chemical properties of the paper surface can be tailored through surface treatment which incorporates different chemicals using various methods, such as initiator chemical vapor deposition (iCVD) (H.-J. Park et al., 2014), corona discharge surface treatment (Rahimi et al., 2015), and printing (Helka Juvonen et al., 2013) **(**Figure 2. 5 a). iCVD is a solvent free vapor-phase polymer-coating method that can provide systematic tailoring of the paper surface into a favourable biochemical surface that has desirable water resistance and adhesiveness, before stacking the paper into a 3D scaffold (H.-J. Park et al., 2014). The iCVD approach polymerizes a functional polymer coating onto the surface of paper using a free radical polymerization process, which can reduce undesirable side chain polymerization reactions which may destroy the functional groups of the polymer coating (Tenhaeff & Gleason, 2008). A recent study used iCVD for the deposition of glycidyl methacrylate polymer (pGMA) on perfluorodecyl acrylate polymer (pFDA) coated paper has greatly increased cell adhesion. (Figure 2. 5 a ii-iv) This is because pGMA is a bio-reactive polymer that contains an epoxy-group that causes the serum protein in medium to bind onto the paper substrate (H.-J. Park et al., 2014). Corona discharge surface treatment has also been used in paper modification to increase surface energy, inevitably increased wettability for cell adhesion. Further, the chemical properties of a paper can be modified by printing various chemical substances onto it to improve cell adhesion (Helka Juvonen et al., 2013; Sarfraz et al., 2012). Previous studies have printed ECM proteins onto the paper surface to facilitate cell adhesion (Arima & Iwata, 2007; Vogler, 1998). Cell adhesion proteins such as vitronectin and fibronectin were successfully printed on paper substrate to enhance cell attachment (Haynes & Norde, 1995; Silva-Bermudez et al., 2011).

Cell-in-gel-in-paper (CiGiP), a multilayer paper-based 3D cell culture platform made of paper and matrigel, is fabricated by patterning hydrophobic and cell culturing zones on monolayer paper using a wax printer, followed by stacking of these papers into a multilayer stack that is held together with mechanical clamps (Ratmir Derda et al., 2011; Bobak Mosadegh, Borna E Dabiri, et al., 2014). A single-layered paper cultured with osteogenically differentiated ADMSC was stacked with another layer of paper cultured with human endothelial cells to promote the formation of vascularized bone *in vivo*, which was then implanted into mice with calvarial bone defect resulting in significantly enhanced bone regeneration *in vivo* (H.-J. Park et al., 2014). This stacking technology is a key feature of CiGiP which enables researchers to design a customized cell culture platform that suite their experimental needs (Ratmir Derda et al., 2009). Another advantage of this system is the detachability of the platform, which enables the examination of cells at a specific layer and area (Ratmir Derda et al., 2011).

A functional "beating" cardiac tissues were successfully created on three types of paper (print paper, chromatography paper, and nitrocellulose membrane). These papers were coated with PDMS and tested for the growth and differentiation of human induced pluripotent stem cells (hiPSCs). Within 5 days, hiPSCs grew well on these paper substrates and have 3D-like morphology. The hiPSCs lost their pluripotency after 5 days on these paper substrates and were fully induced to the targeted cells. The cardiac tissue cells retained their long-term stable contractile frequency of 40-70 beats per minute for 3 months on the print paper and chromatography paper. The human iPSCs grew on the nitrocellulose membrane differentiated into retinal pigment epithelium even under cardiac-specific induction, demonstrating that the properties of the paper and the mechanical cues are involved in regulating stem cell differentiation. This shows that a paper-based cell culture platform is a promising scaffold for the support of various cell functions, including attachment, proliferation and differentiation (Li Wang et al., 2015).

The aforementioned methods showed the modification of paper's surface chemical properties. The bulk properties of paper can also be altered by chemical modification of the cellulose fibers. For example, hydroxylpropyl cellulose (HPC) is a derivative of cellulose with solubility in both water and organic solvent. Once hydrated with water, the HPC forms a soft elastomer with Young's modulus similar to that of soft tissues (Hoo et al., 2013; Levental et al., 2007; Sen et al., 2009). Crosslinking of HPC grafted with methylacryclic anhydride by ultraviolet irradiation forms a hydrophilic network that provides an anchoring site for cell-matrix interaction. To further enhance cell attachment, 1,1'-carbonyldiimidazole activation of the hydroxyl groups of HPC chain can be done to introduce biochemical cues to HPC, which enables HPC to conjugate with matrix protein (acting as active cell binding sites). This hydrophilic network degrades gradually along with cell proliferation, allowing the cells to slowly replace the materials and regenerate the tissues (Aisha Qi et al., 2014).

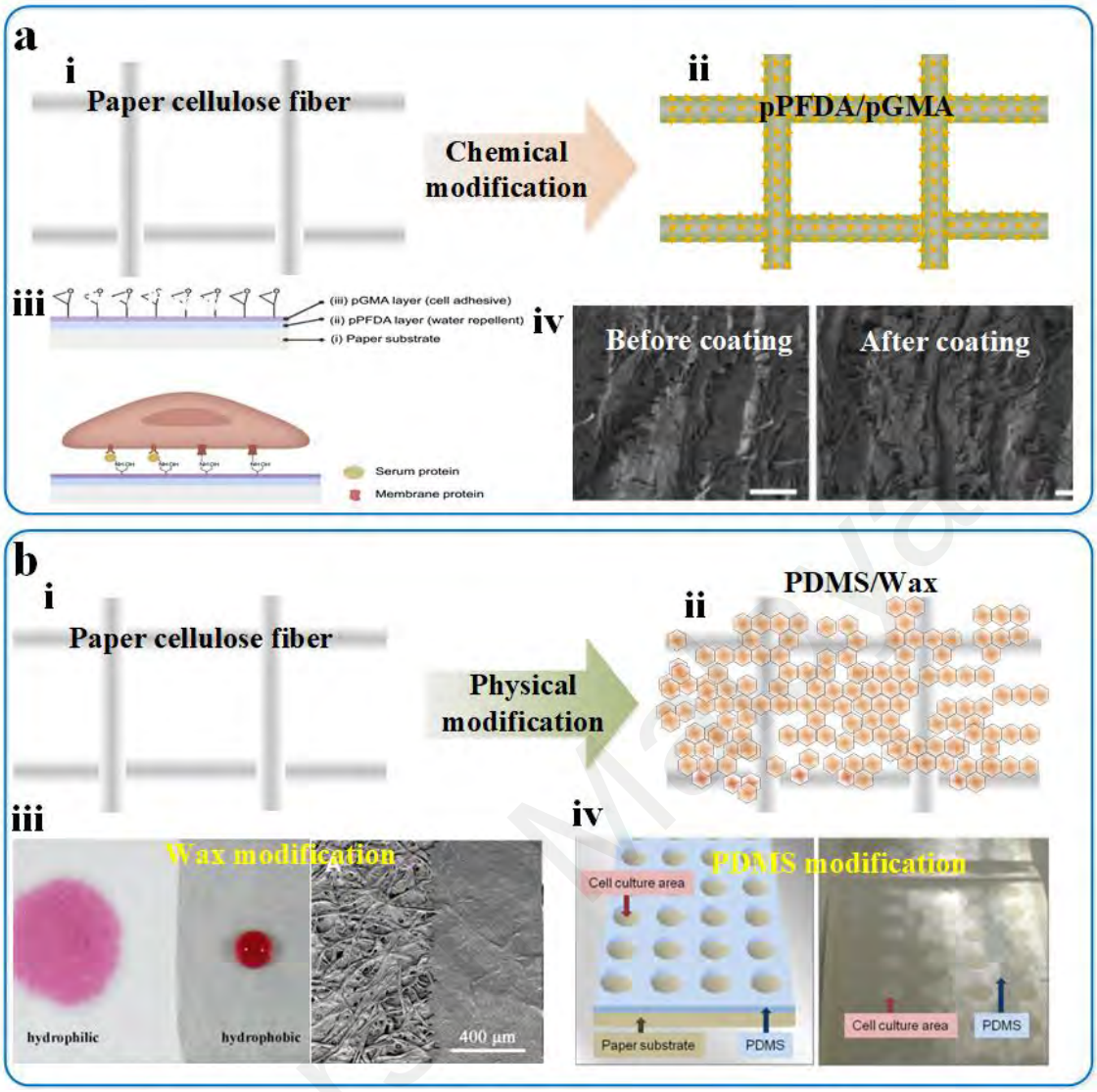

Figure 2. 5: Modification of paper properties for cell culture. a**)** Chemical modification through iCVD coating of various component on paper scaffold for enhanced cell attachment (H.-J. Park et al., 2014). b**)** Physical modification of paper using Wax and Polydimethylsiloxane to modify the hydrophobicity and hydrophilicity of the paper surface. Images reproduced from (Ratmir Derda et al., 2011; Helka Juvonen et al., 2013; Songjaroen et al., 2011). Adapted from K. Ng et al. (2017).

2.3.2 Modification of paper's physical properties for cell culture

The physical microenvironment (*e.g.,* topography, stiffness, roughness and water permeability) has a great impact on cellular behavior, *e.g.,* cell growth pattern, such as direction and orientation (Baharloo et al., 2005; Chung & King, 2011; Discher et al., 2005; G. Huang, Wang, et al., 2012; Min Jin et al., 2012). For instance, cell morphology, adhesion, and migration are affected by the surface topography of the substrate. Materials with smoother surfaces are better at supporting the growth, spreading, and attachment of epithelial cells, whereas materials with a rougher surface are more favorable for the growth, spreading, and attachment of osteoblast cells (Baharloo et al., 2005; Helka Juvonen et al., 2013; Stevens, 2008; L. Wang & Carrier, 2011). Hence, modifying the physical properties of paper can guide cell behavior. In addition, paper stiffness can significantly affect anchorage-dependent cells in terms of their cellular behavior, including stem cell proliferation, adhesion, locomotion, spreading, morphology, striation, and even differentiation (Tse & Engler, 2001).

The physical properties of paper can be tailored through printing and coating of different substances. Previously, it was shown that paper coated with 4 different types of substrate (calcium carbonate/latex binder, kaolin pigments/latex binder, duo kaolin pigments/latex binder, and styrene butadiane/polystyrene) were able to tune the physicochemical properties of the substrate (*e.g.,* topography, roughness and surface energy), which was then used to study cell attachment and growth (Helka Juvonen et al., 2013). These coatings changed the surface properties of paper, including the surface roughness. It was found that paper with low roughness promotes cell growth of human arising retinal pigment epithelial cells (ARPE-19) (Ratmir Derda et al., 2009; Ratmir Derda et al., 2011). Paper has also been coated with a thin layer of highly hydrophobic pFDA to strengthen its mechanical durability and its long-term stability in an aqueous environment, for example, cell culture medium (H.-J. Park et al., 2014).

In another separate study, common laboratory filter papers were modified with plasmonic gold nanorods to act as three-dimensional scaffold for cancer detection (Tian et al., 2012). Hydrophobic materials (*e.g.,* PDMS, wax and Teflon) have low surface energy and hinder cell attachment, allowing them to act as barriers that direct and constrain cell growth in the desired area of the paper (de Silva et al., 2004; Deiss, Matochko, et al., 2014; Frimat et al., 2009; Helka Juvonen et al., 2013) (Figure 2. 5 b). For instance, PDMS was printed on the paper to form 96 individual thin circulars well slabs (hydrophilic zones) that contain hydrogels encapsulating cells, where PDMS functions as hydrophobic barrier to isolate the cell containing zones from each other and prevent the lateral flow of aqueous medium and cell growth across to other zones (Figure 2. 5 iii-iv) (Deiss et al., 2013; Ratmir Derda et al., 2011; Bobak Mosadegh, Borna E Dabiri, et al., 2014).

2.4 Polymer Biomaterials

Polymer based biomaterials have been a popular candidate in tissue engineering applications for many years. The usage of polymer in medical applications dated back to the early 20th century, during World War II some of the prostheses for amputated soldiers was made from rubber. In 1950, polymers such as silicon and polyester resin had become the mainstream in the design and fabrication of prostheses, mainly due to its excellent and tailorable properties (Migonney, 2014). Polymers are still the popular biomaterials to date, mainly due to their tailorable chemical and controllable physical properties that satisfy diverse clinical needs, thus emerged as one of the best candidates in tissue replacement, drug carrier, and prosthesis *(Buddy D Ratner et al., 2004)*.

There are many types of polymers available in the market. Polymer possesses the ability to self-degrade and the degradation products are nontoxic to the host making it the most suitable material for tissue engineering applications. These biodegradable polymers have the upper hand in both short terms, and long-term biomedical applications compare

to other biostable polymer. In short term medical applications, such as suture, biodegradable materials eliminate the need for secondary surgical removal, thus lower the chances of inflammatory and infection reoccurrence. In long term applications, the replacement of the metallic implant with biodegradable polymer implant as the supportive structure in orthopedics application could lower the chances of surgical failure, typically caused by the stress shielding effect of metallic implant (Nair & Laurencin, 2006). The biodegradable implant will slowly degrade and gradually transfer the load to the newly generated ECM, which will eventually take over the load-bearing role in the injury site (G. Huang et al., 2017).

Polymer can be categorized into two distinct groups, which is the synthetic polymer and natural polymer (S. Wang et al., 2010). The natural polymer is generally more favorable in tissue engineering application, due to its biocompatibility, and biodegradable through the hydrolytic mechanism. Synthetic polymer, on the other hand, has its advantage over natural polymer in term of mechanical properties, formability, reproducibility and excellent control over degradation (Griffith, 2000). The clinical use of polymer is decided upon its distinct characteristic. If temporary support for cell attachment is needed, a degradable polymer such as poly-lactic-acid (PLA) and polycaprolactone (PCL) will be used, and such biodegradable polymer will break down slowly and allow replacement by human tissue. Clinically, biodegradable polymer is often used in biodegradable stitches, bone and dental restoration that eliminate the second surgical removal (B.D. Ratner et al., 2004; Sun et al., 2006)).

2.4.1 Polyester

Polycaprolactone (PCL) is one of the earliest synthetic polymer in the world, it was synthesized by Wallace Hume Carother and his team in the early 1930' (Woodruff & Hutmacher, 2010). PCL is a synthetic polymer that falls under the category of aliphatic polyester. The key features of aliphatic polyester that attract considerable attention as

biomaterials are the biodegradability and biocompatibility. PCL can be produced by ring-opening polymerization of caprolactone monomers, the mechanism of polymerization can be done via anionic, cationic, free radical and coordinate polymerization. PCL has excellent characteristics such as biocompatibility, biodegradability and mild immunoresponse, which render it a desirable biomaterial for prosthetic and sutures (Gupta et al., 2007).

In the 1970s, PCL and its copolymer were the popular resorbable polymer in drug-delivery device. PCL has a slower degradation rate, thus it was fabricated into suture materials that need to remain active in drug-delivery for a prolonged period. The relatively weak mechanical properties of PCl were a major drawback, and eventually, PCL was replaced by other materials. In the 2000', PCL was brought back to light when scientist realized that the unique properties of PCL would make it an excellent scaffold in tissue engineering. PCL possesses superior rheological and viscoelastic properties that make the fabrication into scaffold easy. The inexpensive production methods compare to other aliphatic polyester is hugely advantages, examples of such methods are melt spinning and electrospinning (Woodruff & Hutmacher, 2010).

PCL is semi-crystalline at room temperature, it has melting temperature of 59-64^{o}C and glass transition temperature of -60^{o}C. At body temperature, the loosely pack amorphous section in PCL allow permeation of body metabolites *in vivo*. PCL is soluble in organic solvent, but the solubility varies in different solvent. PCL is highly soluble in chloroform, and toluene, while display low solubility in acetone and non-soluble in alcohol (Elbay Malikmammadov et al., 2018).

Degradation of scaffolds is an important property required in tissue engineering application. The biomaterials should have degradation rate that matches the tissue regeneration rate, otherwise, would lead to complication, such as mechanical failure in the injury site and burse release of drugs that will delay the healing process. The degradation of PCL is at a slower rate compared to other polyesters due to the lesser ester

bond in each monomer. Hydrolytic degradation of PCL polymer chain takes a longer time as enzyme need to penetrate deeper into the amorphous region to cleave the ester bond of PCL (Sun et al., 2006). Degradation of PCL biomaterials depends on the factors such as molecular weight, dimension, and microenvironment in the vicinity. Generally, it takes 2-3 years for complete degradation to take place (Elbay Malikmammadov et al., 2018).

2.5 Fibrous polymer scaffolds and fabrication technique

Polymer can be fabricated into various shapes with desired features for tissue in-growth. In tissue engineering, polymer is often fabricated into scaffolds that mimics niche-specific ECM, because such structure will guide cells to develop into the desired phenotype (G. Huang et al., 2017). Type 1 collagen is the fibrillar protein present in ECM, especially in the injury site. The fibrillar structure of collagen provides biochemical and biophysical cue for cell attachment and proliferation in vivo. Fibrous polymer scaffold could mimic the morphological function of collagen fibrils thus provides a better microenvironment to promote cell growth. The nano-sized diameter of fibrous polymer scaffold is close to the size of collagen fiber bundles (50-500 nm)(Smith & Ma, 2004) and the pore size of fibrous polymer scaffold could be fabricated into 5-500 μm, which is the optimal pore size for cell attachment, proliferation, and migration (Pham et al., 2006). Fibrous polymer scaffold that has a gradient in diameter could create scaffold containing gradients in pore size and porosity, and such scaffold appears as an ideal platform for co-culture disease models such as chondrocyte and bone-related disease (Pham et al., 2006).

The striking advancement in technology in the recent decade has brought upon numerous techniques for the fabrication of polymer from a different origin, natural and synthetic, into ECM mimicking fibrous polymer scaffold. Various techniques such as electrospinning, self-assembly, colloidal lithography, phase separation, solution blow spinning, templating, drawing, extraction, and vapour-phase polymerization have been used to fabricate polymer fibers with diameters ranging from micro to nano-size, (Jin et

al., 2018). Among these techniques, three techniques are often used for the fabrication of fibrous polymer scaffold, which is electrospinning, phase separation and self-assembly (Puppi et al., 2014).

2.5.1 Electrospinning

Fibrous polymer scaffold with ultrafine fiber can be produced by electrospinning technique. Electrospinning is capable of producing fibers with diameters ranging from microns to nanometers, that mimic the ECM of the human body, from the suspended droplet of molten polymer or polymer solution (H. Liu & Y. L. Hsieh, 2002). The setup of electrospinning consists of 3 parts (Figure 2. 6): 1) a container attached to a protruded sprue with a small orifice, 2) high voltage power supply, and 3) a collector. In the electrospinning process, a mechanical pump is used to draw the polymer solution out of the container (syringe) through the small orifice (opening of a clinical needle) to form a suspended polymer droplet at the tip of the sprue (needle).The high voltage power supply is used to create an electrostatic field in between the conductive tips (needle), and the collector (conductive plate), the positive terminal is attached to the tips (needle), and the negative terminal is attached to the collector. The electric charge continues to pass through the polymer droplet to destabilize it, the shape of the droplet will shift from hemisphere to conical shape known as the Taylor cone (Yoshimoto et al., 2003). The electrical charge continues to build up in the droplet until it reaches a critical point at which the surface tension of the polymer droplet is overcome, a charged fluid jet will be ejected from the tip of Taylor cone and rapidly accelerated towards the oppositely charged collector. The instability process where the fluid jet will cause a whipping motion that will stretch and splay the fluid jet into forming thin fiber (Suwantong, 2016). Scaffolds that were produced by electrospinning have a few characteristics that are extremely favourable in tissue engineering application, such as possess large surface area to volume

ratio and have porous microstructure with interconnected pores which could promote cell adhesion and proliferation (Yanzhong Zhang et al., 2005).

The properties of electrospun fibers could be altered by a few processing parameters, for examples, polymer viscosity (poise), solvent and collector type. Liu and Hsieh have conducted a study on the processing parameter mentioned above and have reported the effects towards the properties of the electrospun cellulose acetate such as fiber diameter, surface finishing, fiber packing and pore formation. In their study, cellulose acetate was dissolved in a solvent mixture, consist of acetone and dimethylacetamide at ratio 2:1. The polymer solution with viscosity range between 1.2 and 10.2 poise is the optimum viscosity that gave the best result, viscosity lower than 1.2 poise form bead on the fiber, while viscosity higher than 10.2 poise causes instability in the spinning. Paper and water were used as collector in this study, different results were shown in term of fiber morphology, packing density and pores structures. Fibers collected on porous collector (paper and copper mesh) have smoother surfaces and more uniform sizes The scaffold produced are loosely pack and more porous, In contrary, fiber collected on water are not uniform in size and rougher, the scaffold produced are tightly packed and less porous (H. Liu & Y. L. Hsieh, 2002). Electrospinning is advantages over other fibrous scaffold fabrication methods, such as phase separation and self-assembly. The laboratory devices needed by electrospinning process is easy to set up, cheap in price, reproducible and gave good control over fibrous scaffold properties (Elbay Malikmammadov et al., 2018).

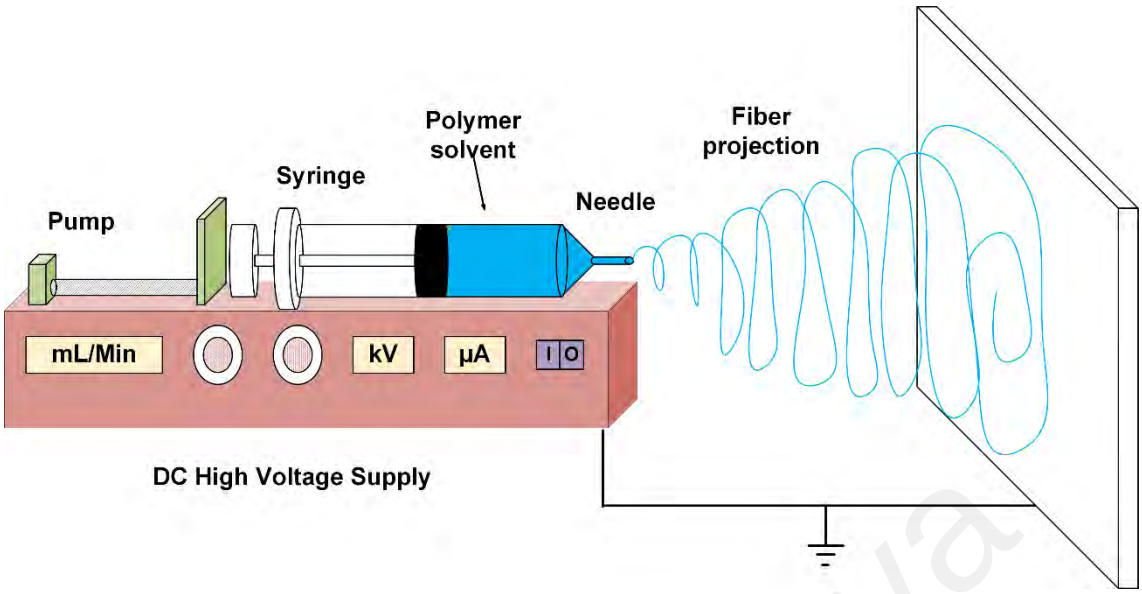

Figure 2. 6: Schematic representation of Electrospinning process

2.5.2 Thermally induced phase separation (TIPS)

Thermally induced phase separation (TIPS) was introduced in the 80's to fabricate microporous membranes. Lately, TIPS has been used to produce fibrous polymer for tissue engineering applications. There are 5 steps involved in the production of fibrous polymer scaffold using TIPS. First, the polymer is dissolved in high heat to become a homogeneous polymer solution. This is followed by the rapid cooling of polymer solution until the temperature is below the glass transition temperature and gelation occur. Rapid cooling forces polymer solution to be separated into a polymer-rich and a solvent-rich phase (gel) (Figure 2. 7a) (Puppi et al., 2014). Subsequently, the solvent-rich phase is extracted by solvent exchange, and the extractant is evaporated (freeze dry) to yield a fibrous polymer scaffold with interconnected porous structure (Figure 2. 7 b-c) (Ishigami et al., 2014). Gelation temperature plays a vital role in determining the porosity of the scaffold, and a low gelation temperature gives rise to a smaller fiber network or vice versa. The porosity and pore size of the scaffold can be manipulated by adding porogen of different sizes and shapes, such as sugar and organic salt, and finally, the porogens are leached out leaving many holes in the scaffold. A porous scaffold is formed. In recent

years, this technique has found its' use in tissue engineering, due to its ability to form ECM mimicking structure (J. F. Kim et al., 2016). The phase separation process can be used to form porous structure with a three-dimensional continuous fibrous network, which resembles the natural structure of collagen in ECM. TIPS can fabricate polymer with fiber size similar to collagen fibrillar, ranging from 50 to 500 nm, and porosity of approximately 98% (Smith & Ma, 2004).

A scaffold that contains a gradient of porosity and pore size can be easily fabricated by TIPS as well, and this architecture constructs closely mimic the hierarchical structure in native ECM (C.-J. Huang & Chang, 2019; Smith & Ma, 2004). A study conducted by Ma and Zhang had reported on the fabrication of nanofibrous poly (L-lactic acid) (PLLA) by using TIPS technique. The results showed that the PLLA scaffold porosity and mechanical properties could be altered by changing the concentration of polymer solution (Ma & Zhang, 1999). Another study also reports that the PLLA scaffold added with porogens could produce nanofibrous structures with an interconnected network of pore after the leaching process (V. J. Chen & Ma, 2006).

TIPS technique is easy to set up, and a low-cost method compares to other methods. This technique also gave reasonable control over the pore size and porosity of the scaffold. However, the thermal treatment step has brought the potential of compromising the intrinsic properties of the polymer and the integrity of bioactive reagent present in the polymer solution (Puppi et al., 2014; Smith & Ma, 2004).

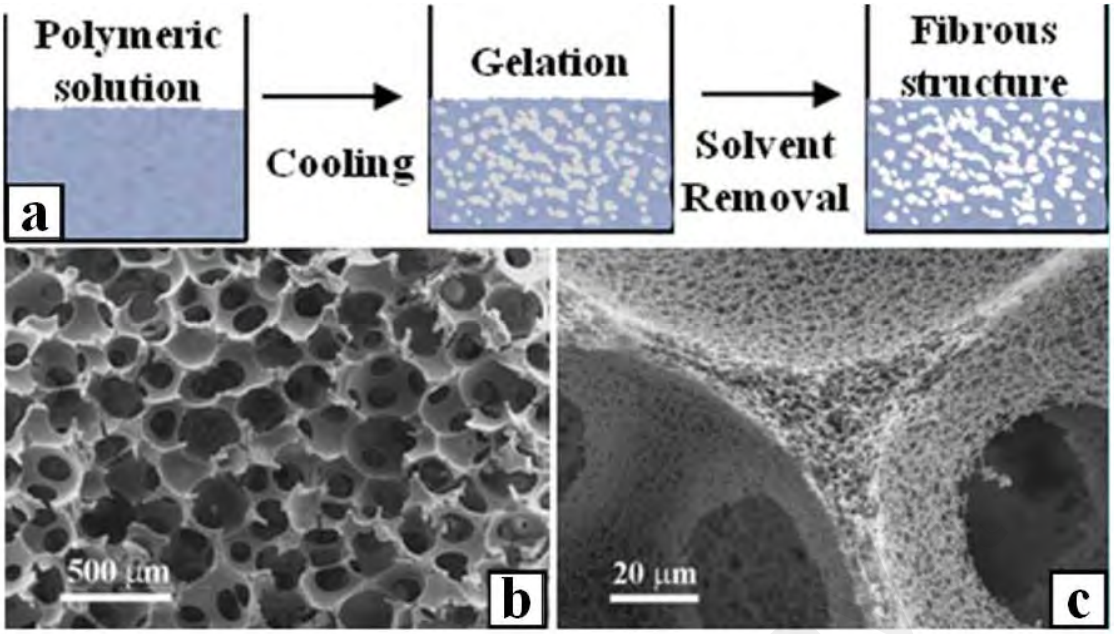

Figure 2. 7: Schematic representation of Thermally induced phase separation (TIPS). (a)TIPS process. SEM micrographs of gelatin structure by TIPS: (b) macropores network and (c) nanofibrous macropores. Adapted from Puppi et al. (2014).

2.5.3 Self-assembly

Self-assembly of fibrous scaffolds, is a bottom-up fabrication method that autonomously organizes the basic building block components into ECM mimicking structures without human intervention. The spontaneous organization of basic building block into structurally defined stable arrangements is governed by short-distance interactions at the molecular level, such as Van der Waals forces, hydrogen bonds, amphiphilic interaction and electrostatic interaction. Self-assembly process naturally occurs *in vivo*, one of the examples is the formation of fibrillar collagen structure in ECM (Thomas et al., 2016).

Scientists has employed this self-assembly strategy to create highly sophisticated 3D fibrous scaffold from different polymers, such as collagen, and thermoplastic. Kraskiewics et al have reported on the use of negatively charged polystyrene bead as a sacrificial template for the self-assembly of hollow collagen sphere. The polystyrene beads attract the attachment of negatively charge collagen to form a network of fiber on

the scaffold's surface. Subsequently, the polystyrene beads were dissolved with solvent, leaving the crosslinked collagen sphere intact (Figure 2. 8 a) (Kraskiewicz et al., 2013). Another group has used a similar approach to fabricate fibrin scaffold using Poly (methyl methacrylate) beads as the sacrificial template instead of polystyrene beads (Figure 2. 8 b) (Saul et al., 2007). Self-assembly method involved complicated chemical reactions and expensive laboratory equipment, it requires extra safety precaution and expert personnel to carry out the fabrication process. Hence, it is more expensive and harder to prosecute compared to electrospinning that only involves nonhazardous solvent and simple device set up.

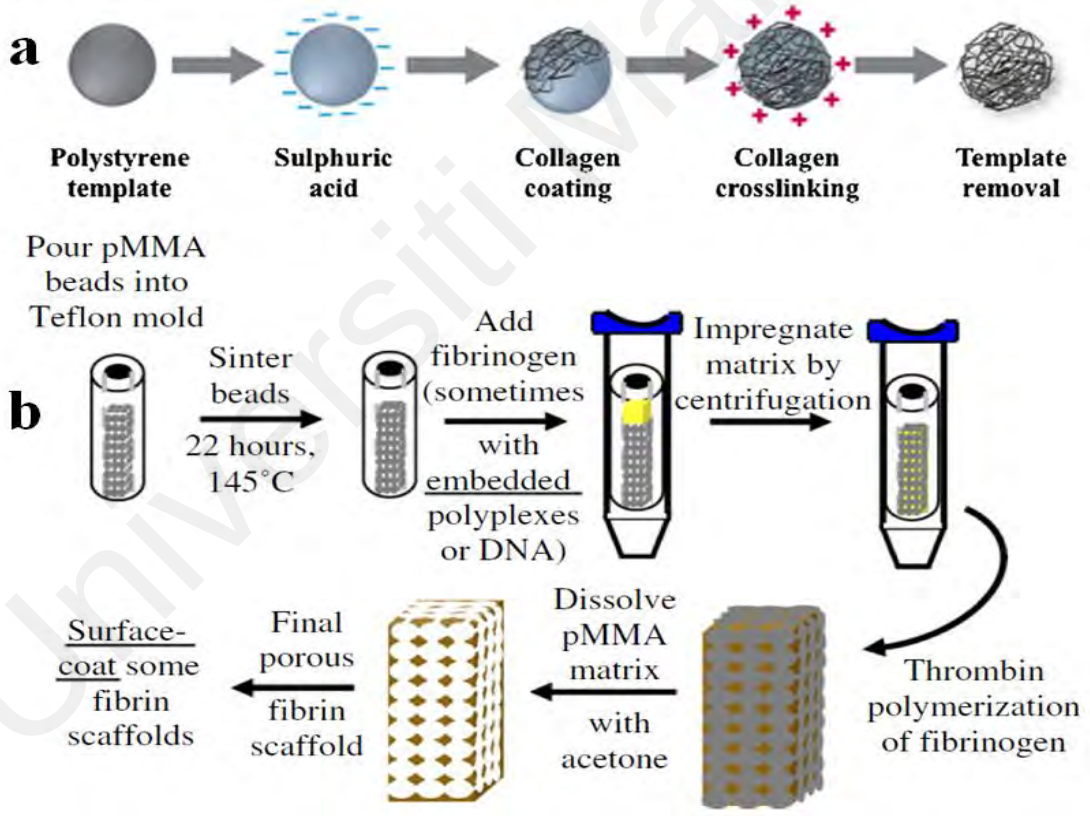

Figure 2. 8: Schematic representation of self-assembly method. a) Flow diagram of production of hollow collagen-based micro-spheres(Kraskiewicz et al., 2013; Thomas et al., 2016) b)Schematic illustration of process for formation of sphere templated fibrin scaffolds (Saul et al., 2007)

2.6 Electrospun PCL fibrous scaffold and its biomedical applications

The use of PCL for fibrous scaffold fabrication has become increasingly popular within the tissue engineering community. The increasing use of PCL possesses ascribe to its superior rheological and viscoelastic properties over other polymers, such as polylactic acid (PLA) and polyglycolic acid (PGA). PCL does not have isomer, which is great advantage over the PLA that exist in 3 types of stereocomplex enantiomer, such as PDLA, PLLA and PDLLA(A. Cipitria et al., 2011). The stereocomplexity of PLA render the fabrication of fibrous scaffold difficult, where specific device and processing parameter that require meticulous monitoring are often required (Zibiao Li et al., 2016). Compared to PLA and PGA, PLA has a lower melting point and it is also soluble in a wide range of solvent. Hence, the manufacturing of PCL scaffold is relatively easy, by manipulating processing parameter (*e.g.*, temperature and solvent type) PCL can be tailor into a wide range of polymer with different properties, such as fiber diameter, pore size and mechanical properties. The versatility of PCL allows it to fit into different fabrication technique. Among all the technique, electrospinning is the most reported technique used in the preparation of fibrous scaffold for tissue engineering application (Elbay Malikmammadov et al., 2018).

Electrospun PCL fibrous scaffold has been actively studied by researchers on its potential in applications for bone regeneration. The conventional method for bone lesion treatment done by using autogenic and allogeneic bone, have the risk of infections and immune response that led to morbidity. Electrospun PCL scaffold shows potential as the alternative approach for bone regeneration; due to its high specific surface area, fibrous structure that resembles fibrillar collagen, high porosity and interconnected pores that positively affect bone cell proliferation (J. R. Venugopal et al., 2008). Venugopal et.al has reported PCL fibrous scaffold that was electrospun into a blend of synthetic biodegradable PCL with gelatin and hydroxyapatite. The incorporation of hydroxyapatite and gelatin have significantly improved tensile properties and osteoblast responses.

Osteoblast proliferation shows significant increase and mineralization was observed throughout the whole scaffold. Another group has reported the fabrication of electrospun composite membrane based on silk fibroin and PCL blend. The addition of PCL into silk fibroin has increased the elongation at break to 5-fold. The *in vitro* cell culture results suggest that the membrane promote cell attachment and the osteogenic differentiation of osteoblast precursor cell (MC3T3-E1). The *in vivo* results suggest that the membrane accelerate the healing rate of tibial fractures on rats (G. Cheng et al., 2018).

2.7 Stem cell

Stem cells are undifferentiated and unspecialized precursor cells that hold the potential for self-renewal and multilineage differentiation into more specialized cell types. Stem cell, owing to its self-renewal and potency, has become an enticing candidate for regenerative medicine, tissue engineering, cellular and gene therapies (Mimeault et al., 2007). Stem cells are classified into 2 major types based on their developmental stage, embryonic stem cells (ESCs) and somatic stem cells (SSCs) (M. Wei et al., 2017). ESCs, harvested from the inner cell mass of blastocysts, have high telomerase activity, great differentiation potential (pluripotency) and infinite self-renewal ability, however, the usage of ESCs are fraughted with ethical, legal and political concerns, thus rendering it less accessible (Lo & Parham, 2009). On the other hand, SSCs can be obtained from less controversial sources such as bone marrow, adipose tissues, cord blood and neural tissues, render it more accessible than ESCs. Hence, SSCs such as Mesenchymal stem cells (MSCs), neural stem cells and adipose-derived stem cells (ADSCs) (Saxena et al., 2010), albeit less potent, have appeared as a favourable stem cell source for tissue regeneration and engineering (M. Wei et al., 2017). Human Induced pluripotent stem cell (hiPSC) that are produced by dedifferentiating SSCs have differentiation potential and self-renewal capability that is similar to ESCs and yet devoid of the ethical problems specific to embryonic stem cells. However, the induction of iPSC from SSCs require complicated

genetic reprogramming that involve the usage of genetic transcription factors, such as (Oct4, Sox2, c-myc, and Klf4), which is expensive, time-consuming and technically challenging (Takahashi & Yamanaka, 2006).

Stem cell research is essential in discovering the secret of human development differentiation, and such research holds great promise in the discovery of new therapy, especially degenerative diseases like myocardial infarction, diabetes and Parkinson's disease. There are a few criteria that need to be fulfilled so that the research and therapy could be carried out in an ethically appropriate manner. Firstly, a waiver of consent needs to be signed by the patient; patient's permission is needed before medical personnel could collect and use the patient's samples; otherwise, it should be discarded. The harvest of stem cell should be done in a minimally invasive manner. The harvested stem cell should be of good quality, which means it should be cultivable to obtain millions of cells and can be differentiated into multiple specific cell types in a reproducible manner. Lastly, the stem cells should be able to be implanted to autologous or allogenic host without inflicting excessive immune response(Lo & Parham, 2009).

2.7.1 Mesenchymal stem cell

Adult mesenchymal stem cells (MSCs) together with hematopoietic stem cells and neural stem cells fall under the category of SSCs or adult stem cell lineage. MSCs also are undifferentiated multipotent stem cell that is capable of self-renewal and able to differentiate to multiple cells of mesenchymal origin, e.g., osteoblast, chondrocytes, adipocytes, and myocytes, triggered by differentiation cues (Mohamed-Ahmed et al., 2018). MSCs has become an important candidate in stem cell-based therapy, because it is copious in different part of the human, including adipose tissue, bone marrow, muscle, tendon, *etc*.

Bone marrow is one of the first sources for stem cell, Friedenstein and colleague are the first that isolate bone marrow-derived stem cell (Bianco et al., 2008). Two populations

of bone marrow stem cells exist in adult bone marrow cells, which is hematopoietic stem cells and MSCs. Hematopoietic stem cells divide to produce mature blood cell lineage such as myeloid and lymphoid, on the other hand, MSCs give rise to cartilage, osteoblasts, chondrocytes, myocytes and adipocytes (Grove et al., 2004). Bone marrow-derived mesenchymal stem cells (BMMSCs) were used extensively in tissue engineering and regenerative medicine. Recent clinical studies have shown that transplanted BMMSCs could heal the patient by regenerating cells and induce vascularization in the damaged area, including pancreas (Hess et al., 2003), liver (Dong et al., 2013), muscle (Tamama et al., 2008), and central nervous system (Dai et al., 2013). However, the harvesting of BMMSCs is more invasive towards donor, the bone marrow aspiration process could inflict suffering to patients and in some serious cases, patient morbidity occurs. These drawbacks have urged scientist to redirect their efforts toward a better alternative for stem cell source (Mohamed-Ahmed et al., 2018).

Adipose tissue exists in all mammalians, it was derived from mesoderm of the 3-germ layer during embryonic development. Adipose tissue is abundant in the human body, about 15%-25% of the total body mass of a young adult is made up of adipose tissue (Badimon et al., 2015). Adipose tissue could be harvest in large quantity from various parts of the body, such as subcutaneous tissues (white adipose tissue) and the intraperitoneal compartment (visceral fat), through methods such as laser-assisted liposuction (LAL), power-assisted liposuction (PAL), and surgical resection. Harvesting adipose-derived stem cells (ADMSCs) is relatively easy and less invasive compared to BMMSCs, and it does not cause serious post-surgical complication and minimal morbidity. Furthermore, the yield of ADMSCs within the stromal vascular fraction (SVF) of subcutaneous white adipose tissue is approximately 2%, which is also higher than BMMSCs that yield in a relatively small amount (0.001–0.01%) (Mohamed-Ahmed et al., 2018). The frequency and yield of ADMSCs cultured in vitro is also higher than BMMSCs. J.K. Fraser et al. (2006) reported on an observation that is to generate

confluent culture at the given time frame of 5-7days, ADMSCs require only 3500 cell cm^2 for initial seeding while BMMSCs require 20 000 -400 000 cell cm^2 (Fraser et al., 2006). Although not identical, ADMSCs is similar to BMMSCs in many aspects; thus, ADMSCs could replace the use of BMMSCs in specific stem cell therapy.

2.7.2 Characteristic of human adipose-derived mesenchymal stem cells

White adipose tissue and Visceral adipose tissue are the two-primary sources of ADMSCs harvesting. White adipose tissue is a preferable source due to 2 reasons; firstly, White adipose tissue is abundant in the subcutaneous area. Secondly, visceral adipose tissue has a more acute inflammatory profile and higher angiogenic potential compare to subcutaneous white adipose tissue (Badimon et al., 2015). The two major sources of subcutaneous white adipose tissue are harvested from abdominal fat and infrapatellar fat pad (IFP) (S. L. Francis et al., 2018). Several steps are required to obtain ADMSCs from the human body, including surgical harvesting, mechanical breakdown, and enzymatic digestion. The harvest protocol and technique of isolation vary among different scientist from the different research laboratory, and this could affect the yield and growth characteristic of harvested cells (Oedayrajsingh-Varma et al., 2006). Besides, the origin of the stem cells might affect the proliferation and differentiation properties of ADMSC, donors from different age group was reported to affect the properties of ADMSC (S. L. Francis et al., 2018; Mohamed-Ahmed et al., 2018). These differences in properties, arise from different handling method, has the potential to jeopardize the exchange of result outcome among scientist, mainly due to concern in data reliability. Thus, with the aim to facilitate reliable knowledge exchange, The International Federation for Adipose Therapeutics and Science (IFATS) and the International Society for Cellular Therapy (ISCT) have proposed the minimum criteria for ADMSC to comply, which is plastic adherence, cell phenotypic surface marker and trilineage differentiation ability. Cell's adhesion to the plastic cultural flask is a curial indicator for stem cell characteristic and

is relatively easy to perform. The plastic adherence test on isolated stem cells is a time-consuming test, where the isolated cell will be incubated for 24-48 hours. The unattached cell will be wash away, and the remaining cell is the ADMSC population. The plastic adherence test has two significant drawbacks, which is time-consuming and lack of phenotypic characterization of ADMSC. Hence, assessment on the phenotype and multilineage potential is needed to identify ADMSC. Phenotypes of cells are tested on its specific surface antigen immunophenotyping with the flow cytometry machine, ADMSC should highly express (>95%) surface marker CD105, CD73, CD90 and CD44, while less in the expression of hematopoietic marker (< 2%), such as CD45, CD34, CD14, CD19 and HLA DQDPDR. A set of surface markers is needed to perform the immunophenotyping because no marker, to date, capable of unambiguously identifies native adipose-derived stromal/stem cells (ASCs).

2.8 Conclusion

From the literature review, it has been shown that paper holds great potential for tissue engineering applications if appropriate modifications are used to improve its chemical and physical properties. Current chemical and physical modification approaches for paper as cell culture biomaterials, despite recent improvements to scaffold performance, still have some unresolved underlying problems. For example, the wax printed paper used in C-i-G-i-P is weak in restricting lateral dissipation of medium from the edge of the paper. Furthermore, Derda et al. also reported that the disassembling of the C-i-G-i-P layers is difficult because the layers are bonded tightly by hydrogel, thus peeling the layer off for analysis could tear off the paper platform. The deposition of chemicals on paper is hard to control, so often chemicals are deposited excessively and unevenly on paper. The following study has been designed to evaluate a simple surface modification technique (dipping paper into a polymer solution), and a more advanced technique (electrospinning), in terms of cellular response including cell viability and proliferation

and cytoskeleton response. Osteoblasts and human adipose derived mesenchymal stem cells (ADMSC) will be used for this study. Both osteoblasts and ADMSC are sensitive to surface topography and used in many studies such as cell-material interactions (Alvarez & Nakajima, 2009; Woo et al., 2007). This study also explores other potential applications of paper in tissue engineering such as stem cell differentiation. With the unique advantages of paper, it has the potential to find a wide spectrum of applications in the biomedical field. We envision that with the unique advantages of paper, it will find a wide spectrum of application in the biomedical field.

CHAPTER 3: METHODOLOGY

3.1 Introduction

This chapter provides detailed procedures on the fabrication and characterisation of paper-based scaffold. Also, the protocols of cell culture and *in vitro* studies are stated thoroughly. A brief workflow of the study is illustrated in Figure 3. 1.

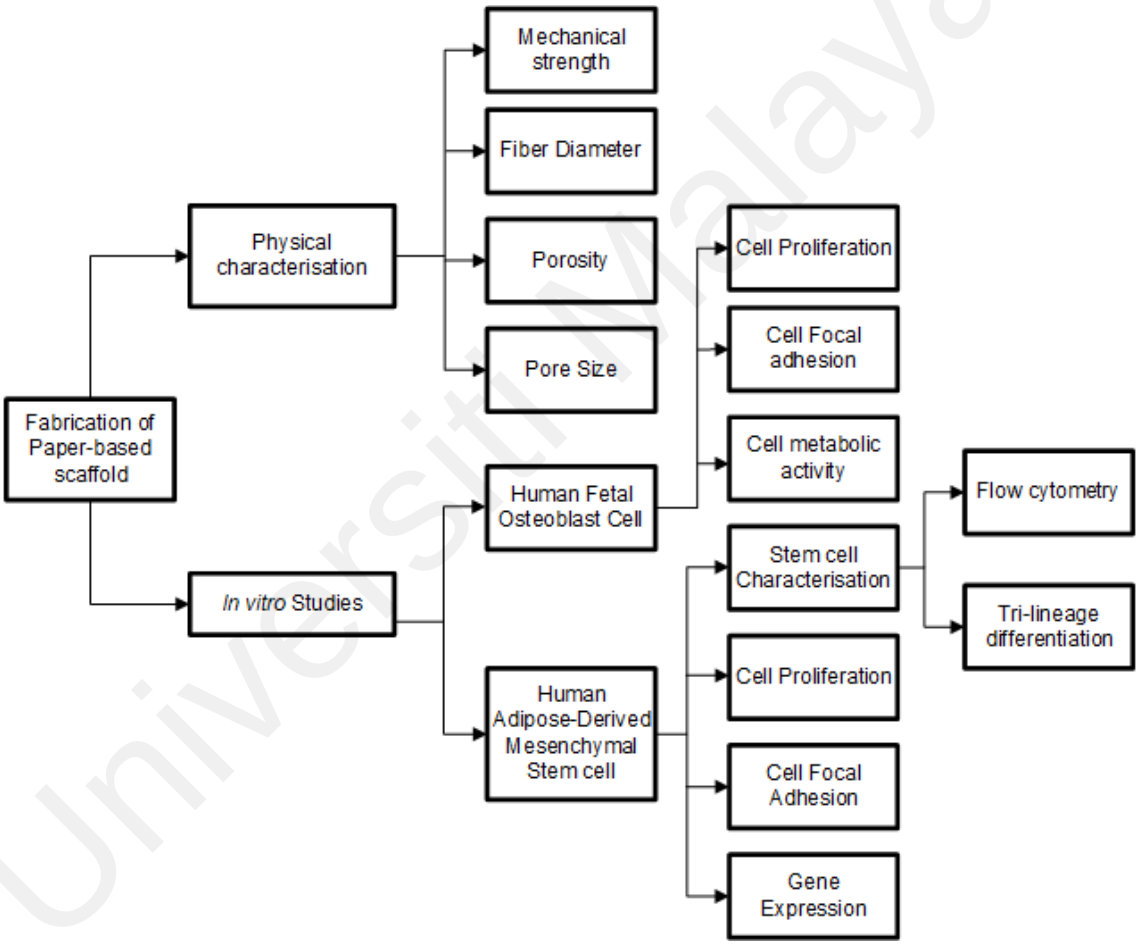

Figure 3. 1: Workflow diagram

3.2 Fabrication and characterisation of PCL/Paper scaffold

3.2.1 Dip-coating of filter paper (DFP)

Whatman filter papers (Whatman® grade 114) were cut into 1x1 cm^2 using a paper guillotine cutter. 10 wt.% PCL solution was prepared by dissolving PCL pellets (Sigma Aldrich, Mn=80000g/mol) in chloroform (Frinedemann Schmidt, Australia), and stirring with a magnetic stirrer for 2 hours to obtain a clear homogeneous solution. The cut filter papers were submerged in the PCL solution for approximately 3 seconds and then left to dry at room temperature overnight (Figure 3. 2 a).

3.2.2 Electrospinning of PCL on Filter paper (ES-PCL/FP)

In this experiment, Whatman filter papers (FP) were coated with PCL via electrospinning method. First, the spinning dope was prepared by dissolving PCL pellets (10% w/v) in a co-solvent mixture, comprising 9 volumetric parts chloroform and 1 volumetric part N, N-dimethylformamide DMF (Sigma Aldrich, USA). The PCL solution was prepared at room temperature in a condensed conical flask and placed on a magnetic stirrer to obtain a clear homogenous solution. The PCL solution was loaded into a 10 mL syringe (Terumo) with a 20 G blunt needle attached at the opening of the syringe and placed horizontally 18 cm from the aluminum collector. The feeding rate of the syringe pump (KD-100, KD Scientific Inc) was adjusted at 3 mL/h. A DC voltage of 12 kV (Gamma High Voltage Research, Ormond Beach, Florida, USA) was connected to the needle while a piece of filter paper (5x 5 cm^2) was placed on the aluminium collector (Figure 3. 2 b). The duration of the electrospin-coating was 30 minutes.

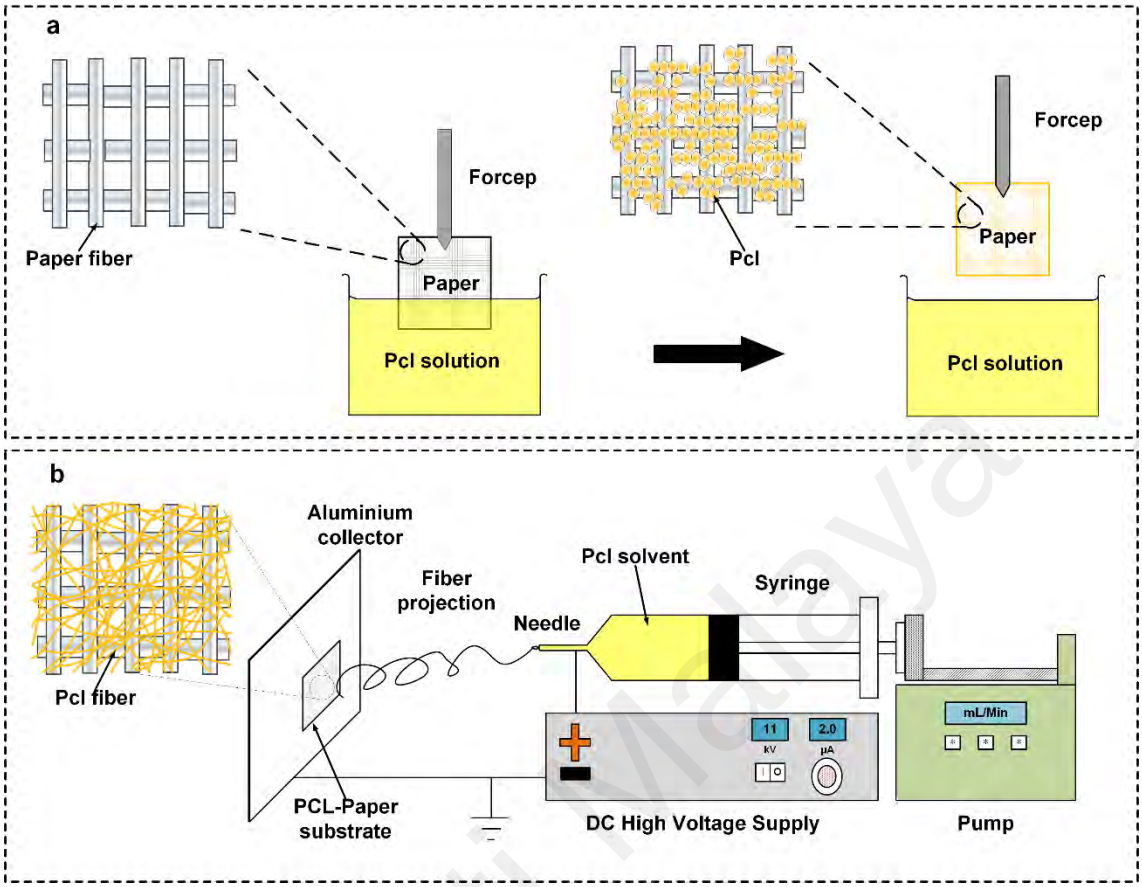

Figure 3. 2: Schematics of filter paper modification. a) Dip-coating of filter paper with PCL solution (DFP), b) Electrospinning of PCL on Filter paper (ES-PCL/FP)

3.2.3 Electrospun PCL (ES-PCL)

For the control study, only PCL sheets were produced, without paper. The PCL sheets were prepared using the same electrospinning device and the setup was identical to the preparation of ES-PCL/FP (refer to 3.2.2). The only difference was that there was no filter paper placed on the aluminium collector. 20 ml PCL solution was electrospun to obtain a scaffold with sufficient thickness for cell culturing.

In total there were four (4) type of scaffolds prepared for the entire studies. These scaffolds are 1) Filter paper (FP)(Control), 2) Electrospun PCL (PCL) (control for ES-PCL/FP), 3) Dip-coated Paper (DP) and, 4) Electrospun PCL on Paper (ES-PCL/FP).

3.2.4 Porosity measurement

The porosity of the scaffolds was measured using a Pycnometer (Marianela, Germany) based on the Archimedes Principle. Absolute ethanol (John Kollin Corporation, United Kingdom) was used as the medium, and gravimetric displacement of liquid was measured at room temperature [32]. The porosity of the scaffolds was calculated based on equation (3.1).

$$\text{Porosity}\ (\%) = \frac{W_2 - W_3 - W_\text{m}}{\rho_\text{e}} \Big/ \frac{W_1 - W_3}{\rho_\text{e}} \times 100 \qquad (3.1)$$

where W1 represents the weight of the pycnometer filled with absolute ethanol, W2 is the weight of the pycnometer filled with absolute ethanol and scaffold, W3 is the weight of the pycnometer and absolute ethanol when the ethanol-soaked scaffold had been taken out from W2, Wm is the dry weight of the scaffold, and ρ_e is the density of the absolute ethanol.

3.2.5 Medium sorption and retention test

This test was carried out to evaluate whether the prepared scaffolds have the ability to hold medium in a dry condition for a time interval. The scaffold was thoroughly dried in a fume hood for 24 hours and the weight was recorded as W_1. Subsequently, the scaffold was immersed in complete medium for 24 hours and the weight was recorded as W_2. The scaffold was then placed in a dry well plate and left in the incubator, and the incubator was set to 37 °C, 5% CO_2 and 95% relative humidity. The weight (W_2) of the scaffold was measured at time intervals of 24 hours until there were no changes in weight. The water absorption (W_R) at time t was calculated with the following equation:

$$\text{W}_\text{R} = \frac{\text{W}_2 - \text{W}_1}{\text{W}_1} \times 100\% \qquad (3.2)$$

3.2.6 Characterization of scaffold mechanical properties

These tests were carried out to evaluate whether different coating techniques have an effect on the mechanical properties of paper-based scaffolds, particularly their tensile strength. The tensile tests were carried out using an INSTRON 3345 device with a load of 100 N based on ASTM D 638. The specimens were punched to dumbbell-shaped geometries with dimensions of 50 mm x 9 mm (length x width). The support span length was set at 50 mm. The testing speed was set at 1 mm/min. The strain (ε) was evaluated as the ratio between the elongation of the specimen Δl and the original length l0 as shown in equation (3.2).

$$\varepsilon = \Delta l / l_0 \qquad (3.3)$$

3.2.7 Evaluation of Surface Morphology

The surface properties of a scaffold have a great influence on cellular responses such as cell proliferation, differentiation and protein synthesis. The coating is able to change scaffold surface properties. Field emission scanning electron microscopy (FESEM) (Carl Zeiss Auriga, Germany) is a great tool to view scaffold especially if the polymers fibers are in nano range. The scaffolds were sputter coated with gold and analysed under FESEM. For scaffolds which were seeded with cells, cell fixation must be conducted prior to gold coating. The fiber diameter and pore size were measured based on the obtained FESEM images using ImageJ software (version 1.48).

3.2.8 Contact angle measurements

Static contact angle was measured with Dataphysics Instruments (OCA 15EC, Filderstadt, Germany). The measurement was carried out at ambient condition with Sessile drop technique. Water was used as probe liquid; equal volume of water was added on different samples by using motor driven syringe. Image of the water droplet on different samples

was taken. Measurement of contact angle were done on the images of the water droplet on the samples (n=6) by using SCA software developed by Dataphysics Instruments (Filderstadt, Germany).

3.3 Cell Culture

3.3.1 Culture of Human Foetal Osteoblastic Cell Line (hFOB)

Human fetal osteoblastic cell lines (hFOB 1.19 No: CRL-11372, ATCC, USA), were used in this research study. HFOB cells were cultured in T-75 flasks (Thermo Fisher Scientific, USA) by using complete growth medium consist of Dulbecco's Modified Eagle's Medium (DMEM F12, Gibco™, USA) with 10% fetal bovine serum (#26140079, FBS, Gibco™, USA), and 1% Geneticin® (G418, Thermo Fisher, USA). The cryopreserved cell was thawed at a rapid rate (> 100℃/min) at 37℃ in a water bath until all ice disappear, rapid thawing is crucial to ensure high viability of cells. After thawing, the cell was washed with complete growth medium and centrifuge at 1800 rpm (K3 series, Centurion Scientific) for 5 minutes to separate the cell pellet from the supernatant liquid. The cell pellet was resuspended in complete growth medium and transferred to a 25cm^2 culture flask. The cells were cultured at 34 °C in a humidified (5% CO2, 95% air) atmosphere. When cells reached 90% confluence, cells were detached with Accutase® (#07920, Innovative Cell Technologies, USA). Cell suspension at a density of 5 ×10^6 cells/ml was prepared for further use. 10 µL of the cell suspension was seed onto each pre-soaked scaffold. The scaffolds were incubated for 2 hours. 1 ml of medium was micropipette into each well to submerge the scaffolds. Only passage 5 cells were used in this study.

3.3.2 Isolation and Culture of Adipose-derived Human Mesenchymal Stem Cell (ADMSC)

Infrapatellar human adipose tissue samples were collected from donors, age between 50-70, who undergo knee surgeries. Ethical approval was received from the Medical Ethics committee University of (Malaya (MECID NO:201993-7798, Appendix A). Samples collected from donors are adipose tissues that were normally discarded as clinical waste. Written consents were acquired from patients prior to surgery. Figure 3. 3 provides a brief intuition on the isolation and culture of ADMSCs. The harvested adipose tissues were washed with phosphate buffer saline (PBS) (Sigma Aldrich, St. Louis, USA), added with 1% of Penicillin-Streptomycin (Gibco, Waltham, Massachusetts, USA), to remove unwanted blood and impurities. A surgical blade was used to remove blood vessels and to mince adipose tissue into smaller pieces prior to enzymatic digestion. Equal volume of 0.1% (w/v) type I collagenase (#LS004196, Worthington, New Jersey) prepared in PBS were added to the minced adipose tissues as shown in Figure 3. 3. The mixture was placed in 37^{o}C 5% CO_2 incubator for an hour for thorough digestion. The digested adipose tissues were centrifuged at 1800 rpm for 5 min to separate the mixture into 3 fractions of digested tissue, which is adipose fraction, fluid portion and stromal vascular fraction (SVF) (Figure 3. 4c). SVF pellet were collected and suspended in ADMSC complete medium before transfer into culture flask. The ADMSC complete medium is composed of Dulbecco's Modified Eagle's medium (DMEM)/Ham F-12, 10% FBS, 1% glutamax (Gibco, Waltham, Massachusetts, USA), and 1% of Penicillin-Streptomycin (Gibco, Waltham, Massachusetts, USA). ADMSCs were cultured in a 5% CO_2 incubator (Galaxy® 170 R, New Brunswick Scientific, USA) at 37℃. To subculture cells, TrypLE express reagent (Gibco, Waltham, Massachusetts, USA) was added to dissociate the cells, and passage 2 cells were used for ADMSC characterization. The characterization tests include cell phenotyping (flowcytometry) and trilineage differentiation (histochemical staining).

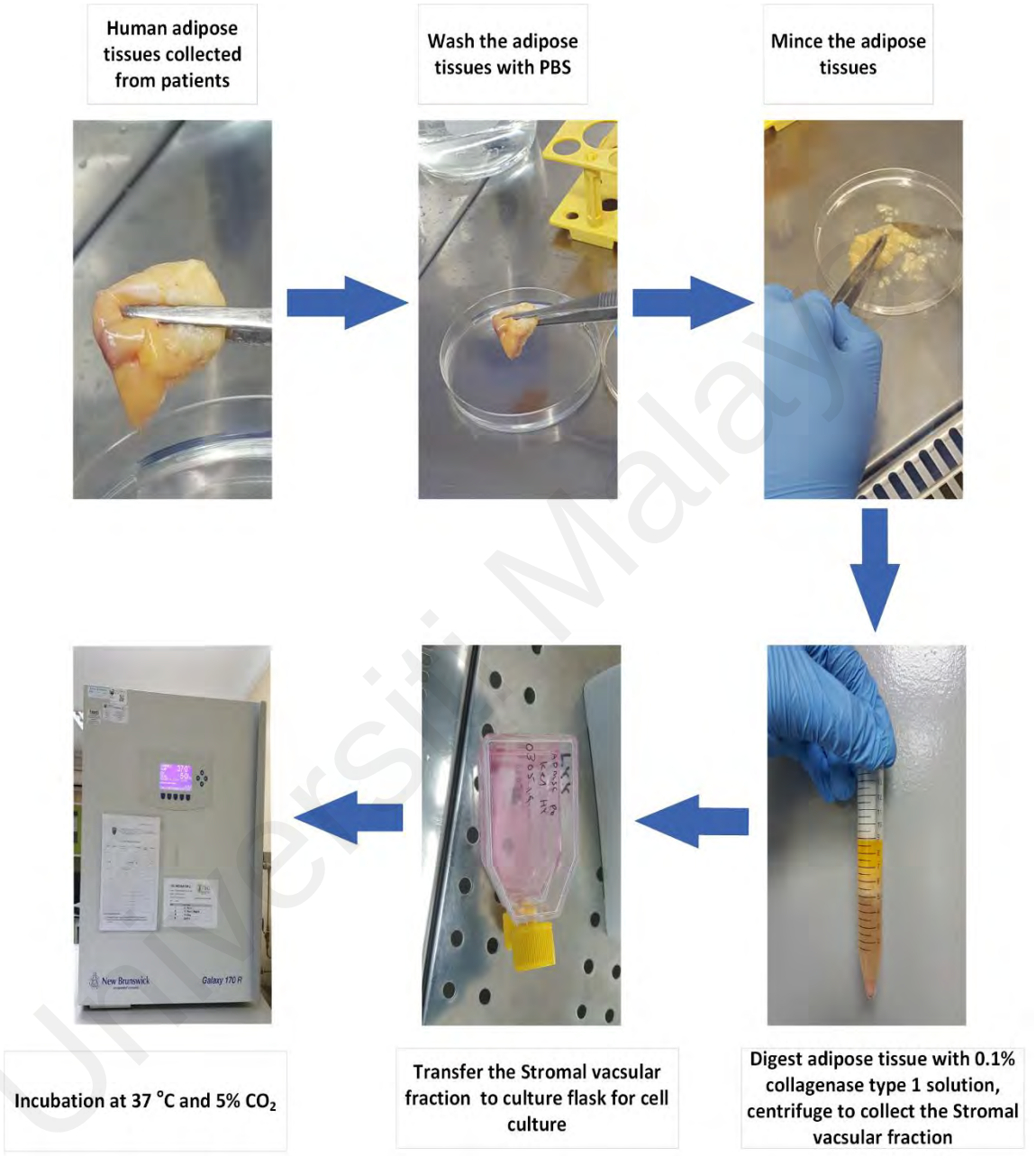

Figure 3. 3 : A flow chart of the procedure involved in ADMSC isolation and culturing

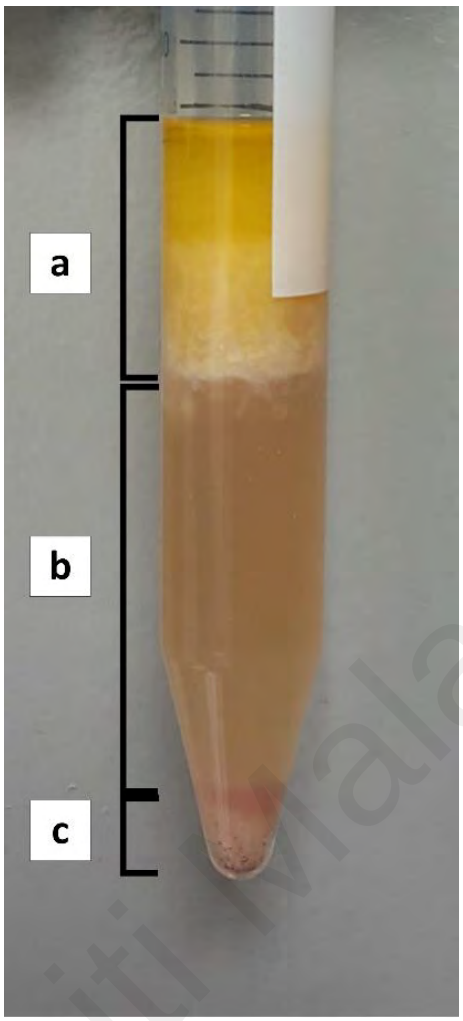

Figure 3. 4: Density gradient separation of ADMSCs. a) adipose fraction, b)fluid fraction c)Stromal Vascular Fraction (SVF)

3.3.3 Characterisation of ADMSCs

ADMSCs can be obtained from different parts of the human body, such as white adipose tissue in infrapatellar fat pad, and visceral adipose tissue in abdominal fat. Procedure of ADMSCs harvestation also differ from person to person. These differences become a barrier that hinders the exchange of experimental findings among researchers, and casts doubt on the credibility of experiment results. In the effort to promoting the interchange of data among researchers, The International Federation for Adipose Therapeutics and Science (IFATS) and the International Society for Cellular Therapy (ISCT) have proposed three minimal criteria for the characterisation of ADMSCs (Baer, 2014; Dominici et al., 2006). The first criteria to comply is, ADMSCs must be plastic-adherent when cultivated in tissue culture flask filled with standard ADMSC complete medium. The second criteria is, ADMSCs should express CD105, CD73, CD90(≥ 90%), and not express the hematopoietic markers CD14, CD34, CD45, CD19 and HLA-DR (≤ 2%). The third criteria to comply is, ADMSCs must have the ability to differentiate into cells of mesenchymal origin *in vitro*, such as adipocytes, chondrocytes, and osteoblasts, when exposed to specific growth signals.

3.3.3.1 Tri-lineage Differentiation of ADMSCs

As mentioned previously in Section 3.3.3, one of the criteria is that ADMSCs must have the ability to differentiate into cells of mesenchymal origin *in vitro*, such as adipocytes, chondrocytes, and osteoblasts, when exposed to specific growth signals. Tri-lineage differentiation study is a common test to evaluate ADMSCs ability to differentiate into cells of mesenchymal origin *in vitro.*

The tri-lineage differentiation study of isolated ADMSCs was performed by using StemPro chondrogenesis, osteogenesis, and adipogenesis differentiation kits (#A10071-01, #A10072-01, #A10070-01, Gibco, Waltham, Massachusetts, USA). The ADMSC

complete medium was prepared in accordance with the protocol provided by manufacturer, and the differentiation Basal Medium was added to Supplement in 9:1 ratio. 50µl Penicillin-Streptomycin (Gibco, Waltham, Massachusetts, USA) was added into the complete medium. ADMSCs at passage 2 were used in this characterisation.

I) Osteogenic Differentiation

ADMSC cell suspension at a density of 1 $\times 10^6$ cells/ml was prepared. 10 µl of cell suspension, approximately 10 000 cells, was added into each well of the 8 well Chamber Slide (Lab-Tek, Nunc, Roskilde, Denmark). The cells were cultured in ADMSC complete medium for three days prior to replacement with osteogenic differentiation medium. For the negative control well, ADMSC complete medium was used instead of osteogenic differentiation medium. After 21 days of incubation, the cells were fixed with 10% formalin solution (#HT501128, Sigma Aldrich, USA) for 30 minutes. The formalin was then discarded and the cells were rinse twice with PBS. Alizarin Red S powder (#A5533, Sigma Aldrich, USA) was used to prepare 1% (w/v) solution by dissolving in 1 g of the powder into 100ml of deionized water. Cells in each well were stained with 1% alizarin red S solution for 5 minutes at room temperature. Finally, the 1% alizarin red S solution was discarded and the cells in each well were rinsed with deionized water prior to observation under microscope for qualitative analysis.

II) Adipogenic Differentiation

ADMSCs cell suspension at a density of 1 $\times 10^6$ cells/ml was prepared. 10 µl of cell suspension, approximately 10 000 cells, was added into each well of the 8 well Chamber Slide (Lab-Tek, Nunc, Roskilde, Denmark). The cells were cultured in ADMSC complete medium for three days prior to replacement with adipogenic differentiation medium. For the negative control well, ADMSC complete medium was used instead of adipogenic differentiation medium. After 14 days of incubation, the cells were fixed with 10%

formalin solution (#HT501128, Sigma Aldrich, USA) for 30 minutes. The formalin was then discarded, and the cells were rinse with PBS. Isopropanol (60%) was added in and stand for 5 minutes. Cells in each well were stained with Oil Red O solution in 99% isopropanol for 10 minutes in room temperature. Finally, the Oil Red O solution in 99% isopropanol was discarded and the cells in each well were rinsed with deionized water prior to observation under microscope for qualitative analysis.

III) Chondrogenic Differentiation

The induction of chondrogenic differentiation used a micromass culture system. A ADMSC cell suspension at a density of 1×10^6 cells/ml was used to prepare for each cell pellet. The cell suspensions were centrifuged at 1600 rpm for 5 minutes to create the cell pellet. The conical tube containing the pellet was slightly loosen for gas exchange and placed in an incubator at 37ºC with 5% CO_2. The ADMSCs complete medium was changed every 2 days, the cell pellet was gently agitated to ensure formation of cell spheroid. After 28 days of incubation, the cell spheroid was gently washed with PBS to avoid rupture of the cell pellet, then the cells were fixed with 10% formalin solution (#HT501128, Sigma Aldrich, USA) for 30 minutes. The fixed cell pellet was then encapsulated with 4% agarose in a cylindrical mold to form a cylindrical specimen. The mold was cooled at 4 ºC for 2 hours to stabilise the dimension of the specimens. The specimens were sent for tissue processing overnight, which include the steps such as dehydrating in ascending concentrations of ethanol and clearing in xylene. Samples were then embedded in paraffin wax and sectioned at 5 μm using a microtome before being mounted on poly-L-lysine-coated glass slides. The sections were then processed for histologic evaluation to observe cartilage matrix by staining with 0.1% Safranin O solution for 5 min. The specimens were rehydrated in 95% alcohol for 5 times followed

by double immersion in absolute alcohol and being mounted onto coverslips with mounting reagent.

3.3.3.2 Flow Cytometry Assay

ADMSC cell suspension at a density of 1 $\times 10^6$ cells/ml was prepared. The cell suspension was placed in one centrifuge tube (15ml) and centrifuged at 1800 rpm for 5 minutes. The cells were resuspended with 1ml of stain buffer (#MAB554656, Becton Dickinson Biosciences, USA), and 500 µl of cell suspension - approximately 500 000 cells - was transferred to one microcentrifuge tube (5ml). A human MSC analysis kit (#PMG562245, Becton Dickinson Biosciences, USA) was used for immunophenotype characterisation of isolated ADMSCs. Cells were then incubated with antibodies labelled with fluorochrome as follows (Table 3. 1): hMSC Positive Cocktail (CD 105-PerCP-Cy5.5, CD 90-FITC, CD 73-APC), PE hMSC Negative Cocktail(CD 34-PE, CD 11b-PE, CD19-PE, CD 45- PE and HLA-DR PE), hMSC positive isotype control cocktail, PE hMSC negative isotype control cocktail, and single stains were added into each tube accordingly based on the technical data sheet. After 30 mins of incubation on ice in the dark, cells were washed and centrifuged with sheath fluid to remove unbound and residual antibodies. Finally, the cells were resuspended in 500 µL sheath fluid and analysed immediately using a flow cytometry system (BD Accuri™ C6 (BD FACSCanto II, Becton Dickinson Biosciences, USA)). For each tube, 10,000 events were acquired from each run. The data were then analysed using BD Accuri™ C6 software (Becton Dickinson Biosciences, USA).

Table 3. 1: Flow-cytometry antibodies and its description

Antibodies	Positive hMSC marker
CD73	ecto-50-nucleotidase
CD90	Thy-1 (T cell surface glycoprotein)
CD105	SH-2, endoglin
Antibodies	Negative hMSC marker
CD11b	integrin alpha M, protein subunit on lecukocytes
CD19	B-lymphocyte antigen
CD34	sialomucin-like adhesion molecule
CD45	leukocyte common antigen
HLA-DR	major histocompatibility class II antigens

3.4 In Vitro Study

Both human fetal osteoblast cells and human adipose-derived mesenchymal stem cells followed the subculturing and cell counting methods explained in the following subsection 3.4.1 and 3.4.2.

3.4.1 Subculturing of cell

Subculturing of cells was performed at 80-90% confluency. The culture medium in the culture flask was removed and PBS (5ml) was added in twice to rinse away the remaining medium. TrypLE express reagent or Accutase® was added, 1ml for 25 cm^2 flask and 4ml for 75 cm^2 flask, into culture flask until all the adherent cells were fully submerged. The culture flask was placed in the incubator for 3-6 minutes to allow the dissociation of attached cells on the culture flask. The flask was frequently check under microscope to observe the changes in morphology of the attached cells on flask. Once the attached cells

shrunk into a spherical shape while remaining attached to the flask, gentle tapping onto the culture flask was applied to assist detachment of cells. Complete medium containing FBS to the cell suspension to inhibit further enzymatic digestion was added. The cell suspension was transferred into a 15 mL centrifuge tube and centrifuged at 1800 rpm (K3 series, Centurion Scientific) for 5 minutes to separate the cell pellet from the supernatant liquid. The cell number was counted before the cell pellet was resuspended into the complete growth medium and transfer to 75cm^2 culture flask. The cells were cultured in a 5% CO_2 incubator at 37 °C. The cell counting procedure is explained in the next section.

3.4.2 Cells counting

A Neubauer haemocytometer was used to perform cell count and trypan blue was used for the exclusion viability testing. Prior to use, the mirror-like surface of Neubauer haemocytometer together with a cover slip must be cleaned by lens paper and ethanol. After the surface was dried, the cover slip was placed on top of the cell counting chamber on the Neubauer haemocytometer. Following from the previous section 3.4.1, after 5 minutes of centrifugation, the supernatant was removed and 1ml of complete medium was added into the cell pellet. A pipette was used to suck the cell suspension up and down in order to get a homogenous cell distribution in the solution before proceeding to cell counting. 20 µl of cell suspension was transferred to the microcentrifuge tube and mixed with equal volume of 0.4% w/v trypan blue solution. Trypan blue is a negatively charge dye that can penetrate the membrane of death cell and stain the cytoplasm into blue. The cell suspension was diluted at an appropriate volume to avoid formation of overlapping cell clusters. The cell suspension was pipetted to the edge of cover slip and allowed to wick into the gap between the cell counting chamber and the cover slip through capillary effect. The Neubauer haemocytometer was then viewed under a direct light microscope with 10X objective. The cell should not overlap on the grid, 90% of the cell should be free from contact with adjacent cell, otherwise, the test was repeated with a different

dilution factor. In this study, cell number was obtained from the 4 larger squares on the outer corner (Figure 3. 5). Viable cell density was calculated with the following formula:

$$\text{cells/ml} = \frac{\text{number of cells counted}}{\text{number of large square counted}} \times \frac{\text{volume of diluted mixture sample}}{\text{volume of original mixture sample}} \times 10\,000 \qquad (3.4)$$

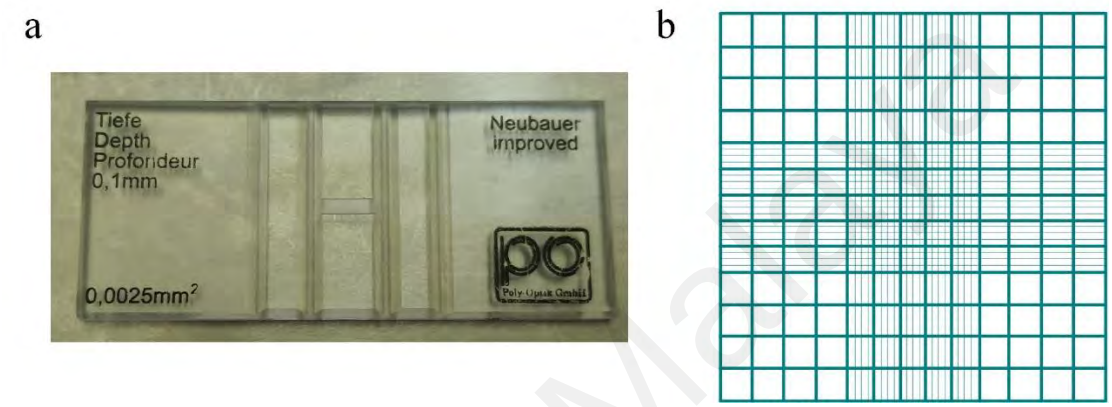

Figure 3. 5: Cell counting apparatus. a) haemocytometer and b) haemocytometer grid

3.4.3 Human Fetal osteoblast cell (hFOB) interactions with Scaffold

hFOBs were seeded on the scaffold at a density of $3x10^4$ cells/cm^2. At the designed time point (Day 1, Day 3, and Day 7), the quality of the cell growth, such as the cell proliferation, metabolic activity, and morphology, was investigated through different assays. Culture medium was changed every 2 days by using complete medium stated herein, unless otherwise stated.

3.4.3.1 Cell adhesion and morphology

The cell adhesion and morphology studies were conducted at time points 1, 3, and 7 days. FESEM (Carl Zeiss Auriga, Germany) was used to observe the cell adhesion and morphology. The scaffolds seeded with cells were washed 3 times in PBS and fixed with 2.4% glutaraldehyde solution (Sigma Aldrich Co.) for 24 hours. After fixing, the

specimens were washed 3 times again with PBS, and placed through a series of graded ethanol solutions for dehydration (30%, 50%, 70%, 90% and 100%) for 10 min each. The scaffolds were placed overnight in a freeze dryer (FreeZone, Labconco, USA) to remove excess liquid prior to sputter coating. The scaffolds were coated with an ultra-thin coating of electrically conducting metal (gold/palladium (Au/Pd)) to improve the scaffold conductivity and avoid build-up of charge due to the accumulation of static electric field. The coated scaffolds were mounted on stud holder by using conductive carbon tape prior to FESEM viewing. The FESEM imaging was performed at 10kV and working distant of 9.1mm.

3.4.3.2 Cell Proliferation

The cell proliferation can be accessed via a Resazurin Reduction assay. The Resazurin Reduction assay quantitatively measured cell proliferation by using a redox indicator. The nonfluorescent resazurin dye (blue) was reduced by cellular mitochondrial enzyme to resorufin that emits red fluorescence. The intensity of red fluorescence was measured via absorbance in a spectrophotometer microplate reader, and the resorufin optical density was taken as the measurement of cellular activity. The Resazurin Reduction assay was performed at three time points, 1, 4, and 7 days. The Resazurin Stock solution was prepared by dissolving 140 mg of Resazurin powder (Sigma-Aldrich, USA) into 1000 ml of phosphate buffer saline (PBS) (Sigma-Aldrich, USA). Resazurin working solution was prepared by mixing stock solution with PBS at a volumetric ratio of 1:9. The Resazurin working solution at 1 ml was added into each well containing scaffold seeded with cells. The 6 or 12 well plates were incubated for 4 hours at 34 °C in a 5% CO_2 incubator for the conversion of resazurin to resorufin. Triplicates of 100 mL of the Resazurin working solutions were aspirated from each well contained scaffold seeded with cells. Resorufin optical densities were then measured using a microplate reader (FLUOstar OPTIMA,

BMG Labtech, GmbH, Ortenberg, Germany) at an absorbance wavelength of 570 nm, and 595 nm set as the reference wavelength. Unseeded scaffolds were incubated under the same conditions in resazurin working solution as blanks and absorbance values were calculated accordingly.

$$\text{Resazurin reduction (\%)} = \frac{(\varepsilon_{ox}\lambda 2)A\lambda 1 - (\varepsilon_{ox}\lambda 1\ )A\lambda 2}{(\varepsilon_{red}\lambda 1)A'\lambda_2 - (\varepsilon_{red}\lambda 2)A'^{\lambda_1}} \times 100 \quad (3.5)$$

$\varepsilon_{ox}\ \lambda_2$ = molar extinction coefficient of alamar blue oxidized form at 600nm
$\varepsilon_{ox}\ \lambda_1$ = molar extinction coefficient of alamar blue oxidized form at 570nm
$\varepsilon_{red}\ \lambda_2$= molar extinction coefficient of alamar blue reduced form at 600nm
$\varepsilon_{red}\ \lambda_1$= molar extinction coefficient of alamar blue reduced form at 570nm
$A\lambda_2$= absorbance value of test wells at 600nm
$A\lambda_1$= absorbance value of test wells at 570nm
$A'\lambda_2$ = absorbance of negative control well at 600nm
$A'\lambda_1$ = absorbance of negative control well at 570nm

3.4.3.3 Cell viability

The Live/Dead Viability/Cytotoxicity Kit (Life Technologies, USA) measures the cell viability based on the integrity of cell membranes. Scaffolds seeded with cells were supplemented with 10 µL of PBS mixture containing calcein-AM and ethidium homodimer-1 in a 1:4 ratio and incubated for 20 minutes at room temperature. The scaffolds were immersed in PBS for 10 minutes prior to laser confocal viewing. Laser confocal microscopy (Leica TCS SP5, Germany) was used to capture the fluorescence images. 3 different areas on the scaffolds were scanned and the images were captured for further analysis.

3.4.3.4 Alkaline Phosphatase (ALP) assay

The Alkaline phosphatase kit (Life Technologies, USA) is used to measure the metabolic activity of hFOB. The activity of alkaline phosphatase (ALP) indicated the presence of osteoblast cells and the formation of new bone. The measurement of ALP

activity in biological samples was done by using p-nitrophenyl phosphate (pNPP), a phosphatase substrate which turned yellow upon dephosphorylation by ALP.

In the ALP detection assay, pNPP substrate was incubated with cell lysate. If there was ALP present in the cell lysate, they converted the pNPP substrate to p-nitrophenol. It was necessary for the cells to be lysed to detect the presence of ALP. Cell seeded sample scaffolds were immersed in 250 µl M-Per mammalian protein extraction and left in the incubator for 10 minutes to allow cell lysis. To prepare pNPP solution, 2 pNPP tablets were dropped into 10 ml of 1 X diethanolamine substrate buffer in a 50 ml centrifuge tube and vortexed until the pNPP tablets completely dissolved. After 10 minutes, cell lysate from each scaffold was transferred into a labelled 1.5 ml microcentrifuge tube and centrifuged at 15000 rpm for 5 minutes using Gryozen 1730MR Refrigerated Benchtop Microcentrifuge. Then, 50 µl of supernatant was taken from each microcentrifuge tube and transferred into a 96 well plate. Subsequently, 150 µl pNPP solution was topped up to each well to obtain a 200ul mixture. The 96 well plates containing the supernatant/pNPP mixture were incubated for 30 minutes at 34 °C in a 5% CO2 incubator, follow by intermediate shaking before placing the 96 well plate into the multiplate reader. The p-nitrophenol concentration was measured using FluoStar Omega Multiplate Reader at 405 nm wavelength. The absorbance reading of p-nitrophenol concentration is recorded and compare with the absorbance versus p-nitrophenol concentration standard curve.

3.4.4 Adipose Derived Mesenchymal Stem Cells (ADMSCs)

ADMSCs were seeded on scaffold with the cell density of $3x10^4$ cells/cm^2. At the designed time point (Day 1, Day 3, and Day 7), the quality of the cell growth, such as cell proliferation, metabolic activity, and morphology, was investigated through different assays. The ADMSC complete medium was changed every 2 days with complete medium stated herein, unless otherwise stated. The osteogenic potential of scaffolds was

investigated through quantitative reverse-transcription polymerase chain reaction (RT-qPCR).

3.4.4.1 Cell adhesion and morphology

The cell adhesion and morphology studies were conducted at time point of day 1, 3, and 7. FESEM was used to observe the cell adhesion and morphology. The scaffolds seeded with cells were washed 3 times in PBS and fixed with 4% glutaraldehyde solution (Sigma Aldrich Co.) for 24 hours. After fixing, the specimens were washed 3 times again with PBS, placed through a series of graded ethanol solutions for dehydration (30%, 50%, 70%, 90% and 100%) for 10 min each. The scaffolds were placed overnight in a freeze dryer (FreeZone, Labconco, USA) to remove excess liquid prior to sputter coating. The specimens were sputter coated with an ultra-thin coating of electrically conducting metal (gold/palladium (Au/Pd)) to improve the scaffold conductivity and avoid build-up of charge due to accumulation of static electric field. The coated scaffolds were mounted on a stud holder by using conductive carbon tape prior to FESEM viewing.

3.4.4.2 Cell Proliferation

The Resazurin Reduction assay was performed at three time points of day 1, 4, and 7. Resazurin Stock solution was prepared by dissolving 140 mg of Resazurin powder (Sigma-Aldrich, USA) into 1000 ml of phosphate buffer saline (PBS) (Sigma-Aldrich, USA). Resazurin working solution was prepared by mixing stock solution with PBS at a volumetric ratio of 1:9. 1ml of Resazurin working solution were added into scaffolds seeded with cells and left in the 5% CO_2 incubator at 37 °C for 4 hours for the conversion of resazurin to resorufin. Triplicates of 100 mL of Resazurin working solution from each scaffold were taken for absorbance measurements. The optical densities were then measured using a microplate reader (FLUOstar OPTIMA, BMG Labtech, GmbH, Ortenberg, Germany) at an absorbance wavelength of 570 nm, with 595 nm set as the

reference wavelength. Unseeded sterilized scaffolds were incubated under the same conditions in resazurin working solution as blanks and absorbance values were calculated accordingly.

$$\text{Resazurin reduction (\%)} = \frac{(\varepsilon_{ox}\lambda 2)A\lambda 1 - (\varepsilon_{ox}\lambda 1\ )A\lambda 2}{(\varepsilon_{red}\lambda 1)A'\lambda_2 - (\varepsilon_{red}\lambda 2)A'^{\lambda_1}} \times 100 \qquad (3.7)$$

Ɛox λ2 = molar extinction coefficient of alamar blue oxidized form at 600nm
Ɛox λ1 = molar extinction coefficient of alamar blue oxidized form at 570nm
Ɛred λ2= molar extinction coefficient of alamar blue reduced form at 600nm
Ɛred λ1= molar extinction coefficient of alamar blue reduced form at 570nm
Aλ2= absorbance value of test wells at 600nm
Aλ1= absorbance value of test wells at 570nm
A'λ2 = absorbance of negative control well at 600nm
A'λ1 = absorbance of negative control well at 570nm

3.4.4.3 Cell viability

The Live/Dead Viability/Cytotoxicity Kit (Life Technologies, USA) measures the cell viability based on the integrity of cell membranes. Scaffolds seeded with cells were supplemented with 10 µL of PBS mixture containing calcein-AM and ethidium homodimer-1 in a 1:4 ratio and incubated for 20 minutes at room temperature. The scaffolds were soaked in PBS for 10 minutes prior to laser confocal viewing. Laser confocal microscopy (Leica TCS SP5 II, Germany) was used to capture the fluorescence images. 3 different areas on the scaffolds were scanned and the images were captured for further analysis.

3.4.4.4 Cytoskeleton assessment

Interaction between cells and materials is an important process that dictates stem cell fate, where the formation of actin filaments could affect various cell-signalling pathways and subsequent stem cell fate. In order to stain F-actin, scaffolds seeded with cells were loaded with Alexa Fluor™ 488 Phalloidin (#A12379, Thermo Scientific, USA). The

nuclei were stained using DAPI. The stains used in this assessment needed to be prepared before the staining commences, to ensure a fully dissolved working solution that is able to give the best staining result. The BSA blocking buffer (1%) was prepared by dissolving 1 gram of bovine serum albumin (#0322, Amresco, Belgium) into 100 mL of PBS. The 0.1% Triton-X100 working solution was prepared by diluting 0.1ml of Triton-x100 stock solution (#85111, Thermo Scientific, USA) with 100 ml of PBS. Phalloidin conjugated with AlexaFlour 488 was diluted with PBS into working solution with a concentration of 12.5 µL/ml. DAPI solution was diluted with PBS into working solution with a concentration of 1 µL/ml. The cytoskeleton assessment was ready to commence once the working solution is vortexed homogeneously.

Before viewing the cytoskeleton, the scaffolds seeded with cells were washed 3 times in PBS and fixed with 4% glutaraldehyde solution (Sigma Aldrich Co.) for 24 hours. After fixation, the scaffolds were rinsed twice with PBS and permeabilized with 0.1% Triton X-100 for 15 minutes at room temperature. The scaffolds were rinsed twice with PBS. The 1% bovine Serum Albumin (BSA) blocking buffer was added in the scaffold for 30 minutes at room temperature. The scaffolds were rinsed twice with PBS to totally remove the blocking buffer. Phalloidin solution was added into the samples for 60 minutes at room temperature. The scaffolds were rinsed twice with PBS, followed by the incubation of scaffolds in DAPI for 10 min at room temperature before the scaffolds were observed with confocal laser scanning microscope (Leica TCS SP5 II, Germany).

3.4.4.5 Gene Expression

The purpose of this experiment is to assess which type of the scaffolds have an osteoinductive effect on ADMSCs. In this experiment, ADMSCs were seeded on the prepared scaffolds and cultured in osteogenic medium (#A10072-01, Gibco, Waltham, Massachusetts, USA). The primers for osteo-lineage genes (runt-related transcription factor 2 (RUNX2), alkaline phosphatase (ALP), type 1 collagen (COL_1), bone gamma-carboxyglutamate protein (BGLAP)) and housekeeping reference gene (Glyceraldehyde 3-phosphate dehydrogenase (GAPDH)) were procured from First BASE laboratories (Table 3. 2).

Table 3. 2: Primers used in RT-qPCR.

Gene	Sequence 5'-3'	length
RUNX2	F: CTA GGC GCA TTT CAG GTG C R: CTG GGC CAC TGC TGA GGA ATT T	F:19 R:22
BGLAP	F:GGA GGG CAG CGA GGT AGT GAA GA R:GCC TCC TGA AAG CCG ATG TGG T	F:23 R:22
ALP	F:GAT GTG GAG TAT GAG AGT GAC G R:GGT CAA GGG TCA GGA GTT C	F:22 R:19
COL_1	F:CCC GCA GGC TCC TCC CAG R:AAG CCC GGA TCT GCC CTA TTT AT	F:18 R:23
GAPDH	F:GCC CCC TCT GCT GAT GGC C R:GGG TGG CAG TGA TGG CAT GGA	F:19 R:21

a) RNA Extraction

In order to run gene expression, the RNA from the cells which were previously seeded on the scaffolds need to be extracted. Blood/Cultured Cell Total RNA Mini Kit (FAVORGEN Biotech Corporation, Ping-Tung, Taiwan) was used for the RNA extraction in this study. Prior to RNA extraction, the working solution was prepared from wash buffer 2 stock solution added with equal volume (750ml) of molecular grad absolute ethanol (# E7023, Sigma Aldrich, USA). To detach cells from scaffolds, 1ml of accutase was added into the sample and follow by shaking (200rpm) for 30 minutes. The cell suspensions were placed in a centrifuge tube (15ml) and centrifuge at 1800 rpm for 5 minutes. Supernatants were

aspirated and PBS was added-in before transferring to the microcentrifuge tube. The cell suspensions were centrifuge at 1800 rpm for 5 minutes again. The supernatants were removed, and the cell pellets were subject to snap-freezing before being stored in a -80 ºC freezer.

The frozen pellets were thawed rapidly in 37 ºC water bath. The cell pellets were spun for the aspiration of excess liquid in the microcentrifuge. 350 µl of FARB Buffer and 3.5 µl of ß-Mercaptoethanol were added to each cell pellet, follow by vigorous vortexing for approximately 1 minutes. The sample mixtures were transferred to filter column (placed on collection tube) and centrifuge at 13,000 rpm for 2 minutes. All the centrifugation from this point onwards were done in -4 ºC and at 13,000 rpm. The clarified supernatant was transferred from the collection tube to microcentrifuge tube, and an equal volume of RNase-free ethanol (70 %) was added, followed by vortexing. The ethanol added sample mixtures were transferred to farb minicolumn (placed on collection tube), and centrifuge for 1 minutes. Flow-through liquid in the collection tube was discarded, 500 µl of Wash Buffer 1 added to the FARB Mini Column and centrifuged for 1 min. Flow-through liquid in the collection tube was discarded, 750 µl of Wash Buffer 2 added to the FARB Mini Column and centrifuged for 1min, this step being repeated twice. The FARB Mini Columns were centrifuge for an additional 3 min to completely remove excess liquid. 50 µl of RNase-free deionized water was added directly on the membrane center of the FARB Mini Column (placed on elution tube) and stood for 1 minutes. The FARB Mini Columns were centrifuged for 1 min to elute RNA. The eluted RNA mixtures were stored in -80 ºC freezer for later use.

b) cDNA conversion

The RNA purity and concentration were measured with the Nanodrop 2000 spectrophotometer (Thermo Scientific) absorbance reading at 260 nm and 280 nm wavelengths. The measurement started with setting the standard for 'blank'. 2 µL of the RNase free water was placed on the lower measurement pedestal and sampling arm was lowered to set the 'blank'. The same step was repeated by using 2 µL of the eluted RNA mixture. Both the upper and lower measurement pedestals were gently cleaned with Kim wipe paper after each measurement. RNA samples with high purity (A260/280>1.8) were used for the subsequent cDNA conversion.

The qPCRBIO cDNA Synthesis Kit (PCR Biosystems, UK) was used to convert the extracted RNA to cDNA. Total RNA samples with concentration of 400 ng each were diluted to a mastermix (reaction volume) of 20 µL containing, 4µL of 5x cDNA Synthesis Mix, 1µL 20x RTase, 13µL RNase free water, and 2 µL of eluted RNA mixture. The mastermix was incubated using a C1000 Thermal cycler (Bio-Rad Laboratories Inc, USA), under thermal cycling conditions as follows: incubation at 42°C for 30 minutes, followed by heat inactivation at 85°C for 10 minutes to denature RTase.

c) Reverse transcription-quantitative polymerase chain reaction (RT-qPCR)

RT-PCR were performed using 2x qPCRBIO SyGreen Blue Mix (PCR Biosystems, UK), and CFX Connect Real-Time PCR Detection System (Bio-Rad Laboratories Inc, USA). Briefly, each reaction volume of 20 µl contained 0.5 µl (100 ng) of cDNA, 0.8 µl of forward primer, 0.8 µl of reverse primer, 7.9 µl ultrapure water and 10 µl SyGreen Blue Mix. The reaction mix was then dispensed into PCR plates and subjected to a cycling program in the CFX Connect Real-Time PCR Detection System. The cycler conditions were set up as follows: initial activation step at 95 °C for 2 minutes, denaturation at 95

°C for 5 seconds, and annealing/extension at 60 °C for 30 seconds. The gene expression level of the control group was normalized to 1.

Table 3. 3shows the summary of Master mix composition for RT-qPCR reaction.

The expression of target genes was normalised to the expression of endogenous control gene. The relative quantities of expressions were calculated using the comparative CT approach. Also, the changes in osteogenic gene expression were shown relative to the control samples. The gene expression level of the control group was normalized to 1.

Table 3. 3: Master mix composition for RT-qPCR reaction

Reagent	volume
2x qPCRBIO SyGreen Blue Mix	10µl
Forward primer (10µM)	0.8µl
Reverse primer (10µM)	0.8µl
cDNA	0.5µl
RNase free water	7.9µl
Total volume per reaction	20.0µl

3.5 Medium deprivation test

This test was performed to evaluate the viability of cells in the scaffold, given that it only holds a limited amount of medium, which will diminish over time. ADMSCs were seeded on the sterilized scaffold with a cell density of 3x104 cells/cm^2. The cell seeded scaffold was left to stand for 2 hours to allow the anchoring of cell onto the scaffold. Subsequently, the scaffold seeded with cells was put into a reservoir of medium for 1 minute to allow the absorption of the medium. Then, the scaffold was transferred to a dry well and placed into a 5% CO2 incubator at 37 °C. At the designed time interval of 24 hours, the quality of the cell growth, such as cell proliferation and cell viability, was accessed by using Resazurin Reduction assay and Live/Dead Viability. The percentages of live cells and dead cells were measured using ImageJ software (version 1.48).

3.6 Statistical analysis

For statistical analysis of biochemical assay results, a minimum of six technical replications (N=6) were used for each group of samples. Data were tested by one-way ANOVA with Turkey post hoc test using IBM SPSS version 23 software (SPSS Inc., Chicago, IL, USA). P-values less than 0.05 ($p<0.05$) were reported as statistically significant.

CHAPTER 4: RESULTS AND DISCUSSION

4.1 Introduction

Paper has recently found widespread application in biomedical fields, especially as an alternative scaffolding material for cell culture owing to its properties, such as fibrous nature, porosity, and flexibility. However, paper on its own is not an optimal material for cell culture, as the architectural structure of paper is similar but not fully identical to the ECM structure, thus modification of paper is necessary to make it a physiologically relevant scaffolding material. The present study focuses on modification of filter paper through electrospin-coating and dip-coating with polycaprolactone (PCL), a promising biomaterial in tissue engineering. This chapter presents the results of cellular morphological analysis, evaluation of cell (hFOB and ADMCSs) viabilities, osteoblast alkaline phosphatase (ALP) activity, live/dead assays for hFOB and ADMCSs and ADMSCs differentiation.

4.2 Morphology and structural characterization of PCL/Paper scaffold

FESEM was used to study the morphologies of 4 different types of scaffolds, namely, electrospun PCL on metal collector PCL (ES-PCL) (Figure 4. 1a), electrospun PCL on filter paper (ES-PCL-FP) (Figure 4. 1b), Filter Paper (FP) (Figure 4. 1c) and dip-coated Filter Paper (DFP) (Figure 4. 1 d**)**. These FESEM images (3000x magnification) were taken using 5.0 kV at working distance of 9mm. The data of the fiber diameters is based on 50 measurements per samples. The histogram of fiber diameters analysis shows that the fiber diameter varies between different modification methods and types of collectors. PCL electrospun on metal collector (ES-PCL) shows an average diameter of 0.79 μm, while PCL electrospun on filter paper shows an average diameter of 0.17 μm. With FP serving as the collecting platform during electrospinning, the produced PCL fibers diameters have reduced by approximately 75% (Figure 4. 1 b). Using filter paper as the

collecting platform helps the removal of solvent from the electrospinning jet, through an adsorption of excess solvent and facilitation of evaporation. Other studies reported that a higher rate of solvent removal leads to formation of fibers with smaller diameters. For example, It has been reported that the porosity of the collector can affect the morphology of the deposited fibers (H. Q. Liu & Y. L. Hsieh, 2002). Porous surfaces such as paper can affect the packing density of the deposited nanofibers as well as lead to faster evaporation of residual solvents due to their higher surface area. Paper has the capability of absorbing liquid through capillary action, owing to its porous structure, which is able to absorb the residual solvent from the deposited fiber spun on the paper (K. Ng et al., 2017). Wannatong *et al.* (2004) also reported that high boiling point solvents such as DMF, when used in electrospinning, could result in the formation of wet fibers on the collector, and that an increase in the evaporation rate of the solvent improved the morphology. Another group reported that the wicking capability and high surface area properties of paper greatly facilitate the solvent removal. The diffusion of solvent out of the porous paper layer, along with the wicking and capillary action could exert a pulling force that could further stretch the fiber to a finer diameter (H. Liu & Y. L. Hsieh, 2002).

Dip-coating is another modification method used in this study, where DFP paper-based scaffold was produced by submerging a FP in a 10 wt.% solution of PCL in chloroform (Figure 4. 1 d). DFP has a similar morphology to FP (Figure 4. 1 c), however, there was a small difference in fiber diameter. FP has an average fiber diameter of 23.93 μm while DFP has an average fiber diameter 20.85 μm, a reduction of 12% in fiber diameter. A layer of PCL solution adheres and coats on the fiber of FP amidst the dipping process. Solidification of the PCL coating on FP fiber is accompanied by a dimensional shrinkage that would compress the cellulose fiber and results in a smaller diameter. Francis et al. mentioned that solidification of polymer is often accompanied by shrinkage due to the coating stress developed during processing. The anchoring of polymer coating on a rigid substrate constrains the in-plane stress relaxation of polymer, causing the accumulation

of in-plane stress that will lead to polymer shrinkage upon solidification (Lei et al., 2002). Other studies reported that solvent molecules in polymer solution increase the hydrodynamic volume as it diffuses through the polymer matrix. The evaporation of solvent upon the solidification process reduces the hydrodynamic volume and results in dimensional shrinkage (Su, 2013).

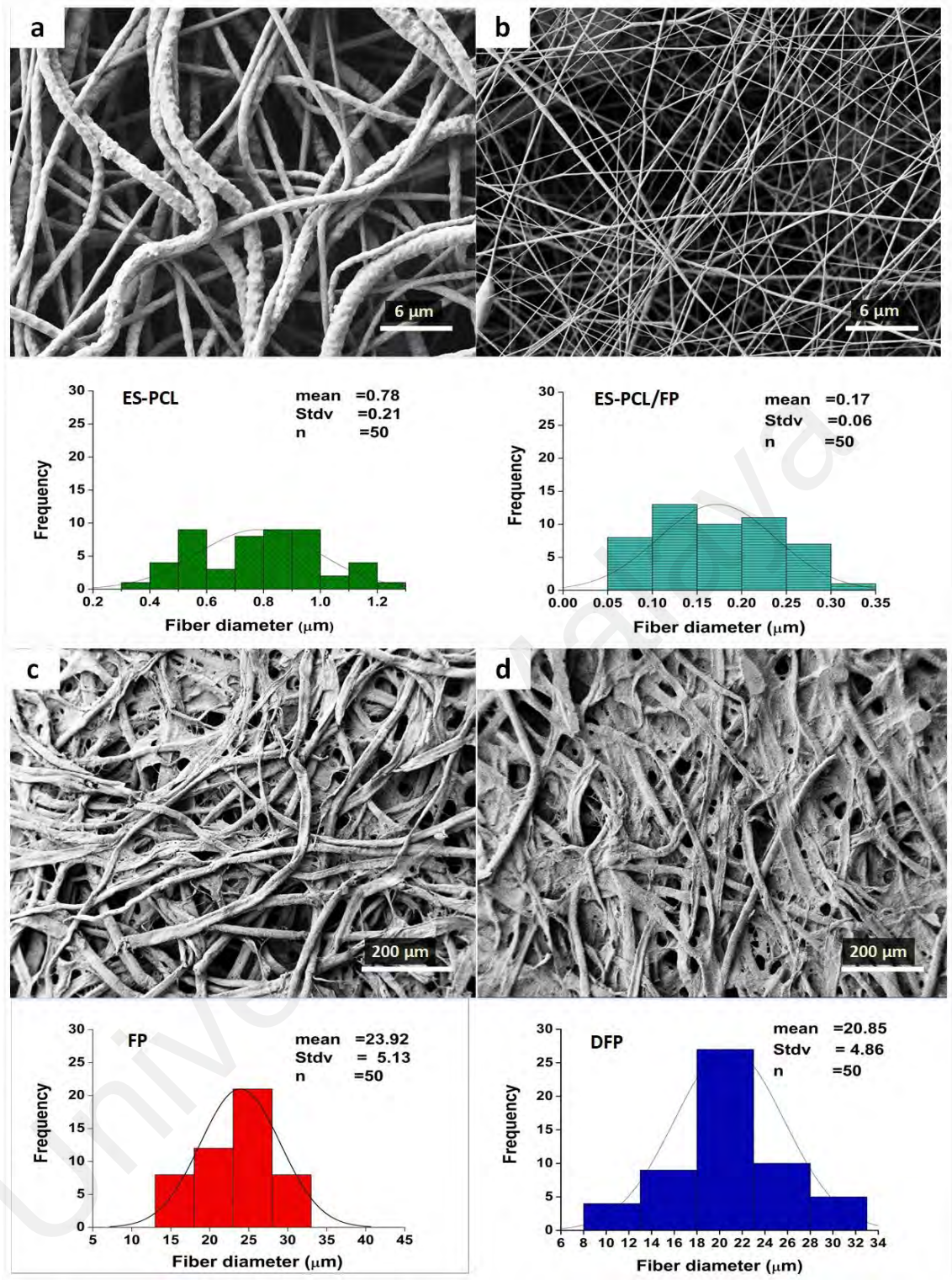

Figure 4. 1: Scaffold morphological analysis**.** FESEM microscopy (plan-view) of (a) ES-PCL, (b) ES-PCL/FP, (c) FP, and (d) DFP of their relevant fiber diameter distribution pattern

4.2.1 Macroscopic dimension (cross-section)

Figure 4. 2 shows the cross-sectional morphology of the scaffolds of ES-PCL, ES-PCL/FP, FP, and DFP. These images show that whilst the bulk architecture properties of all the scaffolds are similar in many aspects, all the scaffolds have a fibrous, porous and interwoven architectural structure. The images of ES-PCL show a more uniform distribution of pores and diameter in its highly porous structure (Figure 4. 2 a), which is typical in electrospun PCL scaffolds (A. Cipitria et al., 2011). Conversely, the pore size and fiber diameter of ES-PCL/FP scaffold varies throughout the structure (Figure 4. 2 b), and it can be observed that there are two layers with distinct architecture structure in the cross-section area (as show by the circle). As mentioned in section 4.2, the fabrication of ES-PCL/FP scaffold involves electrospinning a thin layer of PCL nanofiber (170 nm) on to filter paper with an average fiber diameter of 23.93 μm. These layers form a bimodal scaffold that has the topographical features of both nano and micro fibrous scaffold in the aspects of pores and fiber diameter. Young et al. mentioned that the porosity and fiber diameter of ECM, on the nano and micro scale, are important criteria in the design of tissue specific scaffold. This hierarchical structure of ES-PCL/FP scaffold closely resembles the fibrillar ECM construct in real organs, that is comprised of various macromolecules with sizes ranging from micro to nano scale (Mouw et al., 2014). The ECM mimicking features of ES-PCL/FP has a substantial impact towards determining cellular behaviour and cell fate, which will be discussed in later section. As shown in the circled area of Figure 4. 2 b, the brush-like fibrous PCL fiber on top bound tightly with the paper layer at the bottom, with no visible void or gap in the interface. This good interface is attributed to the solvent diffusion process which exert a force that would pull the fibre toward the paper to form a tightly bind structure (H. Liu & Y. L. Hsieh, 2002). Figure 4. 2 c shows the cross-sectional area of FP. It can be observed that the surface of the FP is rougher compared to DFP, hair-like cellulose fibers are visible on bigger struts (as shown in the circle) and the pores between the cellulose struts are clearly visible (as

shown by the arrow). DFP is FP covered with PCL coating, and the overall structure is rather similar between them, except for the surface and the pore size (Figure 4. 2 d). The PCL coated DFP shows a smoother surface and less hair-like cellulose fibers (show in the circle, Figure 4. 2 d), with the pore between the cellulose strut being partially covered up by the polymer (as shown by arrow, Figure 4. 2 d).

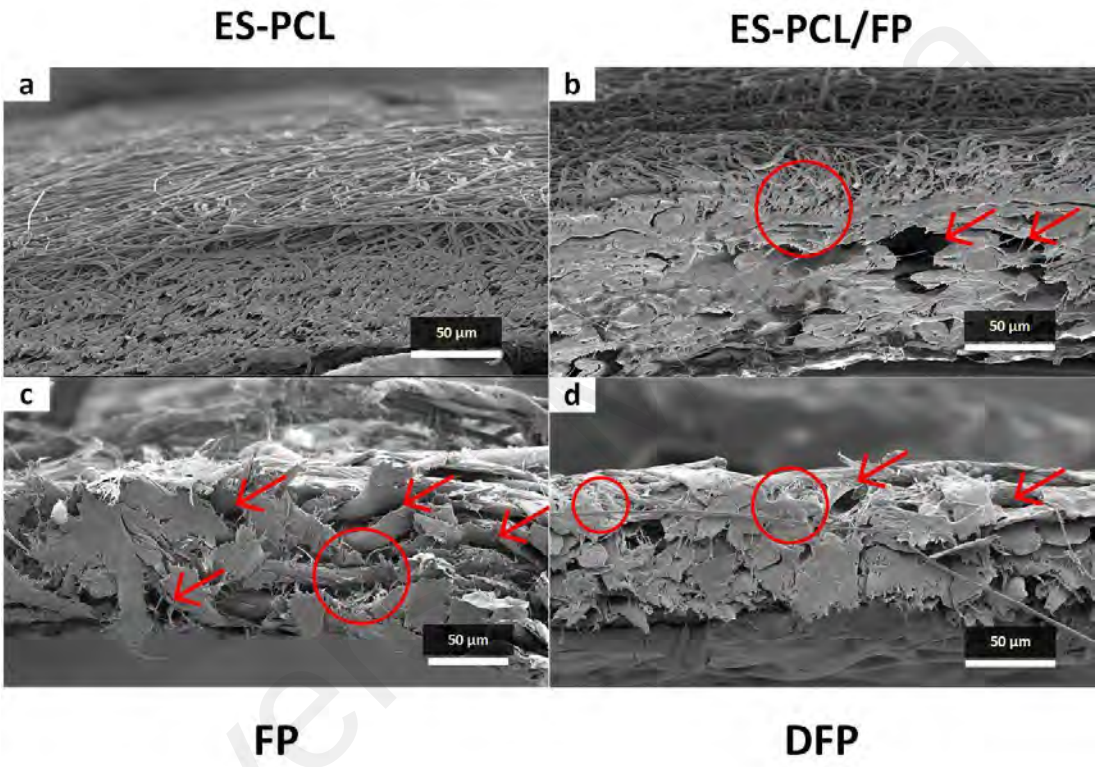

Figure 4. 2: Scaffold morphological analysis. FESEM microscopy on macroscopic dimension (cross-sectional area) of (a) ES-PCL, (b) ES-PCL/FP, (c) FP, and (d) DFP.

4.2.2 Porosity and thickness of scaffolds

Table 4.1 shows the average porosity, pore size, thickness and tensile strength of the 4 types of scaffolds. ES-PCL had the highest porosity (66.71%), followed by ES-PCL/FP (25.26%), then FP (7.55%) and the lowest was DFP (3.23%). The comparison of ES-PCL/FP and FP showed that coating a thin layer of PCL could increase the overall porosity of the scaffold more than two-fold. However, the formation of thinner and straighter fibers on the surface of ES-PCL/FP, as indicated in Figure 4. 1 b, has resulted

in a reduction in pore size. This was due to multiple layers of thin and straight nanofibers overlapping each other and leading to a reduction in the pore size (Puppi et al., 2014; Smith & Ma, 2004). DFP had lower porosity compared to FP as PCL solution had further reduced its porosity as much as 50%. PCL solution penetrates the pores of FP during the dipping process, and the stagnant polymer solidifies and covers a portion of the pore and leads to a reduction in pore size (Figure 4. 1 d),

Table 4. 1: Porosity percentage and thickness of scaffolds.

	ES -PCL	**ES-PCl/FP**	**FP**	**DFP**
Porosity (%)	66.71±2.65	25.26±1.60	7.55±2.76	3.23±0.59
Pore size (µm)	13.11±1.07	5.42±0.22	92.13±11.98	73.67±17.00

4.2.3 Characterization of scaffold mechanical properties and thickness

Table 4.2 shows the tensile strength, Young's modulus, elongation at break and thickness of the 4 types of scaffolds. The mechanical properties of scaffolds were examined by using tensile testing, where the scaffolds were placed at a controlled strain rate (1mm/min) until failure. ES-PCL has the lowest tensile strength and Young's modulus, while ES-PCL/FP with the smallest fiber diameters has the highest tensile strength and Young's modulus (Table 4.2). However, a similar event was not observed in DFP as non-homogenous distribution of PCL within FP does not contribute significantly to the tensile strength and Young's modulus. By reducing the diameter of electrospun fiber to submicron/nano size, superior mechanical properties can be attained (Z.-M. Huang et al., 2003). Wong et al. reported that the effect of fiber diameter towards tensile properties are more dominant when the diameter of PCL electrospun fiber are below 700 nm, Another group also reported that finer PCL fiber was stretched to greater extent during the electrospinning process, giving the fiber a higher degree of molecular

orientation which leads to a higher resistance to tensile force (Lim et al., 2008). The finer fiber of ES-PCL/FP also provides a higher surface area for fiber entanglement and permit a higher fiber packing density. The more densely packed and overlapped nanofibers increased the degree of fiber-to-fiber fusion due to solvent evaporation and chemical reaction, it randomly forms chemical bond like the intra-molecular bonding within the fibrous network, which could lead to a significant increase in tensile strength (X. Wei et al., 2009; Y. You et al., 2006). Besides, the more homogeneously packed nano-sized fibers also allow more fibers interlocking give rise to more interface interaction by Van der Waals forces (X. Wei et al., 2009). In fact, electrospinning caused more PCL to be deposited on the FP (49.69 ± 9.3 µm thickness n=7, (ES-PCL/FP-FP)) in comparison to the dipping method (37.78 ± 22 µm thickness n=7, (DFP-FP)). This shows that electrospinning forms an integrated layer of PCL onto FP and the elastic nature of ES-PCL contributes to tensile properties.

Table 4. 2: Tensile properties of scaffolds

	ES - PCL	**ES-PCL/FP**	**FP**	**DFP**
Tensile Strength (MPa)	1.68±0.23	5.80±0.32	3.52±0.38	3.54±0.17
Young Modulus (MPa)	0.65±0.17	72.99±3.90	57.52±8.71	52.41±5.43
Thickness (µm)	232.07±11.59	258.78±9.03	209.09±0.50	246.87±21.81

4.2.4 Medium sorption and retention

Figure 4. 3 shows the medium retention capacity, measured as the loss of absorbed water from the scaffolds in the incubator, set to 37 °C, 5% CO_2 and 95% relative humidity, with time. ES-PCL/FP absorbed almost 5 times the amount of complete medium of its dry weight, and steadily declined to about 250%, 110%, 26% and 0% on each time point over the 4-days study period. Other scaffolds followed a similar trend with relatively lower initial water sorption abilities and a steady decline to about 0% over the 4-days study period. ES-PCL and DFP have reduced ability to retain medium, with maximum sorption of 195% and 145% on day 0 respectively and lost all the retained the complete medium on day 3. PCL is hydrophobic polymer that has low affinity toward complete medium which mainly comprise of water (Hassan et al., 2006; Elbay Malikmammadov et al., 2018). DFP has the lowest complete medium sorption and retention among all scaffold because the PCL coating has prevented the hydrophilic cellulose fiber of FP from absorbing the medium. The reduced porosity of DFP also lower the possibility of trapping the medium within the scaffold. The ES-PCL that is produced from pure PCL polymer, on the contrary, has higher complete medium sorption and retention due to the higher porosity of ES-PCL compared to DFP (table 4.1). FP contains cellulose fiber that has a high wicking capability to draw and store liquid in its highly porous hydrophilic structure (Cramer et al., 2019; Kelvin Ng et al., 2017). Surprisingly, a layer of electrospun PCL on top of FP gives ES-PCL/FP scaffold the highest medium sorption and retention throughout the time points. The hydrophobic electrospun layer has altered the medium retention ability of the scaffold. Rahimi et al. has fabricated an air-liquid interface PDMS cell culture platform by using duo Janus paper that is hydrophobic on one side and hydrophilic on another side, which platform is capable of maintaining an optimal dynamic flow with the help of Janus paper, and eliminating the need of periodically replacing the medium. Another group also reported that a hydrophobic PDMS layer added on the paper-based medium reservoir has successfully reduce evaporation and prolong the shelf life of

the portable Kirby–Bauer antibiotic susceptibility test point-of-care diagnosis device up to 40 days (Deiss, Funes-Huacca, et al., 2014; Funes-Huacca et al., 2012).

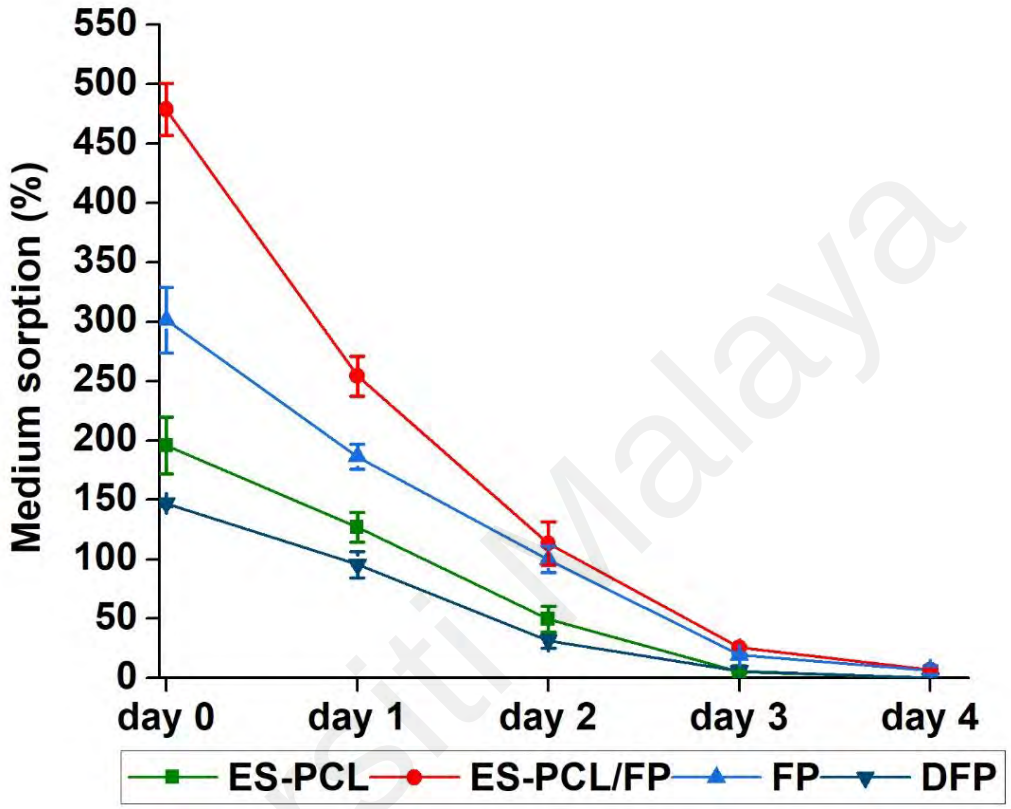

Figure 4. 3: Medium retention analysis. Weight percentage of medium sorption measured at different time point for scaffolds (a) ES-PCL, (b) ES-PCL/FP, (c) FP, and (d) DFP.

4.2.5 Surface contact angle

Contact angles indicate the hygroscopic properties of a surface. The lower the contact angle the more hydrophilic (wettable) the surface is. Hydrophilicity of scaffold dictates a series of biological events, such as cell adhesion, cell proliferation, and protein adhesion (Caridade et al., 2012).

Figure 4. 4 shows the formation of a quasi-spherical arched water drop on different types of scaffolds and its stability over the period of 60 seconds. ES-PCL is the most hydrophobic scaffold among all, it has recorded an average angle of 131.21, followed by

DFP with an average angle of 129.34 (Figure 4. 5). Water droplets form a stable quasi-spherical arched water drop on the surface of ES-PCL and DFP, respectively. Water dropped on the surface of FP does not form any water droplet, and cellulose component within FP is capable of absorbing water molecules into its porous structure through capillary action (Cramer et al., 2019; Yue Zhang et al., 2016).

As illustrated in Figure 4. 4 f-j, the water droplet diminishes gradually in association with contact angle (Figure 4. 5) decrease as time goes on (as shown by the arrow). PCL is inherently hydrophobic and this appears to be its major limitation in biomedical application, as its poor wettability results in poor cell attachment and cell-materials interaction (Masters & Anseth, 2004). Coating of hydrophobic polymer on cellulose paper surface alters the surface energy, modifying the hydrophilic surface of cellulose paper into a hydrophobic surface with low wettability (Ratmir Derda et al., 2011). Zhang et al. fabricated a paper-based hydrophobic/lipophobic surface analytical device by using the dip coating method, with results showing that hydrophobic materials loaded on paper were sufficient to block the interspace of cellulose paper fibers, and render the cellulose paper materials hydrophobic. Dip coating of FP with hydrophobic PCL modified the hydrophilic FP into hydrophobic DFP, the surface contact angle increases from 0^{o} to approximately 129^{o}. Electrospinning a layer of fibrous PCL mat onto FP produced the bilayer ES-PCL/FP, electrospun mat that is composed of fiber with interconnected pores which does not block the interspace of cellulose paper fiber completely. The self-powered capillary action of cellulose paper exerts a wicking forces that slowly pulls the water molecules into the scaffold, reducing the contact angle gradually as a function of time (Zhou et al., 2017).

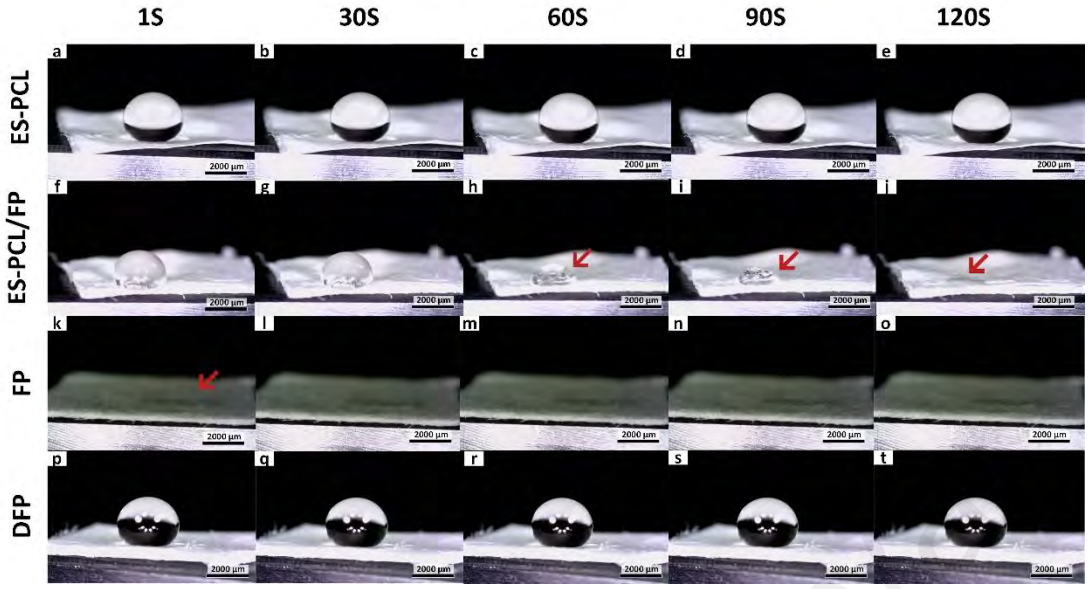

Figure 4. 4: Optical Microscopic images of water droplet on scaffold surface

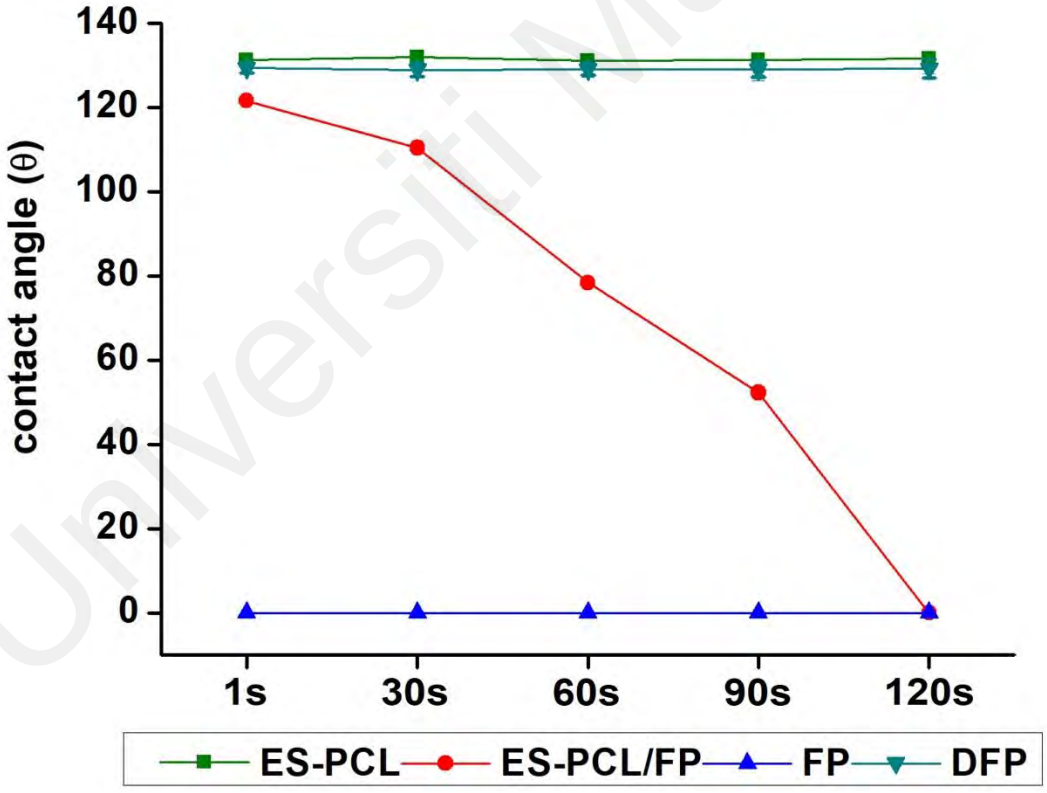

Figure 4. 5: Water contact angle analysis of scaffolds

4.3 In Vitro Study

Tissue engineering scaffolds play a role as an important biological substitute in regenerative medicine clinical applications. Scaffolding biomaterials are often used in the lesion site, to fill the void, to provide temporary structural support, as a reservoir of growth factors, and to enhance cell growth that eventually leads to tissue regeneration (Howard et al., 2008). *In Vitro* studies act as the preliminary studies that give an early intuition on the biocompatibility of scaffold prior to *in vivo* clinical study. A proper evaluation based on the carefully conducted *in vitro* study could prevent unfavourable outcome (Musson et al., 2013). In this study, osteoblasts, and mesenchymal stem cells were selected for cellular response on the PCL polymer modified paper-based scaffolds samples in the aspect of adhesion, proliferation, and differentiation. PCL and paper material have both demonstrated their potential in bone tissue engineering (K.-O. Kim et al., 2013; H.-J. Park et al., 2014) and stem cell (Jin et al., 2018; Elbay Malikmammadov et al., 2018; H.-J. Park et al., 2014), respectively. Thus, the interaction of PCL-modified paper scaffold with osteoblast cells and stem cells would be a subject of interest. The effect of topography and scaffold architecture, towards cellular behaviour will be further discussed in the following section.

4.3.1 Human Fetal Osteoblast 1.19 cell line (hFOB)

The fetal osteoblastic 1.19 cell line (hFOB) is a commercially available clonal human fetal cell line that is immortalized with a temperature-sensitive mutant of SV40 large T antigen (tsA58) (Harris et al., 1995). In vitro model uses hFOB for bone-related studies, such as disease model (Liang et al., 2012), phenomic and genomic study (Xiaomei Liu et al., 2007). HFOB is a well-characterised osteoprogenitor cell line that is capable of multiple passages with minimal karyotype damage (Subramaniam et al., 2002; Yen et al., 2007). HFOB by default will undergo an osteoblastic differentiation pathway. However, when induced with appropriated reagent, it is also capable of multilineage differentiation

into the mesodermal lineages of chondrogenic and adipocytic cell types in addition to its predetermined pathway (Yen et al., 2007).

4.3.1.1 Osteoblast adhesion and morphology

FESEM was used to evaluate morphology, adhesion, and the interaction of hFOB cells within the scaffold. Figure 4. 6 shows the microscopic images of the hFOB cells on the scaffold on day 1, day 4 and day 7. PCL is a synthetic polymer and a biodegradable polyester. It is non-toxic and tissue compatible. PCL was widely used for resorbable sutures, as scaffolds in regenerative therapy and in drug delivery applications. Modification of nitrocellulose membranes with electrospun PCL was able to alter the wicking properties of the membrane and enhanced the protein binding as well as improving detection sensitivity of nucleic acid-based lateral flow assays (C.-H. T. Yew et al., 2018). There were growth factors and proteins present in the fetal bovine serum found in the culture medium, which may have facilitated cell adhesion on the paper-based scaffolds.

For the ES-PCL scaffold (Figure 4. 6 a-c), the cells spread on the surface of the fiber and were more flattened, thicker, and showed less distinct filopodia. As for the ES-PCL/FP scaffolds (Figure 4. 6 d-f), cells were observed to be more elongated, well-anchored to the fiber through distinct filopodia and microvilli and proliferate well along the direction of fiber alignment. Steven et al. (2005) reported that cells that bind on scaffold surface with microscale topography are flattened and spread in a manner that is similar to cells cultured on flat surface. Scaffold with the nanoscale surface, on the contrary, provide greater surface area and more binding site for cell membrane receptor, which is more favorable for cell spreading and proliferation (Puppi et al., 2014). Woo et al. (2003) also reported that nano-fibrous scaffolds allow attachment of osteoblastic cell 1.7 times greater than scaffolds with solid pore walls. In the FP scaffold (Figure 4. 6 g-i), the cells were observed to attach to the struts of cellulose fibers. Figure 4g shows that the

cells bridged between two struts, whereas Figure 4. 6 h-i shows that the cells grew and covered up pores of the cellulose. As for DFP scaffold (Figure 4. 6 j-l), the cells were seen mainly at areas where there are pores. The smooth surface and low porosity of the DFP scaffold (Figure 4. 6 j-l) does not provide a good surface for cells to attach and spread. Cells attached poorly on the flat surface and had short filopodia. Furthermore, the reduced porosity of DFP may have prohibited cell penetration and infiltration within the scaffold. The micrograph clearly shows that the cell morphology and proliferation depend on the topography of the scaffold, such as fiber diameter, orientation and pore size (Badami et al., 2006; Christopherson et al., 2009). Another study reported that the topography of the scaffold influences the growth behaviour of osteoblast cells, results of the study showing that osteoblast attachment and proliferation were greater on a rough surface than the smooth surface (Costa et al., 2013).

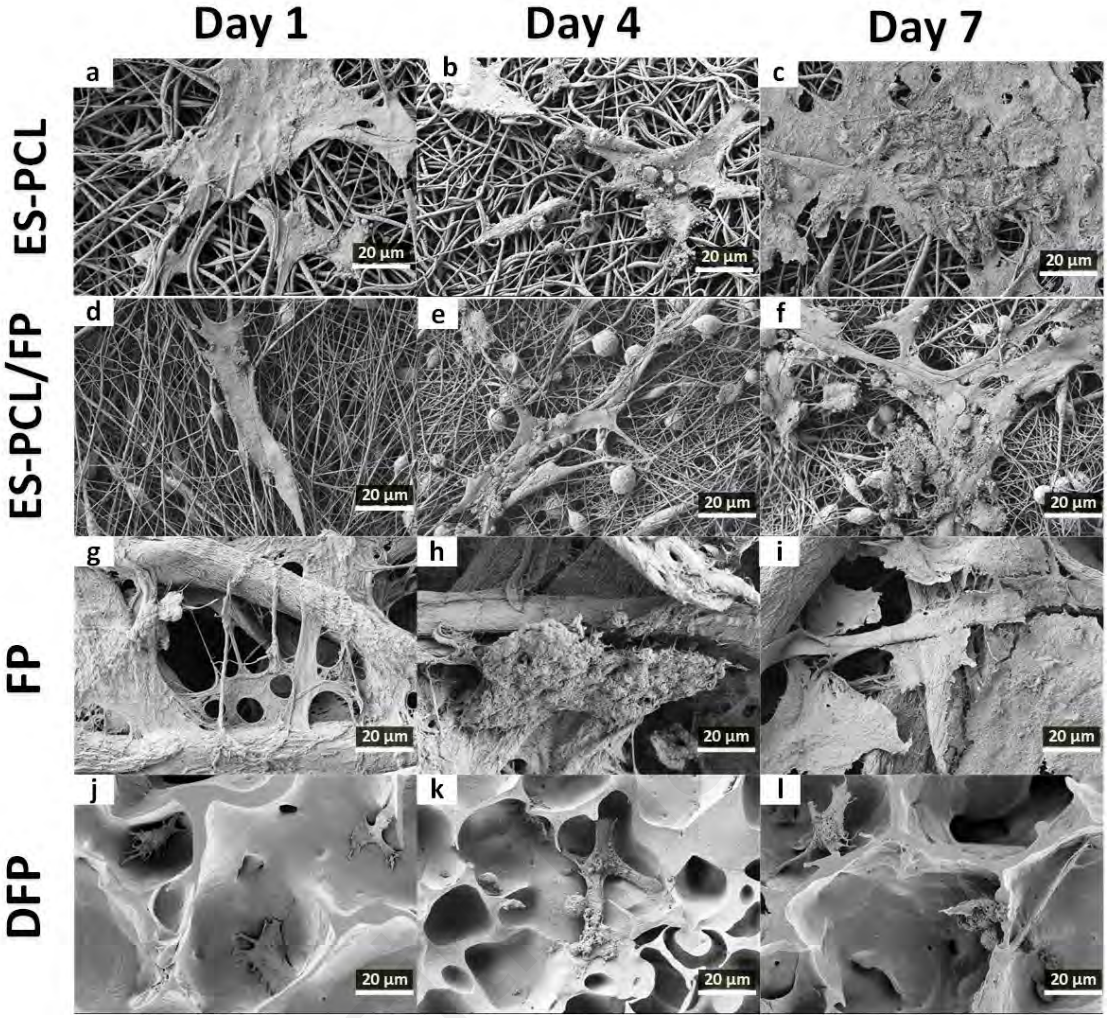

Figure 4. 6: Cell morphological analysis. FESEM images showing the morphology of hFOB plotted separately for each individual scaffold of ES-PCL, ES-PCL/FP, FP, and DFP on different days. The magnification and resolution of all images are the same.

4.3.1.2 Osteoblast Proliferation

Figure 4. 7 shows the proliferation of hFOB measured at the different time points (*i.e.*, day 1, day 4 and day 7) for all groups of scaffolds. ES-PCL showed significantly lower cell proliferation on days 1 and 4 compared to other groups on the same day but reached the same level as FP and DFP on day 7. FP and DFP only indicated significant cell proliferation difference on day 1. While the two groups' cell proliferation continued to rise on days 4 and 7, the difference was insignificant. As shown in Figure 4, the cell proliferation of different scaffolds ascended steadily from day 1 to day 7. The increase in cell proliferation for FP and DFP was not significant throughout the 3-time point when

compared side by side. This result indicate that the dip-coating modification method does not have significant impact on cell growth. Referring to results in the previous section, DFP scaffolds remain in microscopic scale after modification. Puppi et al. (2014) mentioned that cells that adhere on microscopic substrate display phenotypes of cells culture on a 2D flat surface, hence it does not promote significant enhancement in cellular activity. Cell proliferation measured on ES-PCL/FP scaffolds showed significant increase only until day 4, and there was no significant difference between day 4 and day 7. This suggests that the cells on ES-PCL/FP may have reached confluency between the two time points. For ES-PCL scaffold, the cell proliferation on day 1 and day 4 was not significantly different, however there was a sharp increase in cell proliferation after day 4 and there was a difference in cell proliferation between day 4 and 7. This data is in line with the live/dead images (Figure 4. 8 a-b), in which the cell density was almost the same on day 1 as on day 4. Comparison between the groups of scaffolds showed that ES-PCL/FP has the highest cell proliferation of all time points and the difference compared to other groups on the same day was significant. ES-PCL/FP has a hierarchical structure that consist of nano and micro bilayer. This unique ECM mimicking architecture has shown favorable results towards cell growth. The nano-sized fiber on the top layer provides a large specific surface area that eases the adhesion and proliferation of cells (Fang et al., 2010; J. Venugopal et al., 2008). The macro-sized layer at the bottom (FP) is a paper material that can retain fluid, and at the same time, allow diffusion of nutrients across the membrane at a controlled rate. This property renders the FP later to function as a reservoir that could hold the growth factor secreted by the cell, thus creating a feasible microenvironment for cell growth. In native ECM the macro-size fibrous protein, that has interconnected porous structure (physicochemical properties) acts as a reservoir of growth factor and enzyme secreted by cells in vicinity, which play an essential role in dynamic modulation of ECM (Geckil et al., 2010; Hinderer et al., 2016; G. Huang et al., 2017; Nicolas et al., 2020).

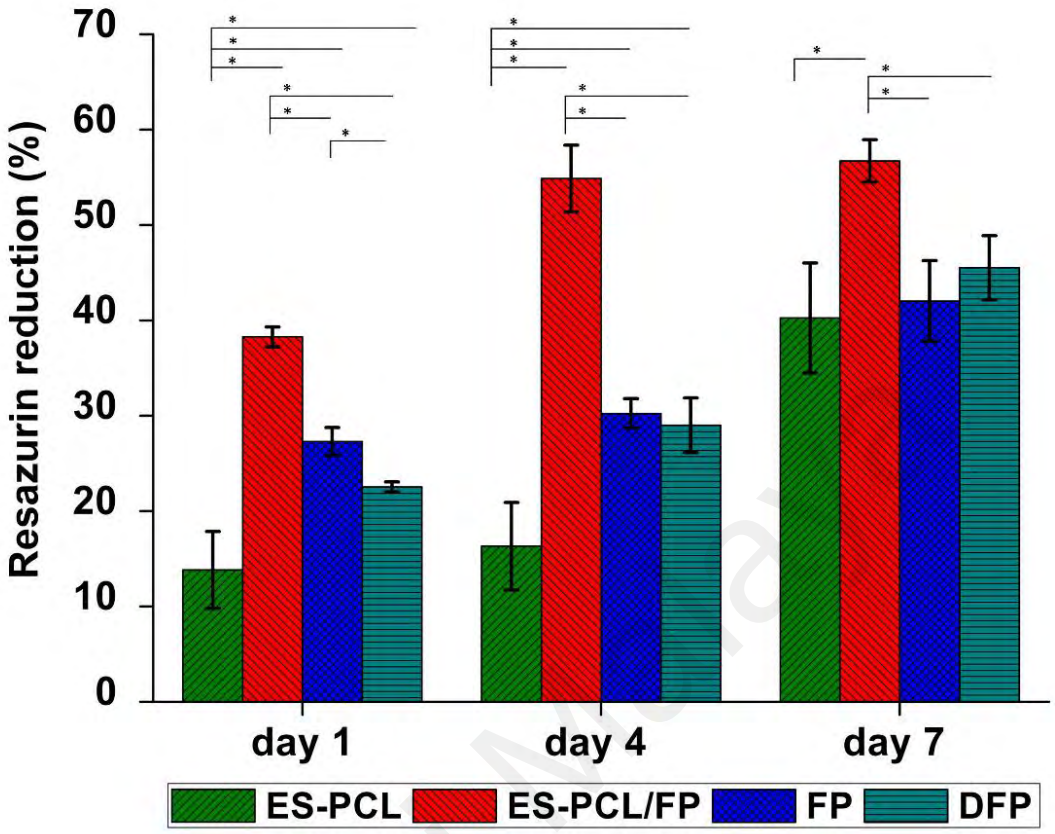

Figure 4. 7: Cell proliferation analysis. Resazurin proliferation assay results for (ES-PCL, ES-PCL/FP, FP, and DFP). The resazurin reduction of hFOB increased on ES-PCL, ES-PCL/FP, FP, and DFP as a function of time. * Indicates statistical significance ($P<0.05$).

4.3.1.3 Osteoblast Viability

Figure 4. 8 shows the microscope images of the scaffolds under fluorescent excitation using live/dead staining. Abundance of green spots indicates the high viability of hFOB cells on the scaffolds in a period of 7-day incubation. As expected, the results suggest that paper and PCL are biocompatible substrates for cell culture. The abundance of green cells could suggest attachment of hFOB cells on the scaffolds as the images exhibited cells anchored on the surface with extended filopodia, a typical characteristic of osteoblast morphology (Nakamura, 2007). There were clearly more live cells on the ES-PCL/FP scaffold in all three-time points (Figure 4. 8 d-f), cells were more well spread, and cell density was higher compared to other scaffolds, on day 7 (Figure 4. 8 c, f, i & l). This

result is in line with resazurin cell proliferation results. The image (Figure 4. 8f) also showed that the ES-PCL/FP surface was confluent with live cells without visible dead cells. DFP and FP scaffolds showed more individual cells clusters that grow in distance, mainly due to the relatively big gap between struts that is difficult for cells to bridge. By day 4 cells on both DFP and FP scaffolds have spread out and occupied more space. The live-dead assay revealed that cell distribution was better on scaffolds with smaller fiber diameters than larger fiber diameters, as reflected by day 7 images (Figure 4. 8 c, f, i & l). Topographic factors such as fiber diameter of a scaffold affect the cell growth, as the scaffolds with a smaller fiber size provide a higher surface area for cell anchoring which leads to both higher cell growth and a more even distribution (Badami et al., 2006; Christopherson et al., 2009).

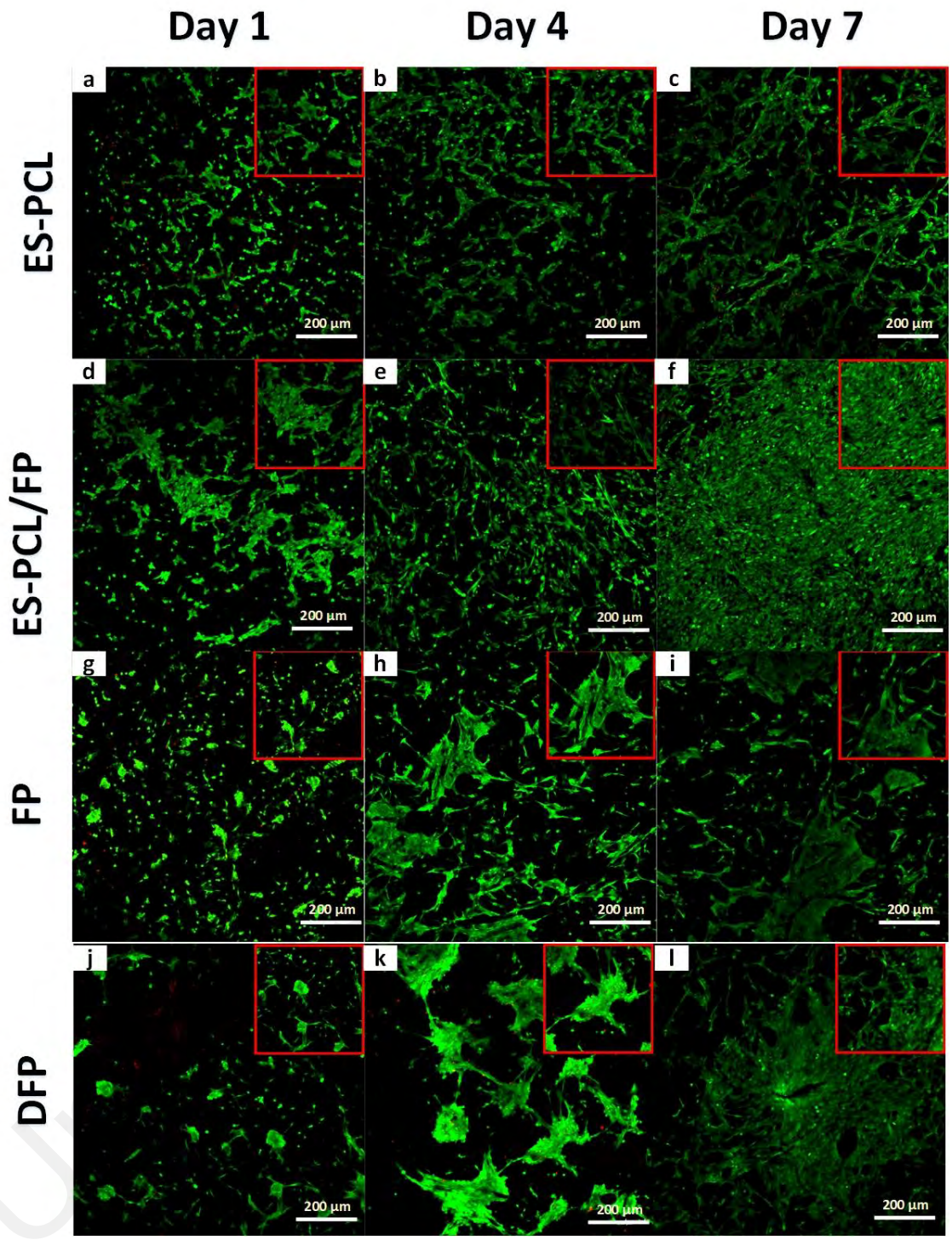

Figure 4. 8: Cell viability analysis. Live/dead confocal of hFOB plotted separately for each individual substrate ES-PCL, ES-PCL/FP, FP, and DFP on different days.

4.3.1.4 Osteoblast metabolic activity

ALP is a time-dependent osteoblastic marker that is often used to examine the osteogenic differentiation pattern (Krishnamurithy et al., 2016). The expression of ALP in bone tissue takes place in the early stages of osteospecific differentiation, and ALP is one of the first expressed functional genes during the bone formation (Niakan et al., 2017) , and mature osteoblasts secrete ALP in a time dependant manner (Yen et al., 2007). Thus, due to its key role in osteogenesis, it has been used as a reliable marker to examine osteogenic activity and osteoblast phenotype (Golub & Boesze-Battaglia, 2007). Figure 4. 9 shows the ALP activity of hFOB measured over a period of 14 days. As shown in the figure 6, the ALP activity on ES-PCL, FP and DFP scaffolds showed an ascending trend from day 1 till day 7. On day 14, DFP and -FP scaffolds showed a slight decrease in ALP activity. The ALP activity of ES-PCL/FP is significantly higher than other groups on all days. The ALP activity of ES-PCL/FP between day 7 and day 14 has not changed significantly, which indicates that the cells have reached confluency, resulting in the ALP activity staying the same. Contact inhibition occur when normal cells reaches confluency, it will cause cell cycle arrest where cells goes into condition resemble quiescence (Leontieva et al., 2014). The ALP activity results are in line with the resazurin assay, in which the ES-PCL/FP scaffold showed the highest readings in both. The ALP activity results also support the live/dead results. It has been reported that better distribution of cells can improve osteospecific differentiation (Sjostrom et al., 2011); based on live/dead assay (Figure 4. 8 f), ES-PCL/FP indicates the highest number of cells and cell spreading all over the surface of the scaffold.

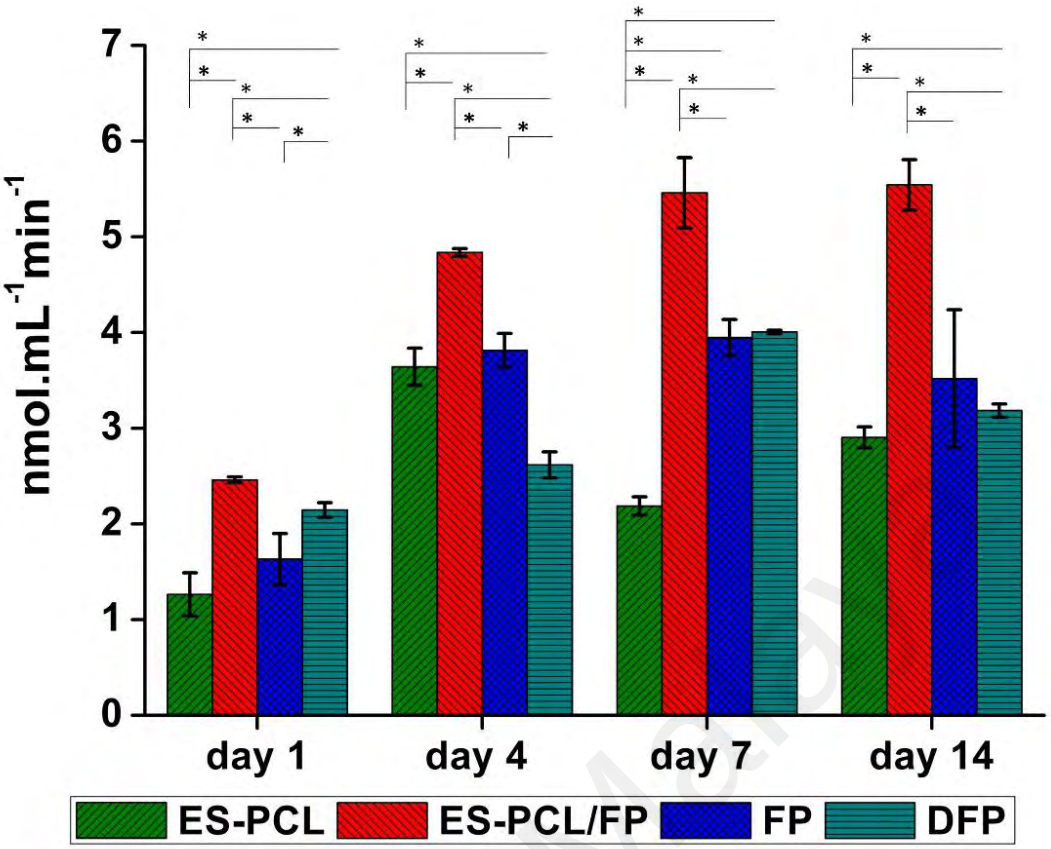

Figure 4. 9: Bone metabolic activity analysis. ALP assay results for hFOB seeded-in (ES-PCL, ES-PCL/FP, FP, and DFP) at different time point. The ALP activity of hFOB increased on ES-PCL, ES-PCL/FP, FP, and DFP as a function of time. The results are statistically significant ($P<0.05$),

4.3.2 ADMSC

The use of stem cells as a means of bone lesion therapy has become a favourable alternative in bone tissue engineering (Mohamed-Ahmed et al., 2018). Mesenchymal stem cells that possess the capability of self-renewal and differentiation into multiple cell lineages have been used extensively in stem-cell therapy. ADMSC has slowly gained popularity in stem-cell therapy due to its less invasive harvesting procedure and its availability in multiple sites. Significant differences were reported in ADMSC harvested from different sites by using different protocols. Hence, a series of tests is needed to confirm the mesenchymal stem cells, with the purpose of effective knowledge exchange and data comparing between research group (Oedayrajsingh-Varma et al., 2006). ISCT has set a few minimal criteria to abide for the claim of stem cells, which includes, plastic adherence, trilineage differentiation and expression of certain surface markers.

4.3.2.1 Characterization of ADMSC

IFATS and ISCT have proposed three minimal criteria for the characterisation of ADMSC(Baer, 2014; Dominici et al., 2006). The first criteria to comply is, ADMSC must be plastic-adherent when cultivated in tissue culture flask filled with standard culture medium. Under light microscopy, stem cells at passage 2 showed fibroblastic spindle shape morphology on day 7 (Figure 4. 10 a) and day 14 (Figure 4. 10 b). On day 7 a colony of stem cells adhered on the plastic cultural flask and surrounded by spindle-shaped cells in the vicinity. By day 14, a confluent growth of stem cells displaying elongated fibroblastic morphology was observed.

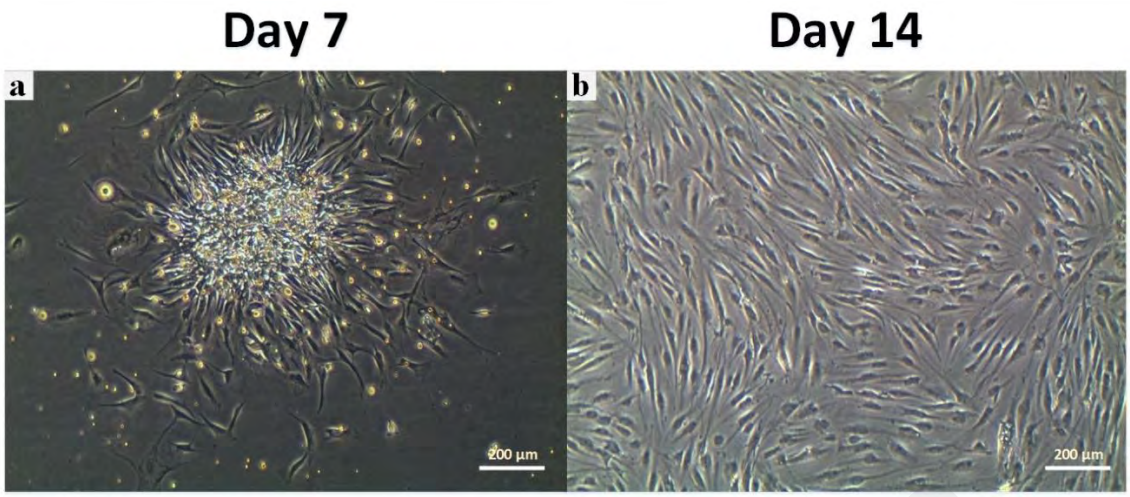

Figure 4. 10: Morphology of ADMSC adhere on plastic flasks. a) Stem cell colony was observed on day 7, Spindle-shaped cells were observed on both day 7 and day 14

(a) Tri-lineage Differentiation of ADMSC

Other criteria for the characterisation are, ADMSC must have the ability to differentiate into cells of mesenchymal origin *in vitro*, such as adipocytes, chondrocytes, and osteoblasts, when exposed to specific growth signals.

I) Osteogenic Differentiation

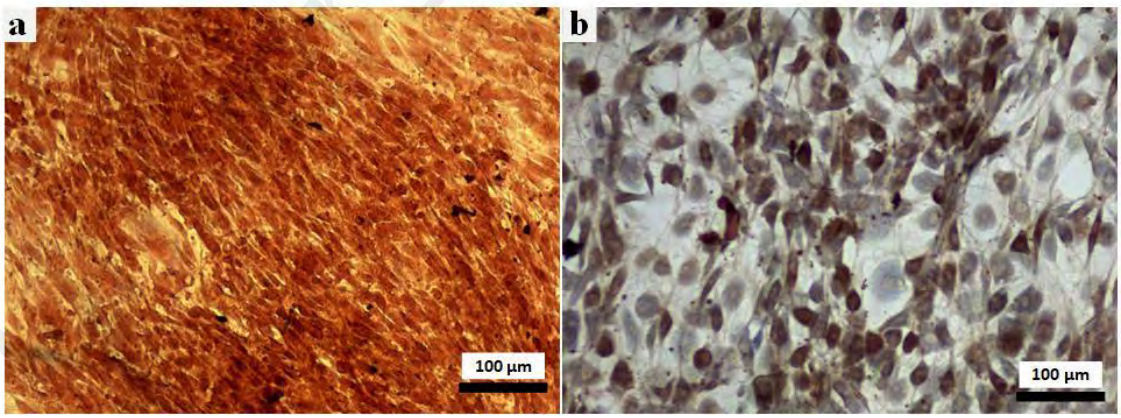

Figure 4. 11: Alizarin S staining of ADMSC cultured in a) osteogenic differentiation medium b) complete medium。

The prominent brick-red colour observed on monolayer cells cultured in osteogenic mediums (Figure 4.11 a) is associated with calcium deposition, indicating the cells were in the early stages of bone formation, where mineral deposition occurs. In contrast, the control sample (Figure 4. 11 b) does not show a brick-red colour under the microscope.

II) Adipogenic Differentiation

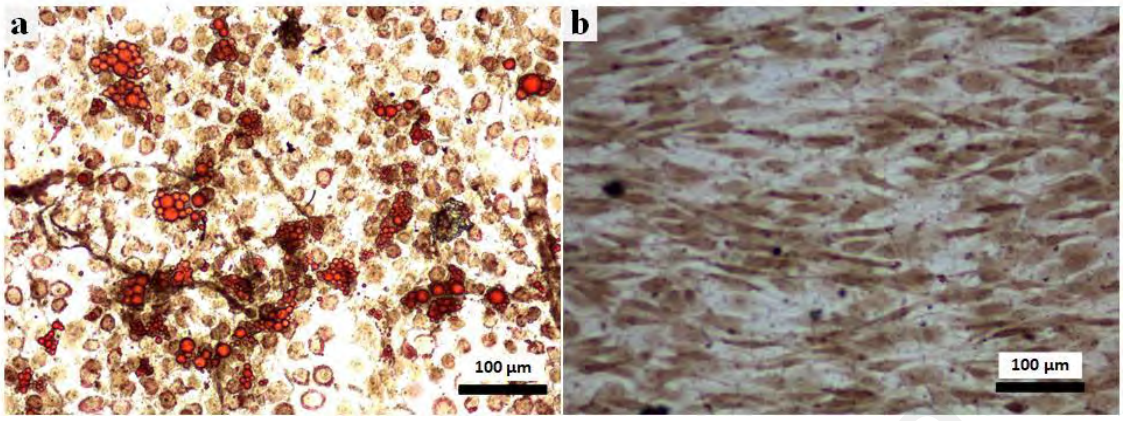

Figure 4. 12: Oil red O staining of ADMSC cultured in a) adipogenic differentiation medium b) complete medium.

Oil red O stain is a chemical dye that reacts with triglycerides and lipid within adipocytes to give a red colour stain. Lipid droplets exist in abundance within the cytoplasm of adipocytes, thus the discovery of redly stained lipid droplet serves as strong evidence for successful adipogenic differentiation from ADMSC. The results of Oil red O staining on the monolayer adipogenic medium induced cell and the monolayer control cell growth in the standard medium are manifested in Figure 4. 12.

III) Chondrogenic Differentiation

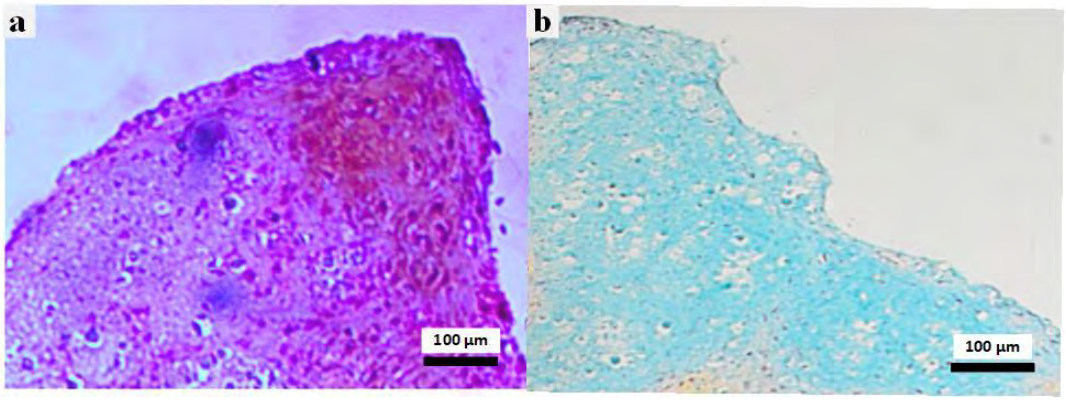

Figure 4. 13: Safranin O staining of ADMSC cultured in a) chondrogenic differentiation medium b) complete medium.

Figure 4. 13 has shown the result of safranin O staining on the histological section of the chondrogenic medium induced cell pellet and control cell. The histological section of the control cell pellet was not positively stained by safranin O, but only positively stained by fast green dye. The chondrogenic induced cell pellet was positively stained by safranin O, which indicated the accumulation of proteoglycan produced by cartilage extracellular matrix.

(b) Flow Cytometry Assay

ADMSC culture expansions from fresh human adipose tissue were confirmed by flow cytometry for the surface marker expression of CD73, CD90, and CD105, as demonstrated in Figure 4. 14. The results obtained show ⩾ 95% expression of cell surface markers such as CD90, CD73, and CD105, while lacking the expression of hematopoietic origin cell surface markers such as CD 34, CD 11b, CD19, CD 45 and HLA-DR.

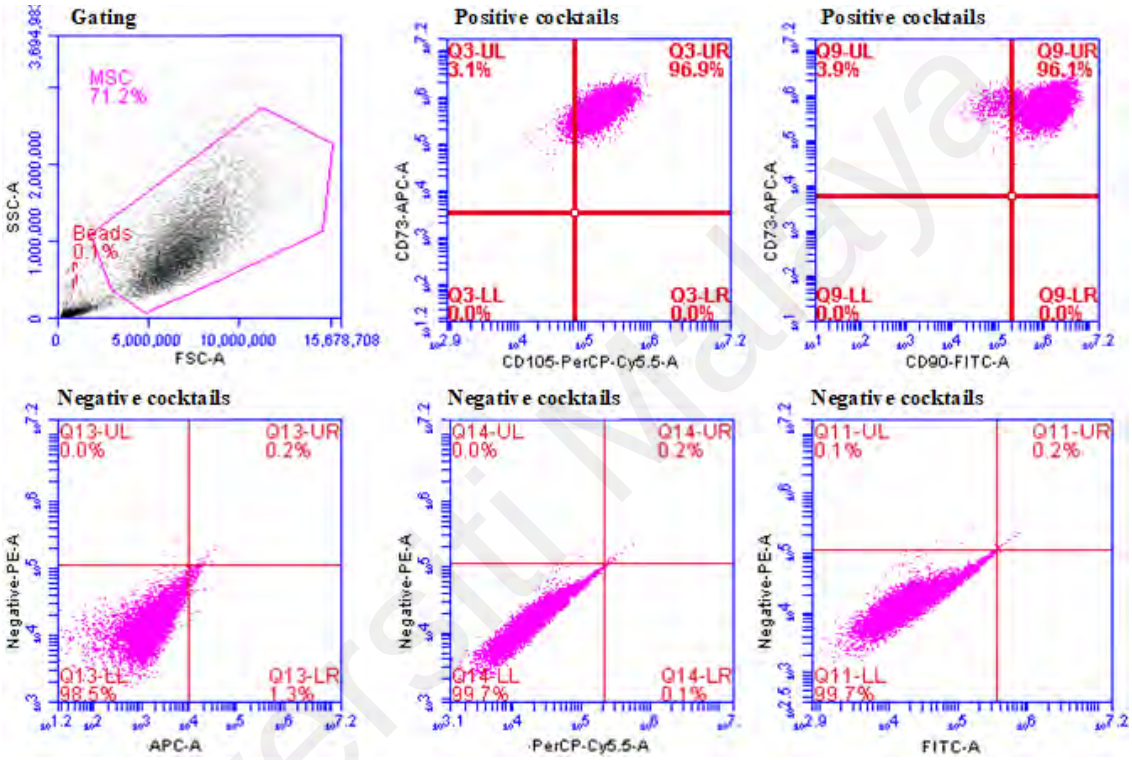

Figure 4. 14: Surface marker expression of ADMSC by using flow cytometric immunophenotyping. The cell expresses positive result for markers such as CD90, CD73, CD105, while negative result for PE-A conjugated markers such as CD 34-PE, CD 11b-PE, CD19-PE, CD 45- PE and HLA-DR PE

4.3.2.2 Cell adhesion and morphology

FESEM was used to evaluate morphology, adhesion, and the interaction of ADMSC with the scaffold. Figure 4. 15 shows the microscopic images of the ADMSC on the scaffolds on day 1, day 4 and day 7. The results show that ADMSC are well-attached and well spread on the surface of fiber of both ES-PCL scaffold (Figure 4. 15 a-c) and ES-PCL/FP scaffolds (Figure 4. 15 d-f). From visual observation ADMSC morphology on

ES-PCL scaffold (Figure 4. 15 a) and ES-PCL/FP scaffolds (Figure 4. 15 d) are similar on day 1. However, on day 4 and day 7, ADMSC grow on ES-PCL/FP scaffolds (Figure 4. 15 e-f) were observed to be thicker, more elongated, well-anchored to the fiber through distinct filopodia and forming a 3D and multicellular network alongside the nanofibrous architectural structure. The nano-scaled features of ES-PCL/FP scaffolds provide a favorable environment for cell growth, where the nano architecture promote cell growth through better adsorption of signaling protein and allow filopodia to anchor more tightly (Woo et al., 2007). Furthermore, the surface features of the ES-PCL/FP scaffolds' nano-scaled PCL fiber are at the similar scale with cell binding receptor, therefore, cell adhesion through receptor driven pathway are possible, thus lead to better cell anchorage along the direction of fiber (Dalby et al., 2014). In the FP scaffold (Figure 4. 15 g-i), the cells were observed to attach to the struts of cellulose fibers. Figure 4. 15 g and h show that ADMSC with rounded shape, attached loosely on the microscale struts with the thin and elongated filopodia. Figure 4. 15 i shows that the cells form cell cluster that covered up pores of the cellulose. As for DFP scaffold (Figure 4. 15 j-l), the cells were seen mainly at areas with smooth surface and low porosity. The morphology of ADMSC on DFP displays fibroblast-like spindle-shaped morphology, that is typical morphology of stem cells cultured on 2D monolayer cultural polystyrene flask (Yin et al., 2020). On day 1 (Figure 4. 15 j), the ADMSC attached on the flat surface of DFP display rounded morphology with protruded cytoplasm and short filopodia, whereas on day 4 (Figure 4. 15 j) the ADMSC display a spindle-like cell morphology elongated filopodia. On day 7 (Figure 4. 15 l), ADMSC on the surface of DFP appeared to have pseudopod-like structures and were longer and flatter. Yin et al. reported a study that compare the senescence-related changes between 2D and 3D cultured ADMSC, results of the study shows that ADMSC, when cultured in 2D platform, displayed a pseudopod-like structures and enlarged flat cellular morphology, which suggest MSC senescence occur (Tobita et al., 2015; Yin et al., 2020).

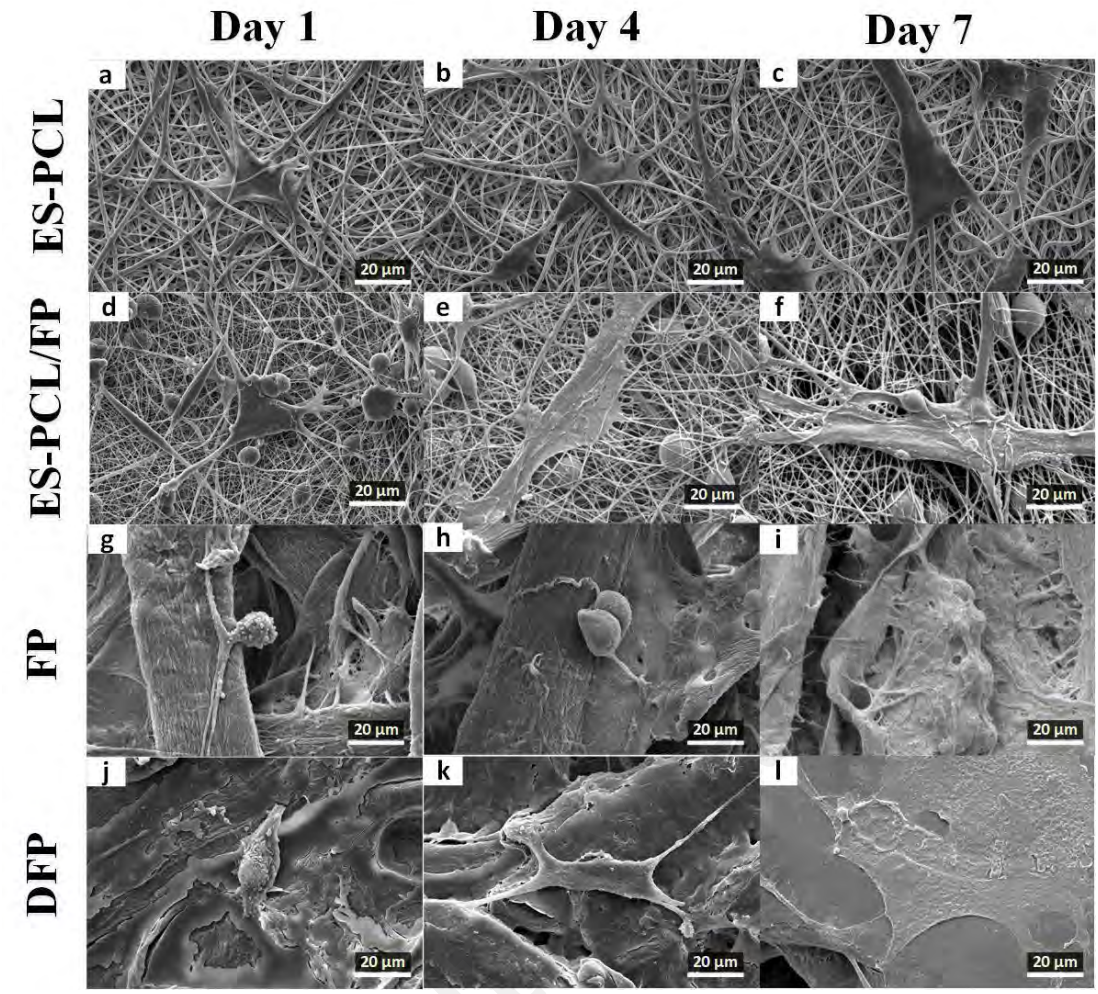

Figure 4. 15: Cell morphological analysis. FESEM images showing the morphology of ADMSC plotted separately for each individual scaffold of ES-PCL, ES-PCL/FP, FP, and DFP on different days. The magnification and resolution of all images are the same.

4.3.2.3 Cell proliferation

Figure 4. 16 shows the proliferation of ADMSC on all groups of scaffolds measured at the different time points (i.e., day 1, day 4 and day 7). ES-PCL showed the lowest cell proliferation on day 1 and day 7 compared to other groups, the cell proliferation ascends to second highest on day 4 but decline to the lowest on day 7. ES-PCL has a 3D porous structure that could enhance cell proliferation as reported by several studies (Ferro et al., 2014; Huh et al., 2011; Karageorgiou & Kaplan, 2005; Yin et al., 2020). However, the hydrophobic nature of PCL could hinder the infiltration and proliferation of cells, as the hydrophobic surface prevents the anchoring and penetration of cells into the porous

structure (Binulal et al., 2014; Elbay Malikmammadov et al., 2018; Woodruff & Hutmacher, 2010; Wu et al., 2010). As shown in Figure 4. 16, FP and DFP cell proliferation result ascend steadily from day 1 to day 7, the increase in cell proliferation being significant throughout the 3-time point. On day 7, the cell proliferation of FP overtakes DFP, but the difference is insignificant. This result shows that the dip-coating modification method does not have significant impact on the growth of ADMSC, which is in accordance with the hFOB results shown in Figure 4. 7. Cell proliferation measured on ES-PCL/FP scaffolds ascend steadily from day 1 to day 7, and the increase in cell proliferation was significant throughout the time point. ES-PCL/FP has the highest cell proliferation on day 4 and day 7, the difference compared to other groups on the same day was significant. The nano-scaled fibrous architecture of ES-PCL/FP provides a high surface area for adhesion of signalling protein, which has significant impact on ADMSC adhesion and proliferation, (Kasten et al., 2014; Veevers-Lowe et al., 2011; Woo et al., 2003). The nano-fibrous architecture could allow filopodia to anchor more tightly, thus providing better adhesion strength on the nano-fibrous scaffolds that could facilitate better cell spreading(W. J. Li et al., 2002; M. Wei et al., 2017). Another study reported that PCL nanofiber scaffold has great compatibility with human mesenchymal stem cells, and it was capable of supporting stem cell adhesion, maintaining viability and accelerating proliferation (Xue et al., 2017). ADMSCs grown on ES-PCL/FP have shown significant up-regulated growth and highest proliferation results, on time points day 1, 4 and 7, that matched the results shown by HFOB grown on ES-PCL/FP in Figure 4. 7. The results demonstrated that electrospinning modification methods show a satisfactory in vitro cytocompatibility with the different types of cell sources and capable of promoting their proliferation rate.

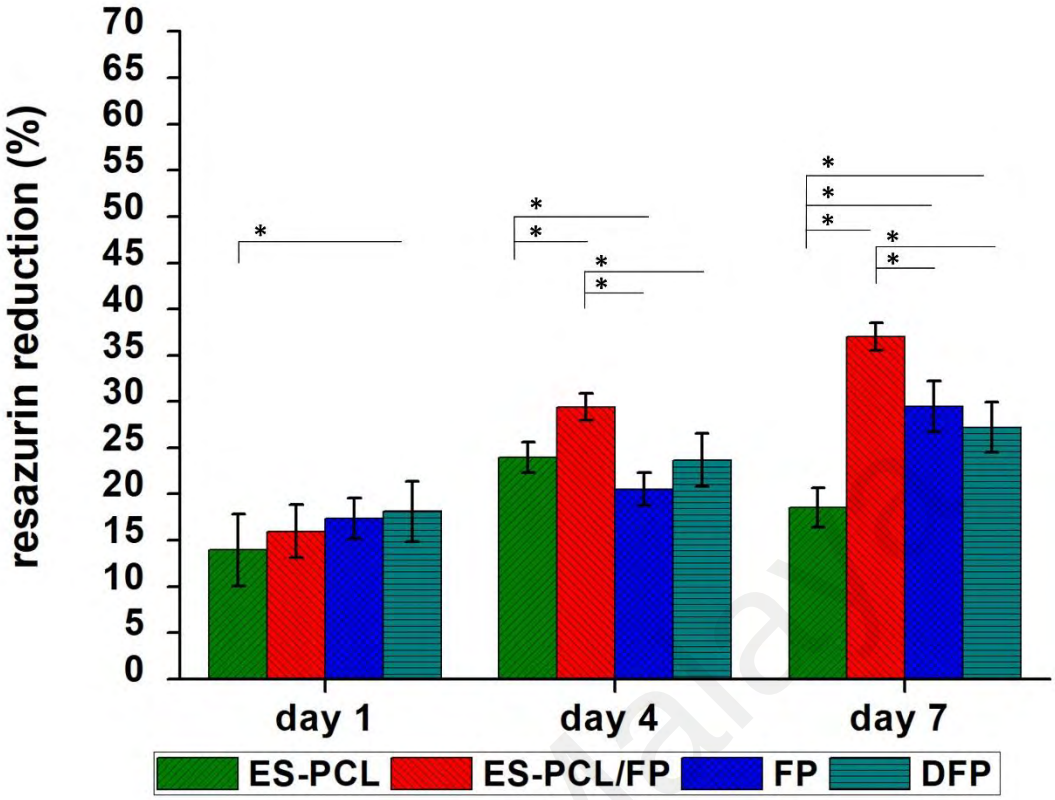

Figure 4. 16: Cell proliferation analysis. Resazurin proliferation assay results for (ES-PCL, ES-PCL/FP, FP, and DFP). The resazurin reduction of hFOB increased on ES-PCL, ES-PCL/FP, FP, and DFP as a function of time. * Indicates statistical significance ($P<0.05$).

4.3.2.4 Cell viability

Figure 4. 17 shows the confocal microscopic image of scaffolds stained with live-dead staining solution, where the calcein reagent will stain the membrane of live cells into green fluorescence, while the ethidium-homodimer reagent will stain the cytoplasm of dead cells into red fluorescence. The confocal images of scaffolds at different time points (i.e., day 1, day 4 and day 7) revealed that the fluorescent spots are mainly green, while red fluorescent spots are hardly visible. The results suggest that paper and PCL paper are biocompatible substrate for the culture of ADMSC. On day 1, the density of live cells on all scaffolds are comparable, which is in line with the cell proliferation results (Figure 4. 16). On day 4, the confocal images of ES-PCL scaffolds showed comparable cell density with day 1 and no visible dead cells on the images. On day 7, red fluorescence dots that

represent dead cell were observed on the confocal images and the density of live cells shows no significant increase compared to previous time point. The poor cell activity on ES-PCL scaffolds may be due to the hydrophobic nature of the polymer (Binulal et al., 2014). ES-PCL/FP scaffold has the most live cell on day 4 and day 7 (Figure 4. 17 e-f), ADMSC were more elongated, and well spread, the cell density was higher compared to other scaffolds. The ES-PCL/FP surface was confluent with live cells without visible dead cells. DFP and FP scaffolds showed more individual cells that are more disperse and grow in distance. This is due to the relatively big gap between the micro size-strut and the relatively big pore that is difficult for cell to bridge. Lowery et al. reported that electrospun PCL fibrous mat with pore size in the range of 6 μm-20 μm support cell bridging over the pore and thus lead to more rapid cell proliferation, while PCL fibrous mat with pore size greater than 20 μm along the single fibers with slower cell proliferation. The analysis of ADMSC by confocal microscopic images showed that the number of live cells are in line with the result of ADMSC proliferation (Figure 4. 16).

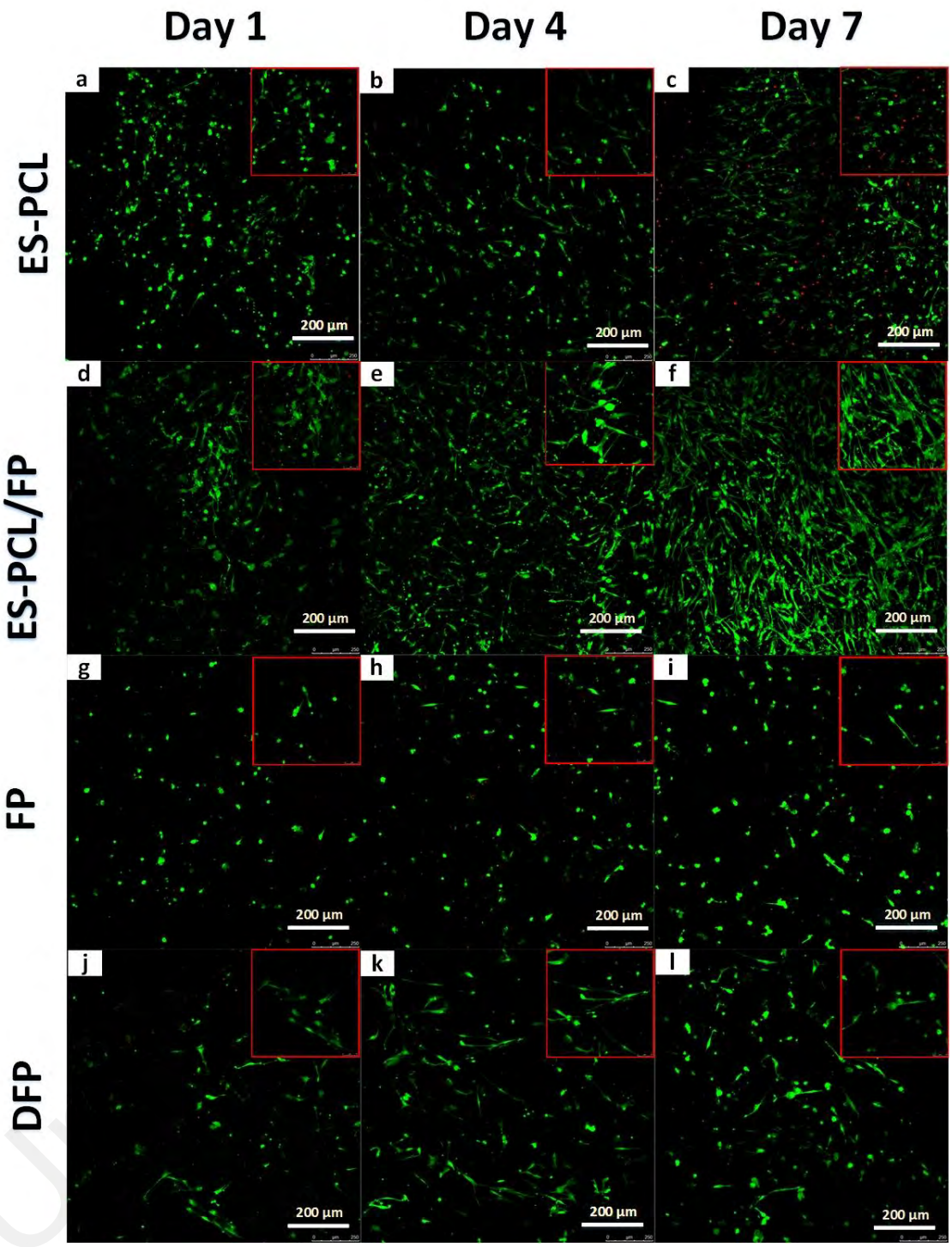

Figure 4. 17: Cell viability analysis. Live/dead confocal of ADMSC plotted separately for each individual substrate ES-PCL, ES-PCL/FP, FP, and DFP on different days.

4.3.2.5 Cell cytoskeleton assessment

Actin-cytoskeleton play an essential role in regulating various cellular process such as morphogenesis, cytokinesis, and migration of cell. The dynamic regulation of actin cytoskeleton in respond to biochemical and biophysical cues is the key factor in determining cellular behaviour and function in development and physiology, in multicellular organism (G. Huang et al., 2017; Tojkander et al., 2012). Interaction between ECM and cell modulates the cell behaviour and gene expression. Researcher have investigated the effect of topography on the cell adhesion and cell fate, the results showed that nano-scaled surface topography is beneficial towards tissue engineering application (Woo et al., 2007; Yin et al., 2020).

Figure 4. 18 shows the confocal microscopic images of scaffolds stain with Rhodamine-Phalloidin and DAPI, where the actin filaments were stained into green fluorescence by Rhodamine-Phalloidin and nucleus were stained into blue fluorescence by DAPI. The confocal images of scaffolds at different time points (i.e., day 1, day 4 and day 7) shows the morphology of actin filament and nucleus on each scaffold. Figure 4. 18 shows the number of adherent cells was noticeably higher on ES-PCL/FP and DFP (Figure 4. 18 d-f, j-l). The surface of the ES-PCL/FP scaffold is covered with more abundance of wide-spread actin filaments compare to DFP. The image (Figure 4. 18d-f) showed that the actin filament on ES-PCL/FP surface present in the vicinity of each nucleus. The actin filament on ES-PCL/FP surface become more abundance on day 4 and day 7. The morphology of the actin cytoskeleton is more widespread compared to other scaffolds and display a spindle-like structure, however, contact inhibition that occur due to the densely packed cell render the cytoskeleton to be less elongated and conform its shape, as shown by arrow (Figure 4. 18 e-f). Although DFP shows comparable cell density with ES-PCL/FP on day 4, but the spreading of actin cytoskeleton is limited, and rather some cells look a bit round compared to ES-PCL/FP. The actin filament is more rounded in shape, less extended filopodia as shown by red arrow (Figure 4. 18 j-k). The number

of adherent cells on ES-PCL and FP were low, indicated by the lower density of blue fluorescent-labelled nuclei on the surface (Figure 4. 18 a-c, g-i). ES-PCL shows elongated actin cytoskeleton on its surface (Figure 4. 18 a-c), the extended filopodia that grow along the fiber were stained green which indicate the formation of cross-linked actin filament (shown by red arrow) (Khurana & George, 2011). Actin cytoskeletons on FP surface were observed to formed at a distance from each other (Figure 4. 18 g-i), the relatively large pore size on FP observed in FESEM images (Figure 4. 1 c &Figure 4. 15 g), impede cell bridging and kept the cell at the cellulose strut. ES-PCL/FP that has the highest values of Young's modulus or stiffness (Table 4. 2) has the most widespread actin cytoskeleton on its surface compared to other scaffolds. Young's modulus or elastic modulus reflect the stiffness or elasticity of scaffolding biomaterials (C. Huang et al., 2015). The stiffness of the scaffold greatly influences the formation of actin cytoskeleton, which mechanical stimulus produced amidst the scaffold-stem interaction can be translated into intracellular signaling that influences the adhesion structure of actin cytoskeleton (Ambriz et al., 2018). Scaffold with increased stiffness will promote the formation of actin cytoskeleton, the actin filament will be more abundance and widespread on stiff scaffold fibers, which is in line with our observation (Figure 4. 18). Huang et al. mentioned that stiff substrate favours the adhesion and formation of actin cytoskeleton of stem cell, which preferentially induce the osteogenic differentiation of stem cell. Another study also reported that shape of stem cell dictates stem cell fate, for instance, osteogenic differentiation led to flatten or spread cell shape (Spandidos et al., 2010; Tay et al., 2013). Gene expression test will be further discussed in the next section, regarding the differentiation of ADMSC.

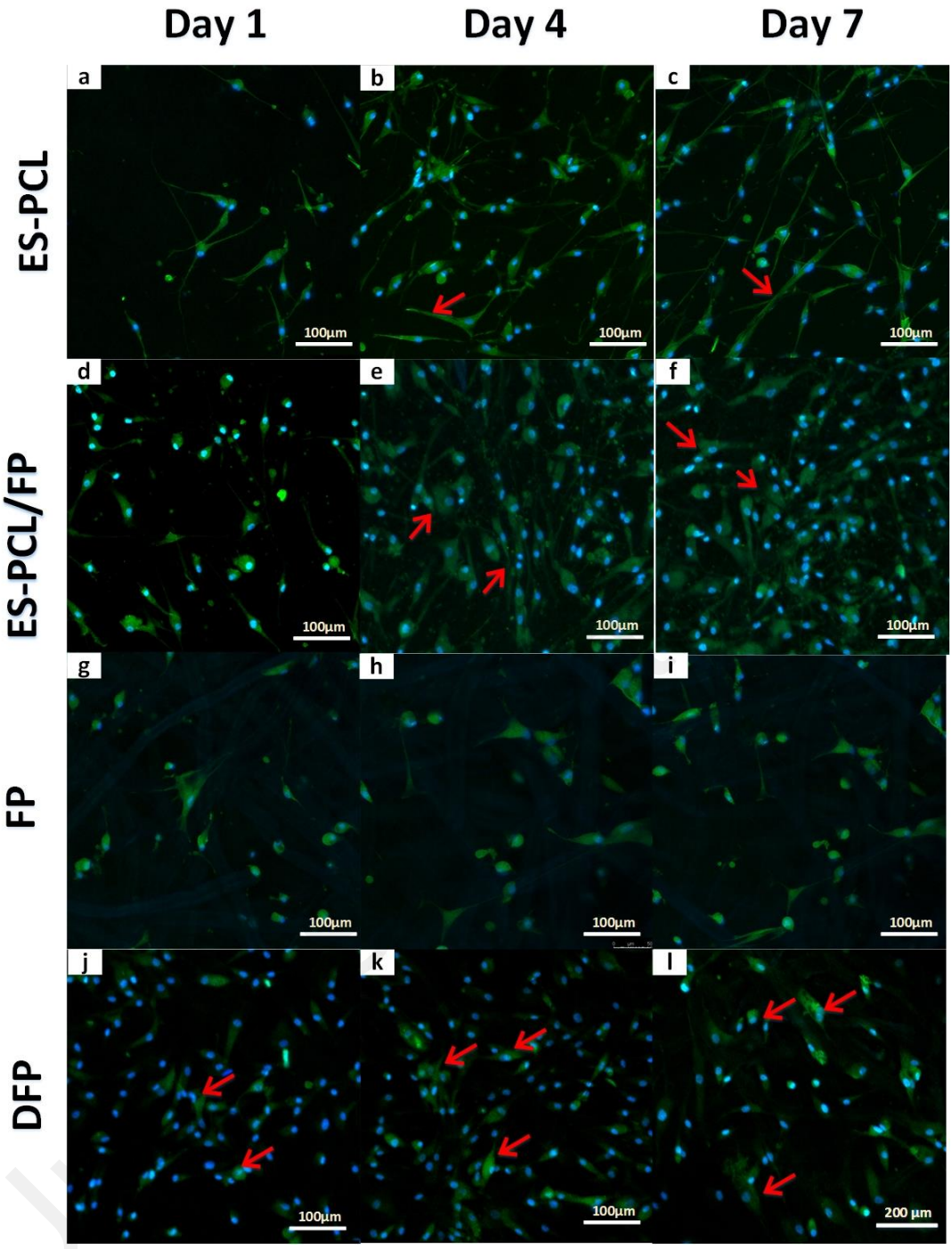

Figure 4. 18: Extracellular matrix analysis. Actin cytoskeleton (Phalloidin) and nuclei (Dapi) confocal imaging results for ADMSC seeded-in (ES-PCL, ES-PCL/FP, FP, and DFP) at different time point.

4.3.2.6 Osteogenic Gene Expression

A comprehensive study into the potential of scaffold materials requires the use of stem cells for *in vitro* study, because MSCs (mainly present in blood and bone marrow) are the first cells attracted into the peri-implant region to colonize the implant surface. The

adhesion interaction of stem cells with topographical surface features of implants dictates cell growth and stem cell fate (Dalby et al., 2014). Surface topography features provide biophysical cues that could synergistically and antagonistically regulate cell behaviour and function, such as spreading, migration, self-renewal, differentiation, and apoptosis (G. Huang et al., 2017). Furthermore, surface topography also induces mechanical stress in cell cytoskeletons that dictate lineage commitment and gene expression. The morphology of stem cells and cytoskeleton distribution are altered to conform with the physical characteristic of surface topography via the process of dynamic interaction (Ambriz et al., 2018; G. Huang et al., 2017). Stem cells with a wide spread cytoskeletal morphology are reported to have a higher tendency towards osteogenesis, the wide spread morphology providing greater cell anchorage that allow the stem cells to conform better to the surface of topography, thus inducing higher cytoskeletal tension and mechanotransduction, essential in osteogenesis (Ambriz et al., 2018; Lavenus et al., 2011). Several studies have reported that nano-scaled PCL fiber could promote and enhance the osteogenic potency of human tissue- derived mesenchymal stem cells. Engler et al. reported that nanoscale topography stimulates human stem cell differentiation and promotes bone mineralisation without osteogenic factors (Engler et al., 2006). Experimental results from scaffolds in previous sections have shown nanoscale fiber size and widespread cytoskeletons, which suggest the possibility of osteogenic differentiation. In this study, the osteogenic potential of ADMSCs on scaffolds was examined by using genes involved in bone formation, such as RUNX2, COL_1, ALP and BGLAP. Generally, successful osteogenic differentiation of ADMSC will show significant up-regulation of early osteogenic gene such as RUNX2, COL_1, and ALP. RUNX2 is the transcriptional activator of osteoblast differentiation that was reported to promote MSC osteogenesis in the early stage (de Peppo et al., 2014; Krishnamurithy et al., 2016; Polini et al., 2011). The expression of RUNX2 and its activity will promote the upregulation of bone specific extracellular matrix, thus increasing the expression of COL_1, and ALP

(M. H. You et al., 2010). BGLAP, that signifies the late stage of osteogenesis, was used in various studies as an indicator that detects the presence of osteocalcin in the mature osteoblast phase.

Figure 4. 19 shows the fold change relative to control over the span of 21 days. The level of expression of ADMSCs cultured on control scaffold is represented by 1. It was hypothesized that the expression of RUNX2, COL-I, ALP and BGLAP would increase in three weeks in response to surface topographical features of scaffolds. Figure 4. 19 shows that level of expression of these four genes (RUNX2, COL_1, ALP and BGLAP) are higher on ES PCL/FP scaffold compared to DFP. However, the level of expression of these genes throughout the 3 time points is not significantly different to control. The lack of expression suggests that osteogenesis does not take place in the 21 day period. Stem cells which grow on rigid surfaces (higher elastic modulus) have a higher tendency to differentiate to osteoblast lineage. Engler et al. reported that MSC cultured on rigid polymeric matric, with Young's modulus greater than 25kPa, show greatest expression of osteogenic transcript. Chemical inducer, such as Dexamethasone, was used in most of the lineage specification study of MSCs ascribed to its great efficiency in directing stem cell differentiation into desired lineage. (Engler et al., 2006; Mooney et al., 1992). However, the results suggest that the biophysical cues exerted by the topography and mechanical stiffness is insufficient to induce osteogenic differentiation. Biophysical cues serve as a double-check mechanism in stem cell differentiation, and need to combine with biochemical cues to promote efficient differentiation of stem cells toward specific lineages (Cao et al., 2011). Solvent used in dissolving polymer prior to electrospinning also affects stem cell differentiation. Elbay et al. reported that acetone was able to promote osteogenesis. Hence, in future study, acetone will be used to replace toluene used in the present study.

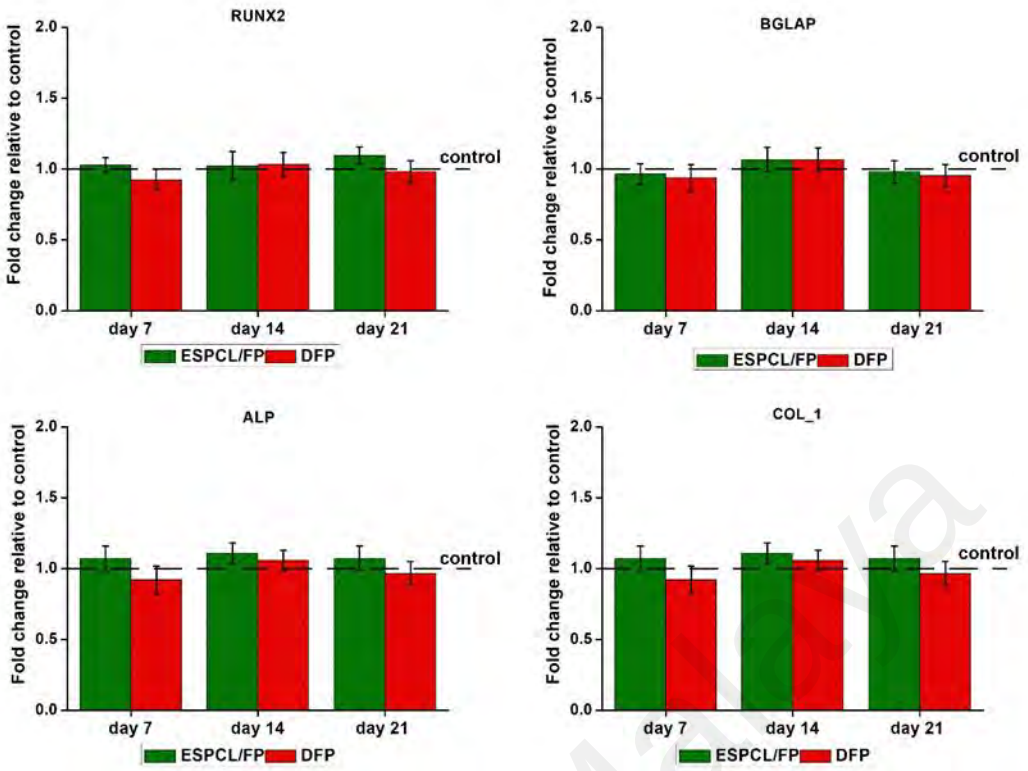

Figure 4. 19: qPCR gene expression of osteogenic markers at three time-points a) RUNX2, b) BGLAP, c) ALP and d) COL_1

4.4 Medium deprivation test

Paper is a cellulose derive 3D substrate that is employed as materials for tissue engineering and biomedical application. Paper is a porous and rigid natural derived material that has shown promising criteria in regenerative medicine application. The porous 3D construct of paper has interconnected pore that allow cell proliferation and migration. This unique ECM mimicking structure of paper scaffold has provided adequate mechanical support for cell growth and also flexibility to fabricate into complex geometry (J. Li et al., 2019). There are two other capabilities of water ascribe to this unique feature of paper, which are wicking capability and liquid storage capability. The potential of wicking and liquid storage capability of paper in the application of point-of-care diagnostic device and microfluidic chips were often reported by researcher (Deiss, Funes-Huacca, et al., 2014; Deka et al., 2020; Rahimi et al., 2015). However, the potential of these properties in cell culture and tissue engineering still await further elucidation. In

this study, we have selected osteoblasts, and mesenchymal stem cells to study their cellular response on the PCL polymer modified paper-based scaffolds samples in limited medium. Cell will grow on the limited medium stored within the 3D porous structure of the scaffold. The viability and proliferation of cell under such medium deprived condition will be discussed in following section.

4.1.1 ADMSC

Figure 4. 20 shows the proliferation of ADMSC measured at the different time points (i.e., day 1, day 2, day 3 and day 4) for all groups of scaffolds, under limited medium conditions. On day 1, the proliferation results between scaffolds are comparable to each other and the difference is not significant. Cell proliferation of ES-PCL, ES- PCL/FP, FP and DFP display a descending trend from day 1 to day 4. DFP shows the lowest proliferation throughout all time points. The cell proliferation results of ES-PCL were higher than FP on day 2 and day 3 but show a drastic decrease on day 4. On day 2, the cell proliferation on ES-PCL/FP increased significantly compared to previous time points and descended steadily on day 3 and day 4. ES-PCL/FP shows the highest cell proliferation on all time points. The cell proliferation was significantly higher than other scaffolds on day 2, day 3 and day 4. The higher cell proliferation on ES-PCL/FP was ascribed to the better medium sorption and retention capability.as shown in Figure 4. 3.

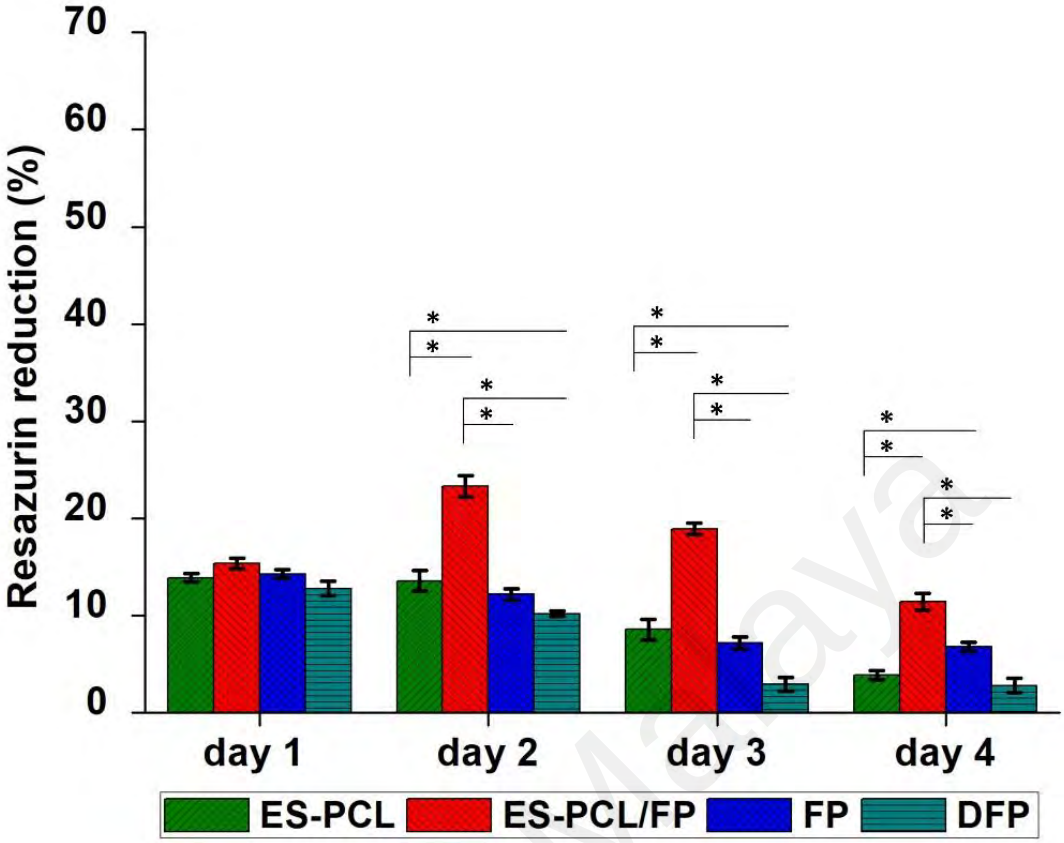

Figure 4. 20: Cell proliferation analysis under medium deprivation condition. Resazurin proliferation assay results for (ES-PCL, ES-PCL/FP, FP, and DFP).

Figure 4. 21 shows a confocal microscopic image of scaffolds stained with live-dead staining solution. There are clearly more live cells on the ES-PCL/FP at each time point (Figure 4. 21 e-h) compared to other scaffolds. The number of live cells drastically increased on day 2, and Figure 4. 21 f shows the highest number of live cells compared to all other scaffolds at different time point. The number of live cells dropped by day 3, live cells are barely visible on day 4 and an abundance of dead cells appeared on the scaffold surface. Figure 4. 22 shows that the percentage of live cells on the ES-PCL/FP was 80% on day 1, 97% on day 2, 97% on day 3, and dropped drastically on day 4 to 23%. The high cell viability is ascribed to high medium absorption and retention ability of the ES-PCL/FP scaffold, the hydrophobic electrospun PCL layer acting as an insulator that slows down the loss of medium via evaporation. DFP and ES-PCL have a low percentage of medium sorption (Figure 4. 3) and does not perform well in this medium

deprivation test. The number of live cells on the surface of DFP (Figure 4. 21 m-o) and ESPCL (Figure 4. 21 a-d) is low compared to other scaffolds. On day 3 and day 4, the percentage of dead cell on DFP had reached 100% (Figure 4. 22) as DFP had lost most of the medium stored within it. ES-PCL scaffold was also covered with dead cells on day 4 (Figure 4. 21 d), and the percentage of live cell was only 10%.

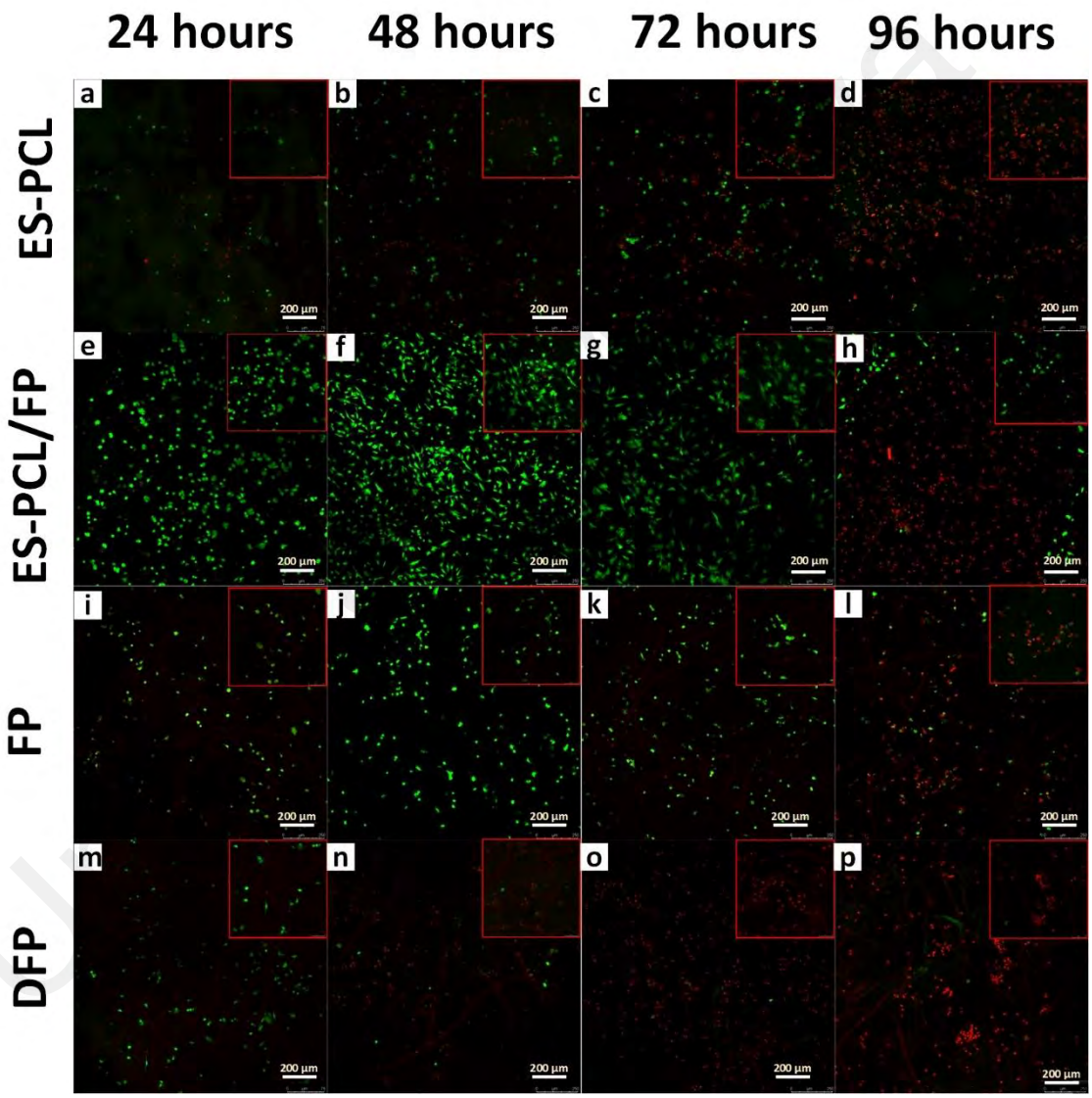

Figure 4. 21: Cell viability analysis under medium deprivation condition. Live/dead confocal of ADMSC plotted separately for each individual substrate ES-PCL, ES-PCL/FP, FP, and DFP on different days.

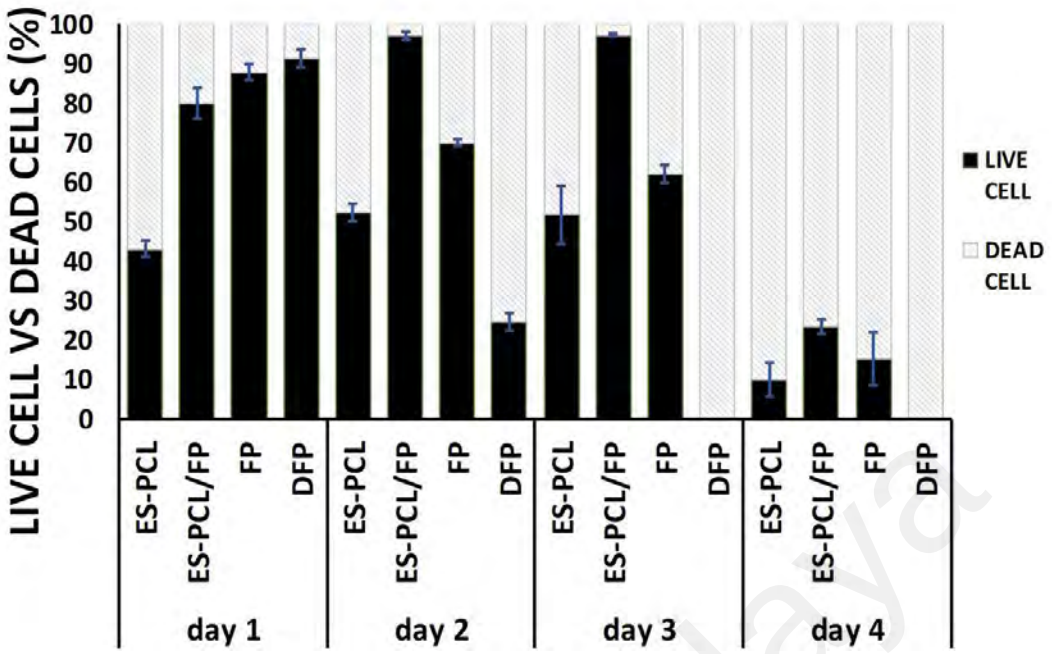

Figure 4. 22: Cell viability analysis on the percentage of live cell vs dead cell under medium deprivation condition. Based on the Live/dead confocal image of ADMSC seeded on each individual substrate ES-PCL, ES-PCL/FP, FP, and DFP on different days.

ADMSCs grown on ES-PCL/FP have shown significant up-regulated growth and highest proliferation results, on time points day 1, 4 and 7, similar results shown by HFOB grown on ES-PCL/FP shown in Figure 4. 7. The results demonstrated that paper as a substrate coated with PCL by electrospinning modification methods show a satisfactory in vitro cytocompatibility with the different types of cell sources and capable of promoting their proliferation rate.

CHAPTER 5: CONCLUSION

As mentioned in section 1.3, 3 objectives have been established for this study. The intention of the study is to improve paper-based scaffolds in terms of their physical properties and biocompatibility, which are the important properties of bioscaffolds for tissue engineering applications. The composite paper-based scaffolds were prepared by coating PCL polymers onto filter paper. Incorporation of PCL onto the filter paper can be achieved via two methods, namely, electrospinning and dip coating. The results show that the electrospinning modification method has an edge over the dip coating method and the physical properties and mechanical performance of ES-PCL/FP scaffold were significantly better than the DFP scaffold. The thin layer of electrospun PCL nanofibers not only produce the bimodal hierarchical structure but also enhance many other properties of the ES-PCL/FP scaffold. Electrospun PCL onto paper has enhanced the tensile strength (5.80±0.32 MPa) and Young's modulus (72.99±3.90 MPa) compared to dip coating paper with PCL (tensile strength 3.54±0.17 MPa and Young's modulus 52.41±5.43 MPa). The higher degree of fiber-to-fiber fusion in the more densely packed and overlapped nanofibers significantly increased the paper's mechanical properties. The hydrophobic thin layer of electrospun PCL on ES-PCL/FP scaffold also reduces the medium evaporation, thus giving it the highest reading in medium sorption and retention tests. The comparison of ES-PCL/FP and FP scaffolds showed that coating a thin layer of electrospun PCL has increased the overall porosity of the scaffold by approximately three-fold. The results of water contact angle analysis also show that the hygroscopic properties are altered by the thin layer of electrospun PCL.

In vitro studies were performed to access the biocompatibility of composite PCL and paper scaffolds. HFOB, and ADMSC were selected to study the cellular response of paper-based scaffolds in adhesion, proliferation, and differentiation. In vitro studies have shown that the cells have responded positively towards ES-PCL/FP scaffold. The use of electrospinning modification significantly improves biocompatibility. HFOB and

ADMSC have shown greater adhesion and bone maturation at an early stage on ES-PCL/FP scaffold. It can be seen in FESEM and confocal images that cells were more widespread and tightly anchored on the surface of ES-PCL/FP scaffold. The abundance of live cells on the surface of ES-PCL/FP scaffold shown by confocal images suggests that ES-PCL/FP is a more favourable substrate for the culture of HFOB and ADMSC. HFOBs cultured on the ES-PCL/FP scaffold also gave rise to significantly improved ALP activity compared to other prepared scaffolds, which indicates improved osteoblast functionality by the nano-sized fiber on ES-PCL/FP scaffold. The significantly improved in vitro results are attributed to the unique ECM-mimicking bimodal structure of ES-PCL/FP. The ADMSC have illustrated a more flatten and well-organized actin cytoskeleton on the ES-PCL/FP scaffold compared to other prepared scaffolds. Despite the widespread actin cytoskeletons suggest the possibility of osteogenic differentiation, the level of expression of osteogenic genes such as RUNX2, COL_1, ALP and BGLAP were not significant over the span of three weeks. ADMSC grown on different scaffolds measured in limited supply of medium shows higher proliferation and viability on ES-PCL/FP scaffold ascribe to its medium sorption and retention capability.

In conclusion, the electrospinning modification method could be an ideal method to fabricate a paper-based scaffold as it was reported it enhanced protein binding to the scaffold (C. T. Yew et al., 2018). There were probably cell adhesion proteins present in the culture medium which mediate cell-material interactions. Physical properties and mechanical properties of ES-PCL/FP scaffold were significantly enhanced as well compared to DFP scaffold. In vitro studies on both hFOBs and ADMSC showed better biocompatibility on ES-PCL/FP scaffold. Results of medium deprivation tests also suggest that ES-PCL/FP scaffold can retain enough medium to support cell growth for 2 days. Collectively, the electrospinning modification method a produced paper-based scaffold that has potential to be used as a portable cell culture platform.

There are several suggestions for future improvement of the paper-based scaffold fabricated in this study. The focus of this study is on the modification of biophysical aspect of scaffold, mainly focused on the effect of topographical cues and architectural structure. Biochemical modification should be done in future work. The effect of bioactive additives and fillers such as hydroxyapatite, bioglass, graphene and growth factors on the biocompatibility and physical properties of scaffold should be investigated. The use of chemical induction medium should also be included in future work to investigate the potential synergistic effects of stem cell differentiation on the paper-based scaffold.

The bimodal structure of ES-PCL/FP scaffold can be adapted for co-culture studies, where interaction of cells such as pancreatic alpha /beta cells, and its effect on insulin and glucagon secretion can be investigated. In addition, mechanical stretching that resembles load bearing in the human body and medium perfusion that simulates interstitial fluid flow can be incorporated into the model to better simulate *in vivo* conditions.

REFERENCES

Abbott, A. (2003). Cell culture: Biology's new dimension. *Nature, 424*(6951), 870-872. Retrieved from http://dx.doi.org/10.1038/424870a

AbdelHafez, F. F., Desai, N., Abou-Setta, A. M., Falcone, T., & Goldfarb, J. (2010). Slow freezing, vitrification and ultra-rapid freezing of human embryos: a systematic review and meta-analysis. *Reproductive biomedicine online, 20*(2), 209-222.

Aghdam, R. M., Shakhesi, S., Najarian, S., Mohammadi, M. M., Tafti, S. H. A., & Mirzadeh, H. (2014). Fabrication of a Nanofibrous Scaffold for the In Vitro Culture of Cardiac Progenitor Cells for Myocardial Regeneration. *International Journal of Polymeric Materials and Polymeric Biomaterials, 63*(5), 229-239. doi:10.1080/00914037.2013.800983

Agrawal, C. M., & Ray, R. B. (2001). Biodegradable polymeric scaffolds for musculoskeletal tissue engineering. *J Biomed Mater Res, 55*(2), 141-150. doi:doi:10.1002/1097-4636(200105)55:2<141::AID-JBM1000>3.0.CO;2-J

Alvarez, K., & Nakajima, H. (2009). Metallic Scaffolds for Bone Regeneration. *Materials, 2*(3), 790-832. doi:10.3390/ma2030790

Ambriz, X., de Lanerolle, P., & Ambrosio, J. (2018). The mechanobiology of the actin cytoskeleton in stem cells during differentiation and interaction with biomaterials. *Stem cells international, 2018*.

Amin, A. M., & Ewais, E. M. (2017). Bioceramic scaffolds. *Scaffolds in Tissue EngineeringMaterials, Technologies and Clinical Applications*, 49.

Amini, A. R., Laurencin, C. T., & Nukavarapu, S. P. (2012). Bone tissue engineering: recent advances and challenges. *Crit Rev Biomed Eng, 40*(5), 363-408. Retrieved from https://www.ncbi.nlm.nih.gov/pubmed/23339648

Arima, Y., & Iwata, H. (2007). Effect of wettability and surface functional groups on protein adsorption and cell adhesion using well-defined mixed self-assembled monolayers. *Biomaterials, 28*(20), 3074-3082.

Azari, P., Hosseini, S., Murphy, B. P., & Martinez-Chapa, S. O. (2018). Electrospun Biopolyesters: Hydrophobic Scaffolds With Favorable Biological Response. *Journal of Public Health International, 1*(1), 5.

Bäckdahl, H., Esguerra, M., Delbro, D., Risberg, B., & Gatenholm, P. (2008). Engineering microporosity in bacterial cellulose scaffolds. *Journal of Tissue Engineering and Regenerative Medicine, 2*(6), 320-330. doi:10.1002/term.97

Badami, A. S., Kreke, M. R., Thompson, M. S., Riffle, J. S., & Goldstein, A. S. (2006). Effect of fiber diameter on spreading, proliferation, and differentiation of osteoblastic cells on electrospun poly(lactic acid) substrates. *Biomaterials, 27*(4), 596-606. doi:10.1016/j.biomaterials.2005.05.084

Badimon, L., Oñate, B., & Vilahur, G. (2015). Adipose-derived mesenchymal stem cells and their reparative potential in ischemic heart disease. *Revista Española de Cardiología (English Edition), 68*(7), 599-611.

Badylak, S. F., Freytes, D. O., & Gilbert, T. W. (2009). Extracellular matrix as a biological scaffold material: Structure and function. *Acta Biomaterialia, 5*(1), 1-13. doi:https://doi.org/10.1016/j.actbio.2008.09.013

Baer, P. C. (2014). Adipose-derived mesenchymal stromal/stem cells: An update on their phenotype in vivo and in vitro. *World journal of stem cells, 6*(3), 256-265. doi:10.4252/wjsc.v6.i3.256

Baharloo, B., Textor, M., & Brunette, D. M. (2005). Substratum roughness alters the growth, area, and focal adhesions of epithelial cells, and their proximity to titanium surfaces. *Journal of Biomedical Materials Research Part A, 74A*(1), 12-22. doi:10.1002/jbm.a.30321

Bhattacharya, M., Malinen, M. M., Lauren, P., Lou, Y.-R., Kuisma, S. W., Kanninen, L., . . . Yliperttula, M. (2012). Nanofibrillar cellulose hydrogel promotes three-dimensional liver cell culture. *Journal of Controlled Release, 164*(3), 291-298. doi:http://dx.doi.org/10.1016/j.jconrel.2012.06.039

Bianco, P., Robey, P. G., & Simmons, P. J. (2008). Mesenchymal stem cells: revisiting history, concepts, and assays. *Cell stem cell, 2*(4), 313-319. doi:10.1016/j.stem.2008.03.002

Binulal, N. S., Natarajan, A., Menon, D., Bhaskaran, V. K., Mony, U., & Nair, S. V. (2014). PCL–gelatin composite nanofibers electrospun using diluted acetic acid–ethyl acetate solvent system for stem cell-based bone tissue engineering. *Journal of Biomaterials Science, Polymer Edition, 25*(4), 325-340. doi:10.1080/09205063.2013.859872

Bissell, M. (2003). Biology's new dimension. *Nature, 424*, 870-872.

Cai, H., Sharma, S., Liu, W., Mu, W., Liu, W., Zhang, X., & Deng, Y. (2014). Aerogel microspheres from natural cellulose nanofibrils and their application as cell culture scaffold. *Biomacromolecules, 15*(7), 2540-2547. doi:10.1021/bm5003976

Camci-Unal, G., Laromaine, A., Hong, E., Derda, R., & Whitesides, G. M. (2016). Biomineralization guided by paper templates. *Scientific reports, 6*(1), 1-12.

Cao, D., Wu, Y.-P., Fu, Z.-F., Tian, Y., Li, C.-J., Gao, C.-Y., . . . Feng, X.-Z. (2011). Cell adhesive and growth behavior on electrospun nanofibrous scaffolds by designed multifunctional composites. *Colloids and Surfaces B: Biointerfaces, 84*(1), 26-34. doi:https://doi.org/10.1016/j.colsurfb.2010.12.005

Caridade, S. G., Merino, E. G., Alves, N. M., & Mano, J. F. (2012). Bioactivity and viscoelastic characterization of chitosan/bioglass® composite membranes. *Macromol Biosci, 12*(8), 1106-1113. doi:10.1002/mabi.201200036

Chen, V. J., & Ma, P. X. (2006). The effect of surface area on the degradation rate of nano-fibrous poly (L-lactic acid) foams. *Biomaterials, 27*(20), 3708-3715.

Chen, Y.-H., Kuo, Z.-K., & Cheng, C.-M. Paper – a potential platform in pharmaceutical development. *Trends in Biotechnology, 33*(1), 4-9. doi:10.1016/j.tibtech.2014.11.004

Chen, Y. H., Kuo, Z. K., & Cheng, C. M. (2015). Paper – a potential platform in pharmaceutical development. *Trends in Biotechnology, 33*(1), 4–9.

Cheng, G., Chen, J., Wang, Q., Yang, X., Cheng, Y., Li, Z., . . . Li, Z. (2018). Promoting osteogenic differentiation in pre-osteoblasts and reducing tibial fracture healing time using functional nanofibers. *Nano Research, 11*(7), 3658-3677. doi:10.1007/s12274-017-1934-3

Cheng, M. L., Lin, C. C., Su, H. L., Chen, P. Y., & Sun, Y. M. (2008). Processing and characterization of electrospun poly(3-hydroxybutyrate-co-3-hydroxyhexanoate) nanofibrous membranes. *Polymer, 49*(2), 546-553. doi:10.1016/j.polymer.2007.11.049

Choi, J. R., Tang, R., Wang, S., Wan Abas, W. A. B., Pingguan-Murphy, B., & Xu, F. (2015). Paper-based sample-to-answer molecular diagnostic platform for point-of-care diagnostics. *Biosensors and Bioelectronics, 74*, 427-439. doi:http://dx.doi.org/10.1016/j.bios.2015.06.065

Chong, Y. K., Toh, T. B., Zaiden, N., Poonepalli, A., Leong, S. H., Ong, C. E., . . . Tang, C. (2009). Cryopreservation of neurospheres derived from human glioblastoma multiforme. *Stem Cells, 27*(1), 29-39. doi:10.1634/stemcells.2008-0009

Christopherson, G. T., Song, H., & Mao, H. Q. (2009). The influence of fiber diameter of electrospun substrates on neural stem cell differentiation and proliferation. *Biomaterials, 30*(4), 556-564. doi:10.1016/j.biomaterials.2008.10.004

Chung, S., & King, M. W. (2011). Design concepts and strategies for tissue engineering scaffolds. *Biotechnology and applied biochemistry, 58*(6), 423-438.

Cipitria, A., Skelton, A., Dargaville, T., Dalton, P., & Hutmacher, D. (2011). Design, fabrication and characterization of PCL electrospun scaffolds—a review. *Journal of Materials Chemistry, 21*(26), 9419-9453.

Cipitria, A., Skelton, A., Dargaville, T. R., Dalton, P. D., & Hutmacher, D. W. (2011). Design, fabrication and characterization of PCL electrospun scaffolds—a review. *Journal of Materials Chemistry, 21*(26), 9419-9453. doi:10.1039/C0JM04502K

Costa, D. O., Prowse, P. D. H., Chrones, T., Sims, S. M., Hamilton, D. W., Rizkalla, A. S., & Dixon, S. J. (2013). The differential regulation of osteoblast and osteoclast activity by surface topography of hydroxyapatite coatings. *Biomaterials, 34*(30), 7215-7226. doi:https://doi.org/10.1016/j.biomaterials.2013.06.014

Cramer, S. M., Larson, T. S., & Lockett, M. R. (2019). Tissue Papers: Leveraging Paper-Based Microfluidics for the Next Generation of 3D Tissue Models. *Analytical Chemistry, 91*(17), 10916-10926. doi:10.1021/acs.analchem.9b02102

Cukierman, E., Pankov, R., Stevens, D. R., & Yamada, K. M. (2001). Taking cell-matrix adhesions to the third dimension. *Science, 294*(5547), 1708-1712.

Dai, G., Liu, X., Zhang, Z., Yang, Z., Dai, Y., & Xu, R. (2013). Transplantation of autologous bone marrow mesenchymal stem cells in the treatment of complete and chronic cervical spinal cord injury. *Brain research, 1533*, 73-79.

Dalby, M. J., Gadegaard, N., & Oreffo, R. O. C. (2014). Harnessing nanotopography and integrin–matrix interactions to influence stem cell fate. *Nature Materials, 13*(6), 558-569. doi:10.1038/nmat3980

de Peppo, G. M., Agheli, H., Karlsson, C., Ekström, K., Brisby, H., Lennerås, M., . . . Petronis, S. (2014). Osteogenic response of human mesenchymal stem cells to well-defined nanoscale topography in vitro. *International Journal of Nanomedicine, 9*, 2499-2515. doi:10.2147/IJN.S58805

de Silva, M., desai, R., & Odde, D. (2004). Micro-Patterning of Animal Cells on PDMS Substrates in the Presence of Serum without Use of Adhesion Inhibitors. *Biomedical Microdevices, 6*(3), 219-222. doi:10.1023/B:BMMD.0000042051.09807.8c

Deiss, F., Funes-Huacca, M. E., Bal, J., Tjhung, K. F., & Derda, R. (2014). Antimicrobial susceptibility assays in paper-based portable culture devices. *Lab on a Chip, 14*(1), 167-171.

Deiss, F., Matochko, W. L., Govindasamy, N., Lin, E. Y., & Derda, R. (2014). Flow-Through Synthesis on Teflon-Patterned Paper To Produce Peptide Arrays for Cell-Based Assays. *Angewandte Chemie International Edition, 53*(25), 6374-6377.

doi:10.1002/anie.201402037

Deiss, F., Mazzeo, A., Hong, E., Ingber, D. E., Derda, R., & Whitesides, G. M. (2013). Platform for High-Throughput Testing of the Effect of Soluble Compounds on 3D Cell Cultures. *Analytical Chemistry, 85*(17), 8085-8094. doi:10.1021/ac400161j

Deka, B., Kalita, R., Bhatia, D., & Mishra, A. (2020). Applications of paper as a support material in biomedical sciences: A decadal review. *Sensors International, 1*, 100004. doi:https://doi.org/10.1016/j.sintl.2020.100004

Derda, R., Laromaine, A., Mammoto, A., Tang, S. K., Mammoto, T., Ingber, D. E., & Whitesides, G. M. (2009). Paper-supported 3D cell culture for tissue-based bioassays. *Proceedings of the National Academy of Sciences of the United States of America, 106*(44), 18457-18462.

Derda, R., Laromaine, A., Mammoto, A., Tang, S. K., Mammoto, T., Ingber, D. E., & Whitesides, G. M. (2009). Paper-supported 3D cell culture for tissue-based bioassays. *Proc Natl Acad Sci U S A, 106*(44), 18457-18462. doi:10.1073/pnas.0910666106

Derda, R., Laromaine, A., Mammoto, A., Tang, S. K. Y., Mammoto, T., Ingber, D. E., & Whitesides, G. M. (2009). Paper-supported 3D cell culture for tissue-based bioassays. *Proceedings of the National Academy of Sciences, 106*(44), 18457-18462. doi:10.1073/pnas.0910666106

Derda, R., Tang, S. K., Laromaine, A., Mosadegh, B., Hong, E., Mwangi, M., . . . Whitesides, G. M. (2011). Multizone paper platform for 3D cell cultures. *PLoS One, 6*(5), e18940. doi:10.1371/journal.pone.0018940

Derda, R., Tang, S. K. Y., Laromaine, A., Mosadegh, B., Hong, E., Mwangi, M., . . . Whitesides, G. M. (2011). Multizone Paper Platform for 3D Cell Cultures. *PLoS ONE, 6*(5), e18940. doi:10.1371/journal.pone.0018940

Dettin, M., Zamuner, A., Roso, M., Gloria, A., Iucci, G., Messina, G. M., . . . Brun, P. (2015). Electrospun Scaffolds for Osteoblast Cells: Peptide-Induced Concentration-Dependent Improvements of Polycaprolactone. *PLoS One, 10*(9), e0137505. doi:10.1371/journal.pone.0137505

Diban, N., & Stamatialis, D. F. (2011). Functional Polymer Scaffolds for Blood Vessel Tissue Engineering. *Advanced Polymers in Medicine, 309-310*(1), 93-99. doi:10.1002/masy.201100038

Discher, D. E., Janmey, P., & Wang, Y.-l. (2005). Tissue Cells Feel and Respond to the Stiffness of Their Substrate. *Science, 310*(5751), 1139-1143. doi:10.1126/science.1116995

Dominici, M., Le Blanc, K., Mueller, I., Slaper-Cortenbach, I., Marini, F., Krause, D., . . . Horwitz, E. (2006). Minimal criteria for defining multipotent mesenchymal stromal cells. The International Society for Cellular Therapy position statement. *Cytotherapy, 8*(4), 315-317.

Dong, X., Pan, R., Zhang, H., Yang, C., Shao, J., & Xiang, L. (2013). Modification of histone acetylation facilitates hepatic differentiation of human bone marrow mesenchymal stem cells. *PLoS ONE, 8*(5).

Engler, A. J., Sen, S., Sweeney, H. L., & Discher, D. E. (2006). Matrix Elasticity Directs Stem Cell Lineage Specification. *Cell, 126*(4), 677-689. doi:https://doi.org/10.1016/j.cell.2006.06.044

Fang, R., Zhang, E., Xu, L., & Wei, S. (2010). Electrospun PCL/PLA/HA Based Nanofibers as Scaffold for Osteoblast-Like Cells. *Journal of Nanoscience and Nanotechnology, 10*(11), 7747-7751. doi:10.1166/jnn.2010.2831

Feinberg, A. W., Wilkerson, W. R., Seegert, C. A., Gibson, A. L., Hoipkemeier-Wilson, L., & Brennan, A. B. (2008). Systematic variation of microtopography, surface chemistry and elastic modulus and the state dependent effect on endothelial cell alignment. *Journal of Biomedical Materials Research Part A, 86A*(2), 522-534. doi:10.1002/jbm.a.31626

Ferro, F., Shields Baheney, C., & Spelat, R. (2014). Three-Dimensional (3D) Cell Culture Conditions, Present and Future Improvements. *Razavi Int J Med, 2*(2), e17803. doi:10.5812/rijm.17803

Francis, L. F., McCormick, A. V., Vaessen, D. M., & Payne, J. A. (2002). Development and measurement of stress in polymer coatings. *Journal of Materials Science, 37*(22), 4717-4731. doi:10.1023/A:1020886802632

Francis, S. L., Duchi, S., Onofrillo, C., Di Bella, C., & Choong, P. F. M. (2018). Adipose-Derived Mesenchymal Stem Cells in the Use of Cartilage Tissue Engineering: The Need for a Rapid Isolation Procedure. *Stem cells international, 2018*, 8947548-8947548. doi:10.1155/2018/8947548

Frantz, C., Stewart, K. M., & Weaver, V. M. (2010). The extracellular matrix at a glance. *J Cell Sci, 123*(24), 4195-4200.

Fraser, J. K., Wulur, I., Alfonso, Z., & Hedrick, M. H. (2006). Fat tissue: an underappreciated source of stem cells for biotechnology. *Trends in biotechnology, 24*(4), 150-154. doi:10.1016/j.tibtech.2006.01.010

Frey, O., Misun, P. M., Fluri, D. A., Hengstler, J. G., & Hierlemann, A. (2014). Reconfigurable microfluidic hanging drop network for multi-tissue interaction

and analysis. *Nat Commun, 5*. doi:10.1038/ncomms5250

Frimat, J.-P., Menne, H., Michels, A., Kittel, S., Kettler, R., Borgmann, S., . . . West, J. (2009). Plasma stencilling methods for cell patterning. *Analytical and Bioanalytical Chemistry, 395*(3), 601-609. doi:10.1007/s00216-009-2824-7

Funes-Huacca, M., Wu, A., Szepesvari, E., Rajendran, P., Kwan-Wong, N., Razgulin, A., . . . Derda, R. (2012). Portable self-contained cultures for phage and bacteria made of paper and tape. *Lab Chip, 12*(21), 4269-4278. doi:10.1039/c2lc40391a

Ge, L., Yan, J., Song, X., Yan, M., Ge, S., & Yu, J. (2012). Three-dimensional paper-based electrochemiluminescence immunodevice for multiplexed measurement of biomarkers and point-of-care testing. *Biomaterials, 33*(4), 1024-1031. doi:http://dx.doi.org/10.1016/j.biomaterials.2011.10.065

Geckil, H., Xu, F., Zhang, X., Moon, S., & Demirci, U. (2010). Engineering hydrogels as extracellular matrix mimics. *Nanomedicine (London, England), 5*(3), 469-484. doi:10.2217/nnm.10.12

Golub, E. E., & Boesze-Battaglia, K. (2007). The role of alkaline phosphatase in mineralization. *Current opinion in Orthopaedics, 18*(5), 444-448.

Goody, M. F., & Henry, C. A. (2010). Dynamic interactions between cells and their extracellular matrix mediate embryonic development. *Molecular Reproduction and Development: Incorporating Gamete Research, 77*(6), 475-488.

Griffith, L. G. (2000). Polymeric biomaterials. *Acta Materialia, 48*(1), 263-277. Retrieved from http://www.sciencedirect.com/science/article/pii/S1359645499002992

Groeber, F., Holeiter, M., Hampel, M., Hinderer, S., & Schenke-Layland, K. (2011). Skin tissue engineering—in vivo and in vitro applications. *Advanced drug delivery reviews, 63*(4-5), 352-366.

Grove, J. E., Bruscia, E., & Krause, D. S. (2004). Plasticity of Bone Marrow–Derived Stem Cells. *STEM CELLS, 22*(4), 487-500. doi:10.1634/stemcells.22-4-487

Gupta, B., Revagade, N., & Hilborn, J. (2007). Poly (lactic acid) fiber: An overview. *Progress in Polymer Science, 32*(4), 455-482.

Harris, S. A., Tau, K. R., Enger, R. J., Toft, D. O., Riggs, B. L., & Spelsberg, T. C. (1995). Estrogen response in the hFOB 1.19 human fetal osteoblastic cell line stably transfected with the human estrogen receptor gene. *Journal of Cellular Biochemistry, 59*(2), 193-201. doi:10.1002/jcb.240590209

Hassan, M., Chong, L., & Sultana, N. (2006). Wettability and water uptake properties of pla and pcl/gelatin-based electrospun scaffolds.

Haynes, C. A., & Norde, W. (1995). Structures and stabilities of adsorbed proteins. *Journal of colloid and interface science, 169*(2), 313-328.

He, X., Park, E. Y., Fowler, A., Yarmush, M. L., & Toner, M. (2008). Vitrification by ultra-fast cooling at a low concentration of cryoprotectants in a quartz micro-capillary: a study using murine embryonic stem cells. *Cryobiology, 56*(3), 223-232.

Hess, D., Li, L., Martin, M., Sakano, S., Hill, D., Strutt, B., . . . Bhatia, M. (2003). Bone marrow–derived stem cells initiate pancreatic regeneration. *Nature biotechnology, 21*(7), 763-770.

Hinderer, S., Layland, S. L., & Schenke-Layland, K. (2016). ECM and ECM-like materials — Biomaterials for applications in regenerative medicine and cancer therapy. *Advanced Drug Delivery Reviews, 97*, 260-269. doi:https://doi.org/10.1016/j.addr.2015.11.019

Holik, H. (2013). *Handbook of Paper and Board*: Wiley.

Hong, B., Xue, P., Wu, Y., Bao, J., Chuah, Y. J., & Kang, Y. (2016). A concentration gradient generator on a paper-based microfluidic chip coupled with cell culture microarray for high-throughput drug screening. *Biomed Microdevices, 18*(1), 21. doi:10.1007/s10544-016-0054-2

Hoo, S. P., Loh, Q. L., Yue, Z., Fu, J., Tan, T. T., Choong, C., & Chan, P. P. (2013). Preparation of a soft and interconnected macroporous hydroxypropyl cellulose methacrylate scaffold for adipose tissue engineering. *Journal of Materials Chemistry B, 1*(24), 3107-3117.

Howard, D., Buttery, L. D., Shakesheff, K. M., & Roberts, S. J. (2008). Tissue engineering: strategies, stem cells and scaffolds. *Journal of anatomy, 213*(1), 66-72.

Hu, J., Wang, S., Wang, L., Li, F., Pingguan-Murphy, B., Lu, T. J., & Xu, F. (2014). Advances in paper-based point-of-care diagnostics. *Biosensors and Bioelectronics, 54*, 585-597. doi:https://doi.org/10.1016/j.bios.2013.10.075

Hu, J., Wang, S., Wang, L., Li, F., Pingguan-Murphy, B., Lu, T. J., & Xu, F. (2014). Advances in paper-based point-of-care diagnostics. *Biosens Bioelectron, 54*, 585-597. doi:10.1016/j.bios.2013.10.075

Huang, C.-J., & Chang, Y.-C. (2019). Construction of Cell–Extracellular Matrix Microenvironments by Conjugating ECM Proteins on Supported Lipid Bilayers. *Frontiers in Materials, 6*(39). doi:10.3389/fmats.2019.00039

Huang, C., Dai, J., & Zhang, X. A. (2015). Environmental physical cues determine the lineage specification of mesenchymal stem cells. *Biochimica et Biophysica Acta, 1850*(6), 1261-1266. doi:10.1016/j.bbagen.2015.02.011

Huang, G., Li, F., Zhao, X., Ma, Y., Li, Y., Lin, M., . . . Xu, F. (2017). Functional and Biomimetic Materials for Engineering of the Three-Dimensional Cell Microenvironment. *Chemical Reviews, 117*(20), 12764-12850. doi:10.1021/acs.chemrev.7b00094

Huang, G., Wang, L., Wang, S., Han, Y., Wu, J., Zhang, Q., . . . Lu, T. J. (2012). Engineering three-dimensional cell mechanical microenvironment with hydrogels. *Biofabrication, 4*(4), 042001.

Huang, G., Zhang, X., Xiao, Z., Zhang, Q., Zhou, J., Xu, F., & Lu, T. J. (2012). Cell-encapsulating microfluidic hydrogels with enhanced mechanical stability. *Soft Matter, 8*(41), 10687-10694.

Huang, Z.-M., Zhang, Y. Z., Kotaki, M., & Ramakrishna, S. (2003). A review on polymer nanofibers by electrospinning and their applications in nanocomposites. *Composites Science and Technology, 63*(15), 2223-2253. doi:https://doi.org/10.1016/S0266-3538(03)00178-7

Huh, D., Hamilton, G. A., & Ingber, D. E. (2011). From 3D cell culture to organs-on-chips. *Trends in Cell Biology, 21*(12), 745-754. doi:http://dx.doi.org/10.1016/j.tcb.2011.09.005

Iqbal, N., Khan, A. S., Asif, A., Yar, M., Haycock, J. W., & Rehman, I. U. (2019). Recent concepts in biodegradable polymers for tissue engineering paradigms: a critical review. *International Materials Reviews, 64*(2), 91-126.

Ishigami, T., Nii, Y., Ohmukai, Y., Rajabzadeh, S., & Matsuyama, H. (2014). Solidification behavior of polymer solution during membrane preparation by thermally induced phase separation. *Membranes, 4*(1), 113-122.

Jin, G., He, R., Sha, B., Li, W., Qing, H., Teng, R., & Xu, F. (2018). Electrospun three-dimensional aligned nanofibrous scaffolds for tissue engineering. *Materials Science and Engineering: C, 92*, 995-1005. doi:https://doi.org/10.1016/j.msec.2018.06.065

Johnstone, R. W. (2002). Histone-deacetylase inhibitors: novel drugs for the treatment of cancer. *Nature Reviews Drug Discovery, 1*(4), 287-299.

Juvonen, H., Maattanen, A., Lauren, P., Ihalainen, P., Urtti, A., Yliperttula, M., & Peltonen, J. (2013). Biocompatibility of printed paper-based arrays for 2-D cell cultures. *Acta Biomater, 9*(5), 6704-6710. doi:10.1016/j.actbio.2013.01.033

Juvonen, H., Määttänen, A., Laurén, P., Ihalainen, P., Urtti, A., Yliperttula, M., & Peltonen, J. (2013). Biocompatibility of printed paper-based arrays for 2-D cell cultures. *Acta Biomaterialia, 9*(5), 6704-6710. doi:http://dx.doi.org/10.1016/j.actbio.2013.01.033

Kadler, K. E., Baldock, C., Bella, J., & Boot-Handford, R. P. (2007). Collagens at a glance. *Journal of cell science, 120*(12), 1955-1958.

Karageorgiou, V., & Kaplan, D. (2005). Porosity of 3D biomaterial scaffolds and osteogenesis. *Biomaterials, 26*(27), 5474-5491. doi:https://doi.org/10.1016/j.biomaterials.2005.02.002

Kasten, A., Naser, T., Brüllhoff, K., Fiedler, J., Müller, P., Möller, M., . . . Brenner, R. E. (2014). Guidance of mesenchymal stem cells on fibronectin structured hydrogel films. *PLoS ONE, 9*(10), e109411-e109411. doi:10.1371/journal.pone.0109411

Khurana, S., & George, S. P. (2011). The role of actin bundling proteins in the assembly of filopodia in epithelial cells. *Cell adhesion & migration, 5*(5), 409-420. doi:10.4161/cam.5.5.17644

Kim, J. F., Kim, J. H., Lee, Y. M., & Drioli, E. (2016). Thermally induced phase separation and electrospinning methods for emerging membrane applications: A review. *AIChE Journal, 62*(2), 461-490.

Kim, K.-O., Kim, B.-S., Lee, K.-H., Park, Y.-H., & Kim, I.-S. (2013). Osteoblastic cells culture on electrospun poly(ε-caprolacton) scaffolds incorporating amphiphilic PEG–POSS telechelic. *Journal of Materials Science: Materials in Medicine, 24*(8), 2029-2036. doi:10.1007/s10856-013-4943-0

Kim, Y., Ko, D., Uhm, S., Chung, K., & Lee, H. (2003). 103 A NEW PAPER CONTAINER FOR THE VITRIFICATION OF BOVINE EMBRYOS. *Reproduction, Fertility and Development, 16*(2), 173-173.

Kim, Y., Uhm, S., Gupta, M., Yang, J., Lim, J.-G., Das, Z., . . . Kim, N.-H. (2012). Successful vitrification of bovine blastocysts on paper container. *Theriogenology, 78*(5), 1085-1093.

Klemm, D., Kramer, F., Moritz, S., Lindström, T., Ankerfors, M., Gray, D., & Dorris, A. (2011). Nanocelluloses: A New Family of Nature-Based Materials. *Angewandte Chemie International Edition, 50*(24), 5438-5466. doi:10.1002/anie.201001273

Kraskiewicz, H., Breen, B., Sargeant, T., McMahon, S., & Pandit, A. (2013). Assembly of protein-based hollow spheres encapsulating a therapeutic factor. *ACS chemical neuroscience, 4*(9), 1297-1304.

Krishnamurithy, G., Yahya, N. A., Mehrali, M., Mehrali, M., Mohan, S., Murali, M. R., . . . Kamarul, T. (2016). Effects of carbon doping on the microstructural, micro/nano-mechanical, and mesenchymal stromal cells biocompatibility and osteogenic differentiation properties of alumina. *Ceramics International, 42*(16), 18247-18256. doi:https://doi.org/10.1016/j.ceramint.2016.08.148

Kuwayama, M. (2007). Highly efficient vitrification for cryopreservation of human oocytes and embryos: the Cryotop method. *Theriogenology, 67*(1), 73-80.

Lane, M., Bavister, B. D., Lyons, E. A., & Forest, K. T. (1999). Containerless vitrification of mammalian oocytes and embryos. *Nat Biotechnol, 17*(12), 1234-1236. doi:10.1038/70795

Lavenus, S., Berreur, M., Trichet, V., Pilet, P., Louarn, G., & Layrolle, P. (2011). Adhesion and osteogenic differentiation of human mesenchymal stem cells on titanium nanopores. *Eur Cell Mater, 22*, 84-96; discussion 96. doi:10.22203/ecm.v022a07

Lee, K.-H., Sun, J.-C., Chuang, C.-k., Guo, S.-F., Tu, C.-F., & Ju, J.-C. (2013). An efficient and mass reproducible method for vitrifying mouse embryos on a paper in cryotubes. *Cryobiology, 66*(3), 311-317.

Lei, H., Francis, L. F., Gerberich, W. W., & Scriven, L. E. (2002). Stress development in drying coatings after solidification. *AIChE Journal, 48*(3), 437-451. doi:10.1002/aic.690480304

Leontieva, O. V., Demidenko, Z. N., & Blagosklonny, M. V. (2014). Contact inhibition and high cell density deactivate the mammalian target of rapamycin pathway, thus suppressing the senescence program. *Proceedings of the National Academy of Sciences, 111*(24), 8832. doi:10.1073/pnas.1405723111

Levental, I., Georges, P. C., & Janmey, P. A. (2007). Soft biological materials and their impact on cell function. *Soft Matter, 3*(3), 299-306.

Levy, I., Nussinovitch, A., Shpigel, E., & Shoseyov, O. (2002). Recombinant cellulose crosslinking protein: a novel paper-modification biomaterial. *Cellulose, 9*(1), 91-98. doi:Doi 10.1023/A:1015848701029

Lewis, G. G., DiTucci, M. J., & Phillips, S. T. (2012). Quantifying Analytes in Paper‐Based Microfluidic Devices Without Using External Electronic Readers. *Angewandte Chemie, 124*(51), 12879-12882.

Li, H., Cheng, F., Robledo-Lara, J. A., Liao, J., Wang, Z., & Zhang, Y. S. (2020). Fabrication of paper-based devices for in vitro tissue modeling. *Bio-Design and Manufacturing*. doi:10.1007/s42242-020-00077-5

Li, J., Liu, X., Tomaskovic-Crook, E., Crook, J. M., & Wallace, G. G. (2019). Smart graphene-cellulose paper for 2D or 3D "origami-inspired" human stem cell support and differentiation. *Colloids and Surfaces B: Biointerfaces, 176*, 87-95.

Li, W. J., Laurencin, C. T., Caterson, E. J., Tuan, R. S., & Ko, F. K. (2002). Electrospun nanofibrous structure: a novel scaffold for tissue engineering. *Journal of Biomedical Materials Research: An Official Journal of The Society for Biomaterials, The Japanese Society for Biomaterials, and The Australian Society for Biomaterials and the Korean Society for Biomaterials, 60*(4), 613-621.

Li, Z., Li, F., Hu, J., Wee, W., Han, Y., Pingguan-Murphy, B., . . . Xu, F. (2015). Direct writing electrodes using ball pen for paper-based point-of-care testing. *Analyst*.

Li, Z., Tan, B. H., Lin, T., & He, C. (2016). Recent advances in stereocomplexation of enantiomeric PLA-based copolymers and applications. *Progress in Polymer Science, 62*, 22-72. doi:https://doi.org/10.1016/j.progpolymsci.2016.05.003

Liang, W., Lin, M., Li, X., Li, C., Gao, B., Gan, H., . . . Yang, M. (2012). Icariin promotes bone formation via the BMP-2/Smad4 signal transduction pathway in the hFOB 1.19 human osteoblastic cell line. *Int J Mol Med, 30*(4), 889-895. doi:10.3892/ijmm.2012.1079

Lim, C. T., Tan, E. P. S., & Ng, S. Y. (2008). Effects of crystalline morphology on the tensile properties of electrospun polymer nanofibers. *Applied Physics Letters, 92*(14), 141908. doi:10.1063/1.2857478

Liu, H., & Hsieh, Y. L. (2002). Ultrafine fibrous cellulose membranes from electrospinning of cellulose acetate. *Journal of Polymer Science Part B: Polymer Physics, 40*(18), 2119-2129.

Liu, H., Qing, H. B., Li, Z. D., Han, Y. L., Lin, M., Yang, H., . . . Xu, F. (2017). Paper: A promising material for human-friendly functional wearable electronics. *Materials Science & Engineering R-Reports, 112*, 1-22. doi:10.1016/j.mser.2017.01.001

Liu, H. Q., & Hsieh, Y. L. (2002). Ultrafine fibrous cellulose membranes from electrospinning of cellulose acetate. *Journal of Polymer Science Part B-Polymer Physics, 40*(18), 2119-2129. doi:10.1002/polb.10261

Liu, X., Lim, J. Y., Donahue, H. J., Dhurjati, R., Mastro, A. M., & Vogler, E. A. (2007). Influence of substratum surface chemistry/energy and topography on the human fetal osteoblastic cell line hFOB 1.19: Phenotypic and genotypic responses observed in vitro. *Biomaterials, 28*(31), 4535-4550. doi:10.1016/j.biomaterials.2007.06.016

Liu, X., & Ma, P. X. (2004). Polymeric Scaffolds for Bone Tissue Engineering. *Annals of*

Biomedical Engineering, 32(3), 477-486. doi:10.1023/B:ABME.0000017544.36001.8e

Liu, Z., Hu, J., Zhao, Y., Qu, Z., & Xu, F. (2015). Experimental and numerical studies on liquid wicking into filter papers for paper-based diagnostics. *Applied Thermal Engineering, 88*, 280-287. doi:http://dx.doi.org/10.1016/j.applthermaleng.2014.09.057

Lo, B., & Parham, L. (2009). Ethical issues in stem cell research. *Endocrine reviews, 30*(3), 204-213. doi:10.1210/er.2008-0031

Lowery, J. L., Datta, N., & Rutledge, G. C. (2010). Effect of fiber diameter, pore size and seeding method on growth of human dermal fibroblasts in electrospun poly(epsilon-caprolactone) fibrous mats. *Biomaterials, 31*(3), 491-504. doi:10.1016/j.biomaterials.2009.09.072

Ma, P. X., & Zhang, R. (1999). Synthetic nano‐scale fibrous extracellular matrix. *Journal of Biomedical Materials Research: An Official Journal of The Society for Biomaterials, The Japanese Society for Biomaterials, and The Australian Society for Biomaterials, 46*(1), 60-72.

Magalhães, R., Nugraha, B., Pervaiz, S., Yu, H., & Kuleshova, L. L. (2012). Influence of cell culture configuration on the post-cryopreservation viability of primary rat hepatocytes. *Biomaterials, 33*, 88-95.

Magalhaes, R., Wang, X. W., Gouk, S. S., Lee, K. H., Ten, C. M., Yu, H., & Kuleshova, L. L. (2008). Vitrification successfully preserves hepatocyte spheroids. *Cell transplantation, 17*(7), 813-828. Retrieved from http://www.ncbi.nlm.nih.gov/pubmed/19044208

Malandrino, A., Mak, M., Kamm, R. D., & Moeendarbary, E. (2018). Complex mechanics of the heterogeneous extracellular matrix in cancer. *Extreme Mechanics Letters, 21*, 25-34. doi:10.1016/j.eml.2018.02.003

Malikmammadov, E., Tanir, T. E., Kiziltay, A., Hasirci, V., & Hasirci, N. (2018). PCL and PCL-based materials in biomedical applications. *Journal of Biomaterials Science, Polymer Edition, 29*(7-9), 863-893. doi:10.1080/09205063.2017.1394711

Malikmammadov, E., Tanir, T. E., Kiziltay, A., Hasirci, V., & Hasirci, N. (2018). PCL and PCL-based materials in biomedical applications. *J Biomater Sci Polym Ed, 29*(7-9), 863-893. doi:10.1080/09205063.2017.1394711

Martinez, A. W., Phillips, S. T., Butte, M. J., & Whitesides, G. M. (2007). Patterned Paper as a Platform for Inexpensive, Low-Volume, Portable Bioassays. *Angewandte Chemie International Edition, 46*(8), 1318-1320. doi:10.1002/anie.200603817

Martinez, A. W., Phillips, S. T., Butte, M. J., & Whitesides, G. M. (2007). Patterned paper as a platform for inexpensive, low-volume, portable bioassays. *Angew Chem Int Ed Engl, 46*(8), 1318-1320. doi:10.1002/anie.200603817

Martino, A., Songsasen, N., & Leibo, S. P. (1996). Development into blastocysts of bovine oocytes cryopreserved by ultra-rapid cooling. *Biol Reprod, 54*(5), 1059-1069.

Masters, K. S., & Anseth, K. S. (2004). CELL–MATERIAL INTERACTIONS. In *Advances in Chemical Engineering* (Vol. 29, pp. 7-46): Academic Press.

Matsunari, H., Maehara, M., Nakano, K., Ikezawa, Y., Hagiwara, Y., Sasayama, N., . . . Nagashima, H. (2012). Hollow fiber vitrification: a novel method for vitrifying multiple embryos in a single device. *J Reprod Dev, 58*(5), 599-608.

Migonney, V. (2014). *Biomaterials*: Wiley.

Mimeault, M., Hauke, R., & Batra, S. K. (2007). Stem cells: a revolution in therapeutics—recent advances in stem cell biology and their therapeutic applications in regenerative medicine and cancer therapies. *Clinical Pharmacology & Therapeutics, 82*(3), 252-264.

Min Jin, C., Ju Young, P., Kyoung Je, C., Jong-Won, R., Dong-Woo, C., & Dong Sung, K. (2012). Micropattern array with gradient size (μPAGS) plastic surfaces fabricated by PDMS (polydimethylsiloxane) mold-based hot embossing technique for investigation of cell–surface interaction. *Biofabrication, 4*(4), 045006. Retrieved from http://stacks.iop.org/1758-5090/4/i=4/a=045006

Mohamed-Ahmed, S., Fristad, I., Lie, S. A., Suliman, S., Mustafa, K., Vindenes, H., & Idris, S. B. (2018). Adipose-derived and bone marrow mesenchymal stem cells: a donor-matched comparison. *Stem cell research & therapy, 9*(1), 168.

Mooney, D., Hansen, L., Vacanti, J., Langer, R., Farmer, S., & Ingber, D. (1992). Switching from differentiation to growth in hepatocytes: control by extracellular matrix. *Journal of cellular physiology, 151*(3), 497-505.

Mosadegh, B., Dabiri, B. E., Lockett, M. R., Derda, R., Campbell, P., Parker, K. K., & Whitesides, G. M. (2014a). Three-dimensional paper-based model for cardiac ischemia. *Advanced Healthcare Materials, 3*(7), 1036-1043. doi:10.1002/adhm.201300575

Mosadegh, B., Dabiri, B. E., Lockett, M. R., Derda, R., Campbell, P., Parker, K. K., & Whitesides, G. M. (2014). Three-dimensional paper-based model for cardiac ischemia. *Adv Healthc Mater, 3*(7), 1036-1043. doi:10.1002/adhm.201300575

Mosadegh, B., Dabiri, B. E., Lockett, M. R., Derda, R., Campbell, P., Parker, K. K., & Whitesides, G. M. (2014b). Three-Dimensional Paper-Based Model for Cardiac Ischemia. *Advanced healthcare materials, 3*(7), 1036–1043.

Mosadegh, B., Dabiri, B. E., Lockett, M. R., Derda, R., Campbell, P., Parker, K. K., & Whitesides, G. M. (2014). Three‐Dimensional Paper‐Based Model for Cardiac Ischemia. *Advanced healthcare materials, 3*(7), 1036-1043.

Mosadegh, B., Lockett, M. R., Minn, K. T., Simon, K. A., Gilbert, K., Hillier, S., . . . Whitesides, G. M. (2015). A paper-based invasion assay: Assessing chemotaxis of cancer cells in gradients of oxygen. *Biomaterials, 52*, 262-271. doi:http://dx.doi.org/10.1016/j.biomaterials.2015.02.012

Mouw, J. K., Ou, G., & Weaver, V. M. (2014). Extracellular matrix assembly: a multiscale deconstruction. *Nature reviews. Molecular cell biology, 15*(12), 771-785. doi:10.1038/nrm3902

Musson, D. S., McIntosh, J., Callon, K. E., Chhana, A., Dunbar, P. R., Naot, D., & Cornish, J. (2013). The Need for Thorough in Vitro Testing of Biomaterial Scaffolds: Two Case Studies. *Procedia Engineering, 59*, 138-143. doi:https://doi.org/10.1016/j.proeng.2013.05.103

Nair, L., & Laurencin, C. (2006). Polymers as Biomaterials for Tissue Engineering and Controlled Drug Delivery Tissue Engineering In K. Lee & D. Kaplan (Eds.), (Vol. 102, pp. 47-90): Springer Berlin.

Nakamura, H. (2007). Morphology, function, and differentiation of bone cells. *Journal of hard tissue biology, 16*(1), 15-22.

Ng, K., Gao, B., Yong, K. W., Li, Y., Shi, M., Zhao, X., . . . Xu, F. (2017). Paper-based cell culture platform and its emerging biomedical applications. *Materials Today, 20*(1), 32-44. doi:https://doi.org/10.1016/j.mattod.2016.07.001

Ng, K., Gao, B., Yong, K. W., Li, Y. H., Shi, M., Zhao, X., . . . Xu, F. (2017). Paper-based cell culture platform and its emerging biomedical applications. *Materials Today, 20*(1), 32-44. doi:DOI 10.1016/j.mattod.2016.07.001

Niakan, A., Ramesh, S., Naveen, S. V., Mohan, S., & Kamarul, T. (2017). Osteogenic priming potential of bovine hydroxyapatite sintered at different temperatures for tissue engineering applications. *Materials Letters, 197*, 83-86. doi:https://doi.org/10.1016/j.matlet.2017.03.057

Nicolas, J., Magli, S., Rabbachin, L., Sampaolesi, S., Nicotra, F., & Russo, L. (2020). 3D Extracellular Matrix Mimics: Fundamental Concepts and Role of Materials Chemistry to Influence Stem Cell Fate. *Biomacromolecules, 21*(6), 1968-1994.

doi:10.1021/acs.biomac.0c00045

Nune, M., Kumaraswamy, P., Krishnan, U. M., & Sethuraman, S. (2013). Self-assembling peptide nanofibrous scaffolds for tissue engineering: novel approaches and strategies for effective functional regeneration. *Curr Protein Pept Sci, 14*(1), 70-84. Retrieved from https://www.ncbi.nlm.nih.gov/pubmed/23544748

O'Brien, F. J. (2011). Biomaterials & scaffolds for tissue engineering. *Materials Today, 14*(3), 88-95. doi:Doi 10.1016/S1369-7021(11)70058-X

Oedayrajsingh-Varma, M., Van Ham, S., Knippenberg, M., Helder, M., Klein-Nulend, J., Schouten, T., . . . Van Milligen, F. (2006). Adipose tissue-derived mesenchymal stem cell yield and growth characteristics are affected by the tissue-harvesting procedure. *Cytotherapy, 8*(2), 166-177.

Oliveira, C., Sepulveda, G., Aguiar, T. Q., Gama, F. M., & Domingues, L. (2015). Modification of paper properties using carbohydrate-binding module 3 from the Clostridium thermocellum CipA scaffolding protein produced in Pichia pastoris: elucidation of the glycosylation effect. *Cellulose, 22*(4), 2755-2765. doi:10.1007/s10570-015-0655-6

Ong, J. L., & Guda, T. (2017). *Translating Biomaterials for Bone Graft: Bench-top to Clinical Applications*: Crc Press.

Park, H.-J., Yu, S. J., Yang, K., Jin, Y., Cho, A.-N., Kim, J., . . . Cho, S.-W. (2014). Paper-based bioactive scaffolds for stem cell-mediated bone tissue engineering. *Biomaterials, 35*(37), 9811-9823. doi:http://dx.doi.org/10.1016/j.biomaterials.2014.09.002

Park, H. J., Yu, S. J., Yang, K., Jin, Y., Cho, A. N., Kim, J., . . . Cho, S. W. (2014). Paper-based bioactive scaffolds for stem cell-mediated bone tissue engineering. *Biomaterials, 35*(37), 9811-9823. doi:10.1016/j.biomaterials.2014.09.002

Parolo, C., & Merkoçi, A. (2013). Paper-based nanobiosensors for diagnostics. *Chemical Society Reviews, 42*(2), 450-457.

Pérez-Tomás, R. (2006). Multidrug resistance: retrospect and prospects in anti-cancer drug treatment. *Current medicinal chemistry, 13*(16), 1859-1876.

Peuster, M., Wohlsein, P., Brügmann, M., Ehlerding, M., Seidler, K., Fink, C., . . . Hausdorf, G. (2001). A novel approach to temporary stenting: degradable cardiovascular stents produced from corrodible metal—results 6–18 months after implantation into New Zealand white rabbits. *Heart, 86*(5), 563-569.

Pham, Q. P., Sharma, U., & Mikos, A. G. (2006). Electrospun Poly(ε-caprolactone)

Microfiber and Multilayer Nanofiber/Microfiber Scaffolds: Characterization of Scaffolds and Measurement of Cellular Infiltration. *Biomacromolecules, 7*(10), 2796-2805. doi:10.1021/bm060680j

Polak, S. (2013). In vitro to human in vivo translation–pharmacokinetics and pharmacodynamics of quinidine. *ALTEX-Alternatives to animal experimentation, 30*(3), 309-318.

Polini, A., Pisignano, D., Parodi, M., Quarto, R., & Scaglione, S. (2011). Osteoinduction of Human Mesenchymal Stem Cells by Bioactive Composite Scaffolds without Supplemental Osteogenic Growth Factors. *PLoS ONE, 6*(10), e26211. doi:10.1371/journal.pone.0026211

Pollock, N. R., Rolland, J. P., Kumar, S., Beattie, P. D., Jain, S., Noubary, F., . . . Whitesides, G. M. (2012). A paper-based multiplexed transaminase test for low-cost, point-of-care liver function testing. *Science translational medicine, 4*(152), 152ra129-152ra129. doi:10.1126/scitranslmed.3003981

Puppi, D., Zhang, X., Yang, L., Chiellini, F., Sun, X., & Chiellini, E. (2014). Nano/microfibrous polymeric constructs loaded with bioactive agents and designed for tissue engineering applications: A review. *Journal of Biomedical Materials Research Part B: Applied Biomaterials, 102*(7), 1562-1579. doi:10.1002/jbm.b.33144

Qi, A., Hoo, S. P., Friend, J., Yeo, L., Yue, Z., & Chan, P. P. (2014). Hydroxypropyl cellulose methacrylate as a photo-patternable and biodegradable hybrid paper substrate for cell culture and other bioapplications. *Adv Healthc Mater, 3*(4), 543-554. doi:10.1002/adhm.201300155

Qi, A., Hoo, S. P., Friend, J., Yeo, L., Yue, Z., & Chan, P. P. Y. (2014). Hydroxypropyl Cellulose Methacrylate as a Photo-Patternable and Biodegradable Hybrid Paper Substrate for Cell Culture and Other Bioapplications. *Advanced healthcare materials, 3*(4), 543-554. doi:10.1002/adhm.201300155

Rahimi, R., Ochoa, M., Donaldson, A., Parupudi, T., Dokmeci, M. R., Khademhosseini, A., . . . Ziaie, B. (2015). A Janus-paper PDMS platform for air–liquid interface cell culture applications. *Journal of Micromechanics and Microengineering, 25*(5), 055015.

Ratner, B. D., Allan S. Hoffman, B. D. R. F. J. S. J. E. L., Knovel, Biomaterials, S. f., Hoffman, A. S., Schoen, F. J., & Lemons, J. E. (2004). *Biomaterials Science: An Introduction to Materials in Medicine*: Elsevier Science.

Ratner, B. D., Hoffman, A. S., Schoen, F. J., & Lemons, J. E. (2004). *Biomaterials science: an introduction to materials in medicine*: Elsevier.

Ravaglioli, A., Krajewski, A., Baldi, G., Tateo, F., Peruzzo, L., & Piancastelli, A. (2008). Glass–ceramic scaffolds for tissue engineering. *Advances in Applied Ceramics, 107*(5), 268-273. doi:10.1179/174367608X341488

Rismani Yazdi, S., Shadmani, A., Burgel, S. C., Misun, P. M., Hierlemann, A., & Frey, O. (2015). Adding the 'heart' to hanging drop networks for microphysiological multi-tissue experiments. *Lab on a Chip, 15*(21), 4138-4147. doi:10.1039/C5LC01000D

Russo, A., Ahn, B. Y., Adams, J. J., Duoss, E. B., Bernhard, J. T., & Lewis, J. A. (2011). Pen‐on‐Paper Flexible Electronics. *Advanced Materials, 23*(30), 3426-3430.

Sapp, M. C., Fares, H. J., Estrada, A. C., & Grande-Allen, K. J. (2015). Multilayer three-dimensional filter paper constructs for the culture and analysis of aortic valvular interstitial cells. *Acta Biomaterialia, 13*(0), 199-206. doi:http://dx.doi.org/10.1016/j.actbio.2014.11.039

Sarfraz, J., Määttänen, A., Ihalainen, P., Keppeler, M., Lindén, M., & Peltonen, J. (2012). Printed copper acetate based H 2 S sensor on paper substrate. *Sensors and Actuators B: Chemical, 173*, 868-873.

Saul, J. M., Linnes, M. P., Ratner, B. D., Giachelli, C. M., & Pun, S. H. (2007). Delivery of non-viral gene carriers from sphere-templated fibrin scaffolds for sustained transgene expression. *Biomaterials, 28*(31), 4705-4716.

Saxena, A. K., Singh, D., & Gupta, J. (2010). Role of stem cell research in therapeutic purpose--a hope for new horizon in medical biotechnology. *Journal of experimental therapeutics & oncology, 8*(3).

Sen, S., Engler, A. J., & Discher, D. E. (2009). Matrix strains induced by cells: computing how far cells can feel. *Cellular and molecular bioengineering, 2*(1), 39-48.

Shalumon, K. T., Sowmya, S., Sathish, D., Chennazhi, K. P., Nair, S. V., & Jayakumar, R. (2013). Effect of Incorporation of Nanoscale Bioactive Glass and Hydroxyapatite in PCL/Chitosan Nanofibers for Bone and Periodontal Tissue Engineering. *Journal of Biomedical Nanotechnology, 9*(3), 430-440. doi:10.1166/jbn.2013.1559

Silva-Bermudez, P., Rodil, S., & Muhl, S. (2011). Albumin adsorption on oxide thin films studied by spectroscopic ellipsometry. *Applied Surface Science, 258*(5), 1711-1718.

Sjostrom, T., Lalev, G., Mansell, J. P., & Su, B. (2011). Initial attachment and spreading of MG63 cells on nanopatterned titanium surfaces via through-mask anodization. *Applied Surface Science, 257*(10), 4552-4558. doi:10.1016/j.apsusc.2010.11.064

Smith, L. A., & Ma, P. X. (2004). Nano-fibrous scaffolds for tissue engineering. *Colloids and Surfaces B: Biointerfaces, 39*(3), 125-131. doi:https://doi.org/10.1016/j.colsurfb.2003.12.004

Sobral, J. M., Caridade, S. G., Sousa, R. A., Mano, J. F., & Reis, R. L. (2011). Three-dimensional plotted scaffolds with controlled pore size gradients: Effect of scaffold geometry on mechanical performance and cell seeding efficiency. *Acta Biomaterialia, 7*(3), 1009-1018. doi:https://doi.org/10.1016/j.actbio.2010.11.003

Songjaroen, T., Dungchai, W., Chailapakul, O., & Laiwattanapaisal, W. (2011). Novel, simple and low-cost alternative method for fabrication of paper-based microfluidics by wax dipping. *Talanta, 85*(5), 2587-2593.

Spandidos, A., Wang, X., Wang, H., & Seed, B. (2010). PrimerBank: a resource of human and mouse PCR primer pairs for gene expression detection and quantification. *Nucleic acids research, 38*(Database issue), D792-D799. doi:10.1093/nar/gkp1005

Stevens, M. M. (2008). Biomaterials for bone tissue engineering. *Materials Today, 11*(5), 18-25. doi:http://dx.doi.org/10.1016/S1369-7021(08)70086-5

Stevens, M. M., & George, J. H. (2005). Exploring and Engineering the Cell Surface Interface. *Science, 310*(5751), 1135. doi:10.1126/science.1106587

Su, W.-F. (2013). Polymer Size and Polymer Solutions. In *Principles of Polymer Design and Synthesis* (pp. 9-26). Berlin, Heidelberg: Springer Berlin Heidelberg.

Subramaniam, M., Jalal, S. M., Rickard, D. J., Harris, S. A., Bolander, M. E., & Spelsberg, T. C. (2002). Further characterization of human fetal osteoblastic hFOB 1.19 and hFOB/ERα cells: Bone formation in vivo and karyotype analysis using multicolor fluorescent in situ hybridization. *Journal of Cellular Biochemistry, 87*(1), 9-15.

Sun, H., Mei, L., Song, C., Cui, X., & Wang, P. (2006). The in vivo degradation, absorption and excretion of PCL-based implant. *Biomaterials, 27*(9), 1735-1740. doi:https://doi.org/10.1016/j.biomaterials.2005.09.019

Suwantong, O. (2016). Biomedical applications of electrospun polycaprolactone fiber mats. *Polymers for Advanced Technologies, 27*(10), 1264-1273. doi:doi:10.1002/pat.3876

Takahashi, K., & Yamanaka, S. (2006). Induction of Pluripotent Stem Cells from Mouse Embryonic and Adult Fibroblast Cultures by Defined Factors. *Cell, 126*(4), 663-676. doi:10.1016/j.cell.2006.07.024

Tamama, K., Sen, C. K., & Wells, A. (2008). Differentiation of bone marrow

mesenchymal stem cells into the smooth muscle lineage by blocking ERK/MAPK signaling pathway. *Stem cells and development, 17*(5), 897-908.

Tay, C. Y., Koh, C. G., Tan, N. S., Leong, D. T., & Tan, L. P. (2013). Mechanoregulation of stem cell fate via micro-/nano-scale manipulation for regenerative medicine. *Nanomedicine, 8*(4), 623-638.

Tenhaeff, W. E., & Gleason, K. K. (2008). Initiated and oxidative chemical vapor deposition of polymeric thin films: iCVD and oCVD. *Advanced Functional Materials, 18*(7), 979-992.

Theocharis, A. D., Skandalis, S. S., Gialeli, C., & Karamanos, N. K. (2016). Extracellular matrix structure. *Advanced Drug Delivery Reviews, 97*, 4-27. doi:https://doi.org/10.1016/j.addr.2015.11.001

Thomas, D., Gaspar, D., Sorushanova, A., Milcovich, G., Spanoudes, K., Mullen, A. M., . . . Zeugolis, D. I. (2016). Scaffold and scaffold-free self-assembled systems in regenerative medicine. *Biotechnology and Bioengineering, 113*(6), 1155-1163. doi:10.1002/bit.25869

Tian, L., Morrissey, J. J., Kattumenu, R., Gandra, N., Kharasch, E. D., & Singamaneni, S. (2012). Bioplasmonic Paper as a Platform for Detection of Kidney Cancer Biomarkers. *Analytical Chemistry, 84*(22), 9928-9934. doi:10.1021/ac302332g

Tobita, M., Tajima, S., & Mizuno, H. (2015). Adipose tissue-derived mesenchymal stem cells and platelet-rich plasma: stem cell transplantation methods that enhance stemness. *Stem cell research & therapy, 6*(1), 1-7.

Tobjörk, D., & Österbacka, R. (2011). Paper electronics. *Advanced Materials, 23*(17), 1935-1961.

Tojkander, S., Gateva, G., & Lappalainen, P. (2012). Actin stress fibers – assembly, dynamics and biological roles. *Journal of cell science, 125*(8), 1855. doi:10.1242/jcs.098087

Tse, J. R., & Engler, A. J. (2001). Preparation of Hydrogel Substrates with Tunable Mechanical Properties. In *Current Protocols in Cell Biology*: John Wiley & Sons, Inc.

Vajta, G., Holm, P., Kuwayama, M., Booth, P. J., Jacobsen, H., Greve, T., & Callesen, H. (1998). Open pulled straw (OPS) vitrification: a new way to reduce cryoinjuries of bovine ova and embryos. *Molecular reproduction and development, 51*(1), 53-58.

Veevers-Lowe, J., Ball, S. G., Shuttleworth, A., & Kielty, C. M. (2011). Mesenchymal

stem cell migration is regulated by fibronectin through α5β1-integrin-mediated activation of PDGFR-β and potentiation of growth factor signals. *Journal of cell science, 124*(Pt 8), 1288-1300. doi:10.1242/jcs.076935

Venugopal, J., Low, S., Choon, A. T., Kumar, A. B., & Ramakrishna, S. (2008). Electrospun-modified nanofibrous scaffolds for the mineralization of osteoblast cells. *Journal of Biomedical Materials Research Part A, 85A*(2), 408-417. doi:10.1002/jbm.a.31538

Venugopal, J. R., Low, S., Choon, A. T., Kumar, A. B., & Ramakrishna, S. (2008). Nanobioengineered Electrospun Composite Nanofibers and Osteoblasts for Bone Regeneration. *Artificial Organs, 32*(5), 388-397. doi:10.1111/j.1525-1594.2008.00557.x

Vogler, E. A. (1998). Structure and reactivity of water at biomaterial surfaces. *Advances in colloid and interface science, 74*(1), 69-117.

Wang, F., Weaver, V. M., Petersen, O. W., Larabell, C. A., Dedhar, S., Briand, P., . . . Bissell, M. J. (1998). Reciprocal interactions between β1-integrin and epidermal growth factor receptor in three-dimensional basement membrane breast cultures: a different perspective in epithelial biology. *Proceedings of the National Academy of Sciences, 95*(25), 14821-14826.

Wang, L., & Carrier, R. L. (2011). *Biomimetic Topography: Bioinspired Cell Culture Substrates and Scaffolds*: INTECH Open Access Publisher.

Wang, L., Huang, G., Sha, B., Wang, S., Han, Y., Wu, J., . . . Xu, F. (2014). Engineering three-dimensional cardiac microtissues for potential drug screening applications. *Current medicinal chemistry, 21*(22), 2497-2509.

Wang, L., Xu, C., Zhu, Y., Yu, Y., Sun, N., Zhang, X., . . . Qin, J. (2015). Human induced pluripotent stem cell-derived beating cardiac tissues on paper. *Lab on a Chip*.

Wang, S., Lu, L., Wang, C., Gao, C., & Wang, X. (2010). Polymeric biomaterials for tissue engineering applications. *International Journal of Polymer Science, 2010*.

Webb, A., Clark, P., Skepper, J., Compston, A., & Wood, A. (1995). Guidance of oligodendrocytes and their progenitors by substratum topography. *Journal of cell science, 108*(8), 2747-2760. Retrieved from http://jcs.biologists.org/content/108/8/2747.abstract

Wei, M., Li, S., & Le, W. (2017). Nanomaterials modulate stem cell differentiation: biological interaction and underlying mechanisms. *Journal of Nanobiotechnology, 15*(1), 75. doi:10.1186/s12951-017-0310-5

Wei, X., Xia, Z., Wong, S.-C., Baji, A. J. I. J. o. E., & Biomechanics, C. (2009). Modelling of mechanical properties of electrospun nanofibre network. *1*(1), 45-57.

Wolf, K., Mazo, I., Leung, H., Engelke, K., Von Andrian, U. H., Deryugina, E. I., . . . Friedl, P. (2003). Compensation mechanism in tumor cell migration mesenchymal–amoeboid transition after blocking of pericellular proteolysis. *The Journal of Cell Biology, 160*(2), 267-277.

Woo, K. M., Chen, V. J., & Ma, P. X. (2003). Nano ‐ fibrous scaffolding architecture selectively enhances protein adsorption contributing to cell attachment. *Journal of Biomedical Materials Research Part A: An Official Journal of The Society for Biomaterials, The Japanese Society for Biomaterials, and The Australian Society for Biomaterials and the Korean Society for Biomaterials, 67*(2), 531-537.

Woo, K. M., Jun, J.-H., Chen, V. J., Seo, J., Baek, J.-H., Ryoo, H.-M., . . . Ma, P. X. (2007). Nano-fibrous scaffolding promotes osteoblast differentiation and biomineralization. *Biomaterials, 28*(2), 335-343. doi:https://doi.org/10.1016/j.biomaterials.2006.06.013

Woodruff, M. A., & Hutmacher, D. W. (2010). The return of a forgotten polymer—Polycaprolactone in the 21st century. *Progress in Polymer Science, 35*(10), 1217-1256.

Wu, H., Wan, Y., Dalai, S., & Zhang, R. (2010). Response of rat osteoblasts to polycaprolactone/chitosan blend porous scaffolds. *Journal of Biomedical Materials Research Part A, 92A*(1), 238-245. doi:doi:10.1002/jbm.a.32376

Xu, F., Wu, C. a. M., Rengarajan, V., Finley, T. D., Keles, H. O., Sung, Y., . . . Demirci, U. (2011). Three ‐ Dimensional Magnetic Assembly of Microscale Hydrogels. *Advanced Materials, 23*(37), 4254-4260.

Xue, R., Qian, Y., Li, L., Yao, G., Yang, L., & Sun, Y. (2017). Polycaprolactone nanofiber scaffold enhances the osteogenic differentiation potency of various human tissue-derived mesenchymal stem cells. *Stem cell research & therapy, 8*(1), 148. doi:10.1186/s13287-017-0588-0

Yan, W., Zhang, Q., Chen, B., Liang, G.-T., Li, W.-X., Zhou, X.-M., & Liu, D.-Y. (2013). Study on Microenvironment Acidification by Microfluidic Chip with Multilayer-paper Supported Breast Cancer Tissue. *Chinese Journal of Analytical Chemistry, 41*(6), 822-827. doi:http://dx.doi.org/10.1016/S1872-2040(13)60661-1

Yen, M. l., Chien, C. C., Chiu, I. m., Huang, H. I., Chen, Y. C., Hu, H. I., & Yen, B. L. (2007). Multilineage differentiation and characterization of the human fetal osteoblastic 1.19 cell line: a possible in vitro model of human mesenchymal progenitors. *STEM CELLS, 25*(1), 125-131.

Yew, C.-H. T., Azari, P., Choi, J. R., Li, F., & Pingguan-Murphy, B. (2018). Electrospin-coating of nitrocellulose membrane enhances sensitivity in nucleic acid-based lateral flow assay. *Analytica chimica acta, 1009*, 81-88.

Yew, C. T., Azari, P., Choi, J. R., Li, F., & Pingguan-Murphy, B. (2018). Electrospin-coating of nitrocellulose membrane enhances sensitivity in nucleic acid-based lateral flow assay. *Anal Chim Acta, 1009*, 81-88. doi:10.1016/j.aca.2018.01.016

Yin, Q., Xu, N., Xu, D., Dong, M., Shi, X., Wang, Y., . . . Jin, H. (2020). Comparison of senescence-related changes between three-and two-dimensional cultured adipose-derived mesenchymal stem cells. *Stem cell research & therapy, 11*(1), 1-12.

Yoshimoto, H., Shin, Y. M., Terai, H., & Vacanti, J. P. (2003). A biodegradable nanofiber scaffold by electrospinning and its potential for bone tissue engineering. *Biomaterials, 24*(12), 2077-2082. doi:https://doi.org/10.1016/S0142-9612(02)00635-X

You, M. H., Kwak, M. K., Kim, D. H., Kim, K., Levchenko, A., Kim, D. Y., & Suh, K. Y. (2010). Synergistically enhanced osteogenic differentiation of human mesenchymal stem cells by culture on nanostructured surfaces with induction media. *Biomacromolecules, 11*(7), 1856-1862. doi:10.1021/bm100374n

You, Y., Won Lee, S., Jin Lee, S., & Park, W. H. (2006). Thermal interfiber bonding of electrospun poly(l-lactic acid) nanofibers. *Materials Letters, 60*(11), 1331-1333. doi:https://doi.org/10.1016/j.matlet.2005.11.022

Young, J. L., Holle, A. W., & Spatz, J. P. (2016). Nanoscale and mechanical properties of the physiological cell–ECM microenvironment. *Experimental Cell Research, 343*(1), 3-6. doi:https://doi.org/10.1016/j.yexcr.2015.10.037

Yusop, A. H., Bakir, A. A., Shaharom, N. A., Abdul Kadir, M. R., & Hermawan, H. (2012). Porous Biodegradable Metals for Hard Tissue Scaffolds: A Review. *International Journal of Biomaterials, 2012*, 641430. doi:10.1155/2012/641430

Zhang, X., Catalano, P. N., Gurkan, U. A., Khimji, I., & Demirci, U. (2011). Emerging technologies in medical applications of minimum volume vitrification. *Nanomedicine, 6*(6), 1115-1129.

Zhang, Y., Ouyang, H., Lim, C. T., Ramakrishna, S., & Huang, Z.-M. (2005). Electrospinning of gelatin fibers and gelatin/PCL composite fibrous scaffolds. *Journal of Biomedical Materials Research Part B: Applied Biomaterials, 72B*(1), 156-165. doi:10.1002/jbm.b.30128

Zhang, Y., Ren, T., Li, T., He, J., & Fang, D. (2016). Paper-Based Hydrophobic/Lipophobic Surface for Sensing Applications Involving Aggressive